Engineering Lantibiotic-Inspired Chimeric Antimicrobials

Charlotte Emma Prattley

Thesis submitted to the University of Nottingham for the degree of Doctor of Philosophy

January 2019

Abstract

Microbial control is important in both human health and food safety. Naturally occurring antimicrobial peptides, such as nisin, have been used extensively to preserve a variety of food products, yet resistance remains uncommon. Both food protection and medical applications urgently require the development of new chimeric antimicrobials, inspired by natural compounds. Ideal antimicrobial peptides possess both specific recognition of targets found universally in bacteria and low haemolytic activity.

We propose to engineer lantibiotic-inspired, lipid II targeting engaging short peptides and chimeric antimicrobials with a targeting domain and a pore forming moiety. This study analyses the properties of candidate compounds N12L, N12D, N12LM2 and N12DM2. N12 represents a section inspired by the first 12 residue target-recognition motif of the common food preservative and antimicrobial nisin. D/L denotes cysteine chirality at position 3 and 7. M2 depicts the presence of magainin II, a pore forming antimicrobial with poor target recognition. Two disulphide bridges can construct macro-cyclic peptides, mimicking rings A and B of nisin.

Interaction of the N12D motif is independent of its cyclisation state. Fluorescent microscopy showed that semi-cyclic N12D binds extensively to *Bacillus subtilis*. Cyclic N12DM2 displayed reduced leakage in the presence of lipid II, but not geranyl geranyl pyrophosphate (GGPP) and showed thermally stable interaction with N-acetylmuramyl-L-alanyl-D-isoglutamine hydrate (MurNAc-dipeptide) through CD studies. Linear N12DM2 was inactive against *Micrococcus luteus*

unless combined with PGLa (peptide with N-terminal glycine and C-terminal leucinamide), a peptide within the magainin family. This suggests that peptides with the N12D motif bind to MurNAc-dipeptide and in the case of the N12DM2 this prevents the action of magainin II.

Antimicrobial activity was demonstrated by cyclic N12L against *M. luteus* and foodborne pathogens *Listeria monocytogenes* and *Staphylococcus* spp., while its linear form is mostly inactive at comparable concentrations. This shows that for N12L to be active it needs to be cyclised. When evaluated against components of lipid II, cyclic N12LM2 displayed interaction with isopentenyl pyrophosphate (I-PP) but did not interact with MurNAc-dipeptide. Some interaction was seen for linear N12L and I-PP, suggesting that increased interaction of N12L with pyrophosphates occurs as the degree of cyclisation increases. This is supported by the fluorescence microscopy, as semi-cyclic N12L-TAM binds *B. subtilis*. In conclusion, cyclised N12L has the most potential as an antimicrobial out of the peptides synthesised and properties assessed.

Acknowledgements

I would like to thank the BBSRC and DuPont for funding the project. Thanks to those at Diamond Light Source, Oxford, for the SAXS and CD assistance.

I am grateful for the unfailing enthusiasm and guidance of my supervisor, Boyan Bonev. I'm also greatly appreciative for the support and microbial advice of my DuPont supervisor Mette Ryun-Drasbek and her team.

Thanks to Dave Tooth for the HPLC/MS guidance and Chris Gell for the microscopy expertise. Thanks also to Divya for the late-night leakage assay assistance.

Big thanks to Alice for the wisdom and tea breaks, and to Marvin for answering all my computational questions.

This would not have been possible without the moral support of my parents and sister. Thanks to my dad for proofreading the many pages.

Special thanks to my mum for patiently listening to my mostly incoherent science-ish ramblings, for the great advice and for keeping me going when I couldn't. The past two years have been the hardest and I couldn't have got through it without you.

Finally, thanks to Monty and Odin for being the best canine companions, always.

Publications

Lanne, A. B. M., Goode, A., Prattley, C., Kumari, D., Drasbek, M. R., Williams, P., Conde-álvarez, R., Moriyón, I., Bonev, B. B. "Molecular recognition of lipopolysaccharide by the lantibiotic nisin." *Biochimica et Biophysica Acta – Biomembranes*, vol. 1861, no. 1, pp. 83-92, 2019.

Contents

Chapter 1 Introduction

Antimicrobial resistance (AMR) is a severe growing global issue and the clock is ticking. If we don't act now, by 2050 10 million people a year could die as a result of AMR. This is not just a devasting health issue but also has massive economic and financial implications. A loss of $100 trillion in global production will be seen by 2050 if no action is taken. The development of new therapies for diseases will be redundant if AMR is not addressed. Routine surgery will carry a massive risk of fatal post-operative infections. [1]

A recent review on AMR by Jim O'Neill outlines a strategy to tackle the issue, which includes significant investment in the AMR research sector, formation of a global AMR coalition and innovation fund, a global public awareness campaign, improved hygiene and sanitation, reduction of the use of antibiotics in agriculture, improved surveillance of AMR and promotion of vaccines. [1] The World Health Organisation (WHO) has a similar global action plan in place and is making progress, for example countries are completing AMR self-assessment surveys that report their advancement towards these goals. [2]

Investment in the development of new antimicrobials is not appealing to pharmaceutical companies because antibiotic treatment is short-term; it is more profitable to focus on long-term health issues. It is vital that investment and cooperativity comes from all sectors to achieve success in addressing this issue.

Following Jim O'Neill's recommendations, the UK government has recently released its plan to address AMR, which includes a new payment scheme. The National Institute of Health and Clinical Excellence (NICE) and NHS England will

pay the pharmaceutical companies for drugs based on their value to the NHS. This will provide an incentive for antibiotic development and production. [3]

Another aspect is food security. Foodborne pathogens and their toxic by-products pose a serious threat to human health and food safety. This class of pathogenic bacteria includes *L. monocytogenes*, *Staphylococcus aureus*, *Bacillus* spp.*, Clostridium botulinum*, *Escherichia coli*, *Salmonella* spp. and *Pseudomonas* spp.. [4] To prevent food spoilage and ensure food safety, bactericidal and bacteriostatic preservatives are used in food worldwide. Currently the list of EU approved food preservatives includes chemical additives such as acetates, benzoates, borates, carbonates, lactates, nitrates/nitrites, parabens, propionates, sorbates and sulphites. Also included are two antimicrobial compounds, nisin and natamycin. Nisin is produced by *Lactococcus lactis* and is active against a broad spectrum of bacteria while natamycin is an antifungal primarily from *Streptomyces natalensis*. [5] [6]

In recent years there has been a demand from consumers for complete transparency in relation to the content of their food. Consumers are becoming increasingly aware of food additives, this has driven a need for chemical free food. The demand for safe nutrition supplied to a rapidly growing global population and consumer awareness, encourage the production of nature-inspired, effective food preservatives. The aim of this work is to address such a demand by designing novel antimicrobial peptides (AMPs).

1.1 Structure of bacterial cell envelope and targets

Identifying bacteria-specific targets is vital for developing suitable antimicrobials.

Crossing or acting upon bacterial membranes is a challenge most antimicrobials face. The development of a magic bullet for all pathogenic bacteria is exceptionally challenging due, in part, to the varying structure of bacterial cells. Gram-positive bacteria contain only one membrane enclosed in a thick peptidoglycan layer comprised of varying long carbohydrate chains connected *via* peptide crosslinks. In contrast Gram-negative bacteria possess both inner and outer membranes, separated by the periplasm, with a thinner peptidoglycan layer in-between, the outer layer of the outer membrane is comprised of lipopolysaccharide (LPS). [7]

AMPs have varying modes of action that exploit specific vulnerabilities in bacteria. AMPs such as indolicidin cross the membrane to reach their intracellular targets, whereas nisin and subtilin target lipid II on the outer leaflet of bacterial membranes. Other AMPs, such as magainin II and melittin, don't bind specific targets but instead interact with negative membranes to form pores. [8] [9]

1.2 Peptidoglycan Synthesis

One pathway that is unique and essential to bacteria is peptidoglycan synthesis. The structure of peptidoglycan and its mechanism of synthesis are specific to bacteria, which offers the opportunity to identify highly specific targets. In fact, the enzymatic action and intermediates involved in peptidoglycan synthesis present the most successfully exploited pharmacological targets (figure 1.2.1).

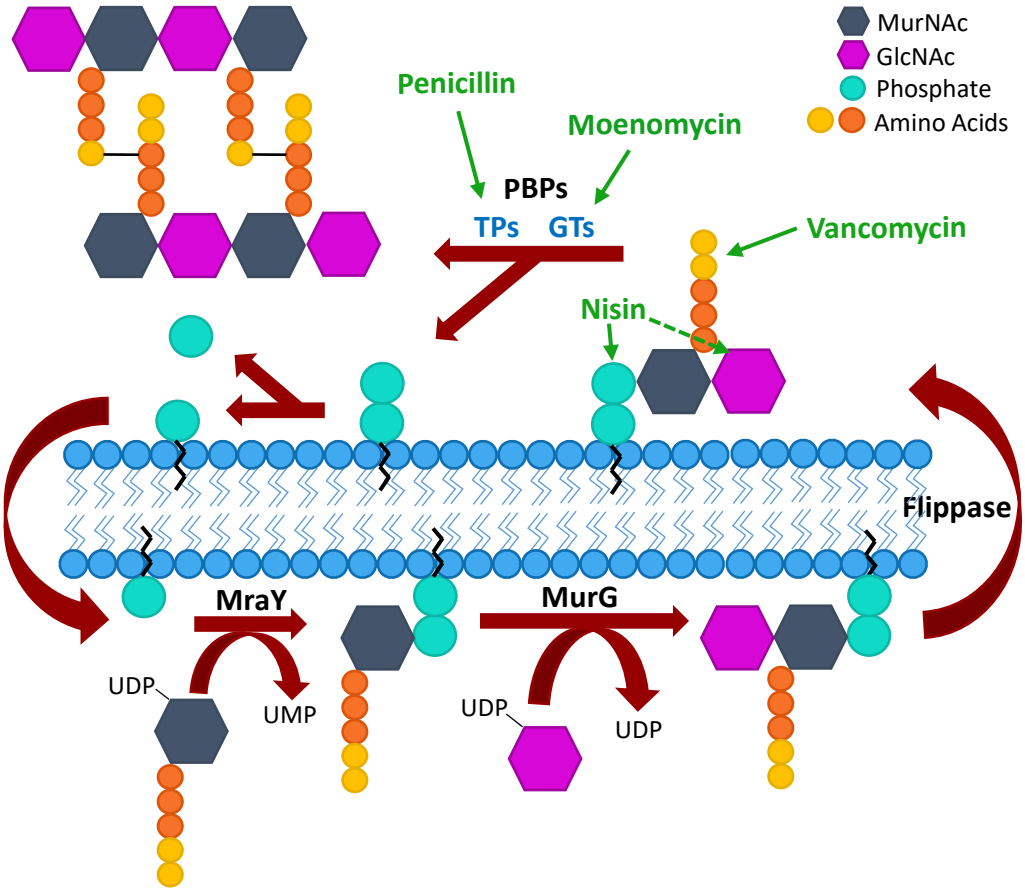

Figure 1.2.1: Membranes stages of peptidoglycan synthesis. Attachment of MurNAc-5pep-phosphate (dark blue) to undecaprenyl monophosphate (turquoise) by MraY, followed by the addition of GlcNAc (purple) by MurG. Lipid II is flipped to the outer leaflet and GlcNAc-MurNAc-5pep is incorporated into the growing peptidoglycan by glycosyltransferases (GTs) and peptide crosslinks formed by transpeptidases (TPs). Conserved residues are in orange and those in yellow are residues where mutation has been observed. The interaction sites of various antibiotics and nisin are indicated by the arrows (green).

Complete peptidoglycan synthesis includes cytoplasmic synthesis steps to produce the components required for the stages in figure 1.2.1. The late membrane stages of peptidoglycan synthesis involve the attachment of MurNAc-5Pep-phosphate to undecaprenyl monophosphate (11P) in the membrane by MraY, forming lipid I. MraY is a phospho-N-acetylmuramoyl-pentapeptide-transferase of 360 residues (39.9 kDa) with 10 transmembrane helices. [10] Lipid I then receives GlcNAc *via* a 4-1' glycosylation to form lipid II,

catalysed by MurG. This transferase is 355 residues (37.8 kDa) and contains two domains. The C-terminal domain is most likely involved in binding uridine diphosphate (UDP) -GlcNAc; the N-terminal domain is hypothesised to bind lipid I and interact with the membrane through a hydrophobic patch. This process occurs on the cytoplasmic leaflet of the bacterial membrane to enable the production of mature peptidoglycan, lipid II must be translocated to the outer leaflet. [11] [12] [13]

There are several possible flippases that could translocate lipid II. Three candidates have been experimentally evaluated and hypothesised to perform this function – MurJ, FtsW and Amj. It is unclear which membrane protein or proteins accomplish this transport. [9] [10]

After translocation to the outer leaflet of the membrane, GlcNAc-MurNAc-5Pep is cleaved from the pyrophosphate. The undecaprenyl pyrophosphate anchor is recycled and returned to the inner leaflet. The disaccharide of GlcNAc-MurNAc-5Pep is incorporated into the peptidoglycan by a glycosyltransferase (GT) and becomes available for transpeptidation. [16]

Transglycosylation is the formation of long polysaccharide strands from GlcNAc-MurNAc-5pep derived from lipid II. Transpeptidation is the subsequent formation of peptide crosslinks. These two processes are completed by penicillin-binding proteins (PBPs) that are divided into 3 classes – A, B and C. PBPs in class A and B are high molecular weight PBPs involved in late stage peptidoglycan synthesis whereas class C PBPs are low molecular weight and are involved in remodelling of the peptidoglycan. [17] The structure of class A PBPs includes a transpeptidase (TP) domain N terminally linked to a GT domain. The

structure of class B PBPs contain an N terminus made up of small domains, possibly involved in protein-protein interactions but more importantly provides a platform for the C terminal TP domain to reach the peptidoglycan. [18]

Different species of bacteria possess different PBPs. The PBPs present in each species are complementary and facilitate transglycosylation and transpeptidation. For example, PBP1a and PBP2 are found in *E. coli*, the former having a GT-TP role and the latter a cell elongation-specific TP role. In fact PBP2, a class B PBP, stimulates the GT activity of PBP1a, a class A PBP. [19] Peptidoglycan synthesis is reliant on PBP organisation, which in turn are themselves regulated. Lipoproteins LpoA and LpoB present in *E. coli* bind to the UB2H domains of PBP1a and PBP1b, respectively. This binding stimulates the activity of the PBPs. [20] Transpeptidation occurs in a two-step reaction: firstly, the terminal D-Ala residue is removed, then an amino group of a residue within a neighbouring pentapeptide forms a peptide bond with the new terminus. [21] During cell growth and division hydrolases cleave glycosidic bonds and amide crosslinks at various points within the peptide chains of the peptidoglycan to allow remodelling. Cleavage of glycosidic bonds is performed by *N*-acetylglucosaminidases, lysozymes and lytic transglycosylases. Amide cleavage is performed by various amidases, endopeptidases and carboxypeptidases. [22] Antibiotics, such as penicillin and carbapenams, are effective because of their structural similarity to the D-Ala-D-Ala motif present in the peptidoglycan. They bind and inhibit the transpeptidase activity of PBPs, preventing the completion of peptidoglycan maturation. [21] Bacteria have developed a mechanism of resistance to these β-lactam antibiotics in the form of β-lactamases. These

enzymes inhibit antibiotic action by hydrolysing compounds such as penicillin. It is possible to counter this by using the antibiotic in combination with β-lactamase inhibitors. The challenge with this arises from the diversity of β-lactamases present in varying bacteria, as inhibitors are specific to classes of these enzymes. [23]

Transglycosylases are another target for inhibition of the peptidoglycan synthesis pathway. Moenomycin A is effective against Gram-positive bacteria and has been used in animal feed stocks. This antibiotic mimics the structure of an undecaprenyl-containing intermediate, which allows competitive binding to the active sites of GTs. Moenomycin A has not been approved for use in humans due to its poor pharmacokinetic properties. [21] [24]

1.3 Lipid II: An AMP/Antibiotic target

Peptidoglycan intermediates such as lipid II are unique to bacteria and are excellent targets for drug development. Lipid II is currently targeted by naturally developed AMPs and antibiotics. It is an ideal, bacteria-specific target for potential AMPs that is explored extensively in this study. Lipid II is the mature peptidoglycan intermediate present in the outer leaflet of bacterial membranes prior to transglycosylation. It is comprised of N-acetylglucosamyl-N-acetylmuramyl pentapeptide (GlcNAc-MurNAc-5pep) and anchored to the membrane by a 1-pyrophosphoryl undecaprenyl (11PP) chain (Figure 1.3.1).

Lipid II delivers the monomeric block GlcNAc-MurNAc-5pep to the nascent peptidoglycan on the outer leaflet of the plasma membrane.

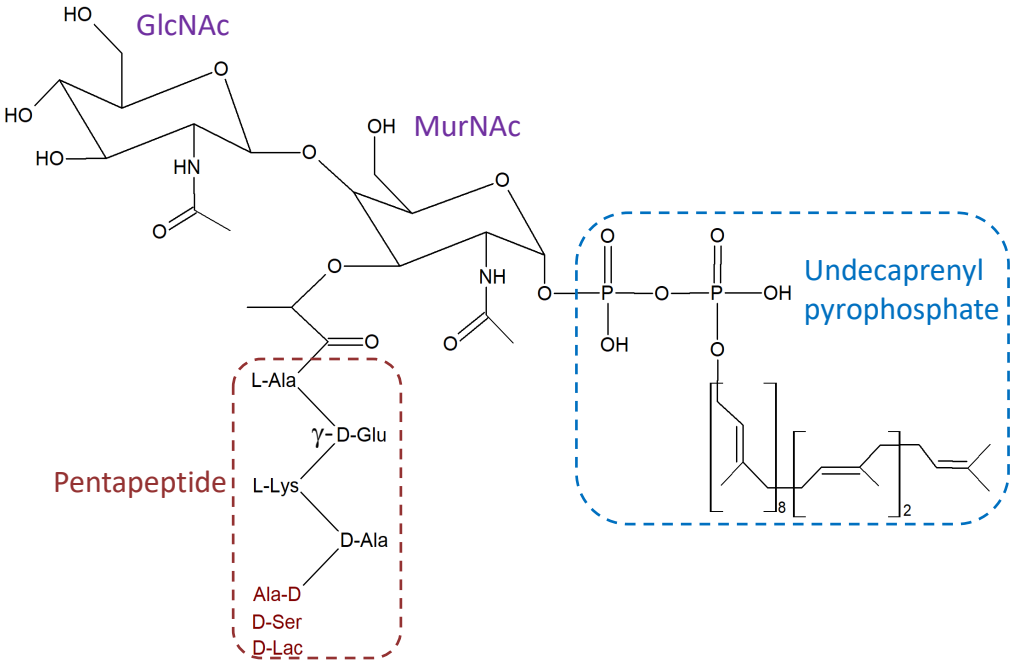

Figure 1.3.1: Structure of lipid II. Alternative position 5 residues for Gram-positive bacteria are in red.

The pentapeptide chain can be targeted by antibiotics such as vancomycin. Produced by the bacteria *Amycolatopis orientalis*, vancomycin and its semi-synthetic derivative telavancin bind the D-Ala-D-Ala motif in the pentapeptide and prevent transpeptidation. [25] [26] However, vancomycin-resistant enterococci contain the modified D-Ala-D-Lac pentapeptide chain, while vancomycin-resistant *S. aureus* possess the D-Ala-D-Ser motif (figure 1.3.1). The presence of D-Lac in position 5 prevents the formation of a hydrogen bond between vancomycin and D-Ala, that results in 1000 fold reduced antimicrobial activity. [27] The D-Ser substitution also results in decreased binding of vancomycin, conferring vancomycin resistance in these strains. [28]

Oritavancin is a glycopeptide antibiotic, similar to vancomycin, approved by the Food and Drug Administration (FDA) in 2014 to treat skin infections. It is effective against vancomycin-resistant *Enterococci* and methicillin-resistant *S. aureus* (MRSA). This antibiotic has multiple targets within lipid II that have yet to be fully characterised. Computational modelling suggests that oritavancin interacts with the pentaglycine chain present in *S. aureus*. [28]

Antibiotics are also known to target other domains of lipid II, besides the pentapeptide chain. Bacitracin is a 12-residue peptide containing one ring formed by an isopeptide bond. This antibiotic is produced by both *B. subtilis* and *B. licheniformis* and is effective against Gram-positive bacteria. It requires a divalent metal ion to bind specifically to the pyrophosphate domain of undecaprenyl pyrophosphate in a 1:1:1 stoichiometry (11PP:Zn:Bacitracin). [29] The mechanism of action is unclear as lysis of bacterial membranes is only observed when applying bacitracin at a concentration 2 orders of magnitude higher than the minimum inhibitory concentration (MIC). Bacitracin is used in combination with neomycin and polymyxin B as the topical antiseptic NEOSPORIN®, approved by the FDA in 1971. [30] This combination is an effective treatment as polymyxin B is active against Gram negative bacteria, such as *Pseudomonas aeruginosa* and *Klebsiella pneumoniae*. [31]

In 2015 the antibiotic teixobactin was discovered in soil samples. Produced by *Eleftheria terrae,* this monocyclic 11 residue peptide contains enduracididine, methylphenylalanine, four D form amino acids and, similarly to bacitracin, one ring. Although it was found to be mostly ineffective against Gram negative bacteria, activity was observed against Gram positive bacteria, such as *M.*

tuberculosis, *C. difficile*, *B. anthracis* and *S. aureus*. *In vitro*, *M. tuberculosis* and *S. aureus* did not develop resistance to teixobactin. Teixobactin inhibits peptidoglycan synthesis by binding to lipid I and II in a 2:1 stoichiometry and is able to bind in the presence of modified pentapeptide. [32] It interacts specifically with the pyrophosphate of 11PP but does not bind when a monophosphate is present. This peptide causes no haemolysis and is not toxic to eukaryotic cells. Due to the labour-intensive method of producing and purifying teixobactin, chemical synthesis has been considered. Enduracididine and D form residues are expensive components therefore modification has been attempted. Individual replacement of the former and the latter resulted in reduced activity. [33] [34]

Antimicrobials developed in nature that inhibit bacterial growth by interacting with lipid II include, copsin and nisin. Copsin, a 161 amino acid fungal defensin derived from the basidiomycete *Coprinopsis cinerea*, has also been shown to bind lipid II. The amino acid at position 3 in the pentapeptide chain is crucial for binding, however binding is not dependent on the identity of the amino acid present at this site. Copsin's activity against a vancomycin-resistant strain of *E. faecium*, which contains D-Lac in position 5, demonstrates that its binding is also independent of the amino acid in this position. [35]

1.4 Bacteriocins

The lantibiotic nisin also targets lipid II, primarily interacting with the pyrophosphate moiety. It also has a second binding site on MurNAc-5pep. [36] The mechanism of action of this antimicrobial is appealing as it is independent of the sequence of the pentapeptide chain. Nisin is the lead compound used in

this study and its mechanism of action is discussed in detail in section 3.9. Nisin falls into the type-A(I) bacteriocin class. Bacteriocins are broadly classified into three groups; class I, II and III. Class I is the lantibiotic containing class that is subdivided into type-A(I), A(II) and B. [16] [36]

1.4.1 Type-A(I) Lantibiotics

Type-A(I) includes bacteriocins below 5 kDa that contain (β-methyl)lanthionine rings. All compounds in this class contain a common identifying feature, a FNLD motif in the leader peptide between positions -15 and -20, which is essential for modification enzymes to bind, and a conserved proline at position -2. Peptides within type-A(I) are modified by two enzymes (LanA and B). These subclasses also vary in the method of removal of their leader peptides and export. Type-A(I) members have their leader peptide removed by a serine protease, LanP, and export is completed by LanT. Examples of antimicrobials belonging to type-A(I) includes nisin, subtilin, epidermin, gallidermin and mutacin 1140. [9] [37]

1.4.2 Type-A(II) Lantibiotics

Type-A(II) lantibiotics are similar to those in type-A(I). They are also less the 5 kDa and posttranslationally modified. Differences occur in the mechanism of modification. Leader sequences of the peptides in this class contain a GG or GA cleavage site, allowing processing by modification enzymes present in the producer strain and the production of the mature peptide. Members of this group are modified by one enzyme (LanM) to produce their mature forms. LanT has a dual function for peptides in this group, performing both cleavage and export. Lacticin 481, sublancin and plantaricin C belong to this class. [9]

1.4.3 Type B Lantibiotics

These are mainly small globular peptides that have their leader peptides removed during maturation, examples include cinnamycin and mersacidin. [38] The latter has 4 heterocyclic rings and some flexibility is conferred by its glycine rich region within ring 2. Rings 1 and 3/4 of mersacidin form intermolecular hydrogen bonds. This interaction and the hydrogen bonds within ring 2 give rise to its globular structure. [9] [37] Mersacidin also contains a cysteine positioned N-terminally to the Abu. Interaction of these residues forms ring A, a reversed methyl-lanthionine ring that is a contrast to those formed in type-A(I) peptides. [37]

1.5 Structure of Nisin

The lantibiotic nisin, also as known as food preservative E234, is used in foods such as dairy, meat and bakery products but also in beverages such as beer. The 34 residue mature cationic nisin contains 5 lanthionine rings, constructed by the formation of thioether bonds. Although 8 nisin variants exist, nisin A and Z were discovered in 1928 and 1991, respectively, and are the two most commonly investigated. [39] Nisin A possesses a histidine at position 27 whereas nisin Z contains asparagine. This change does not alter activity or prevent the formation of the lanthionine rings, all 5 (A-E) are still present (figure 1.5.1). [40] [41] [42]

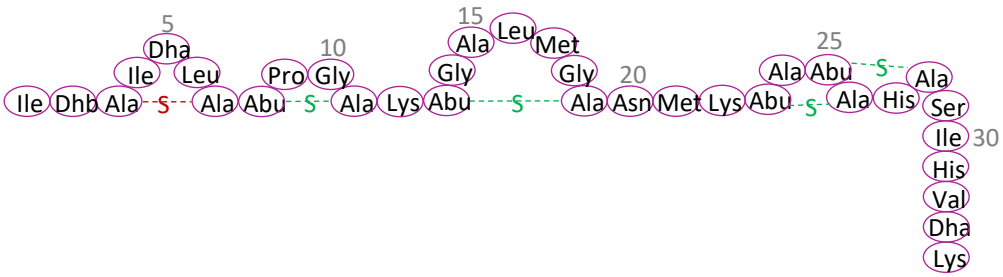

Figure 1.5.1: Structure of nisin A with residues in rings, including the lanthionine ring A (red) and β-methyl-lanthionine rings B-E (green). Posttranslationally modified residues; dehydrobutyrine (Dhb), dehydroalanine (Dha) and aminobutyric acid (Abu).

The structure of nisin includes a flexible region between rings C and D, formed by residues 20-22. This flexibility is also present in subtilin and may aid activity. [9] Nisin is effective in the treatment of gastrointestinal infections, such as *Clostridium difficile*-associated diarrhoea and is comparatively inert against common intestinal microbiota. However, nisin undergoes degradation by pancreatin in the upper gastrointestinal tract due to the double bond within the Dha residues that makes nisin more susceptible to proteolytic cleavage. [43] [44] [45]

1.6 Biosynthesis of Nisin

Mechanisms often found in nature are used to design novel systems. It is important to understand in detail the natural synthesis of AMPs as this can inform the design of a recombinant system for large-scale production.

Several strains of *L. lactis* produce all but one nisin variant, nisin U, which is produced by *Streptococcus* spp.. *L. lactis* possesses a gene cluster that codes for proteins involved in the modification, transportation and proteolytic cleavage of nisin. This cluster also encodes a sensory kinase, response regulator, lipoprotein and ABC exporter. [42]

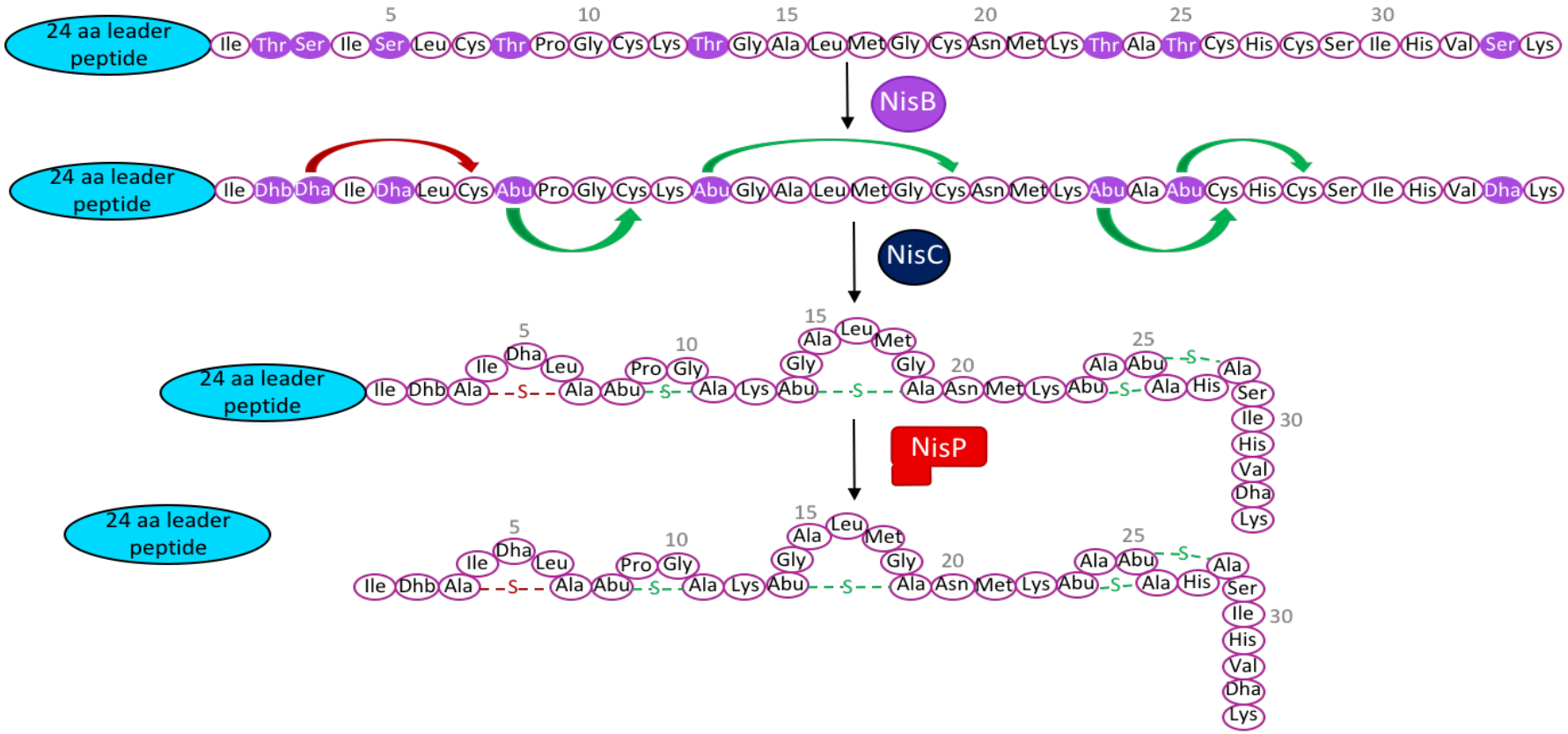

Figure 1.6.1: Biosynthesis of nisin. Amino acids in purple are those dehydrated by NisB. Lanthionine ring A (red) and β-methyl-lanthionine rings B-E (green) are formed by cyclase NisC. The leader peptide is cleaved by NisP.

After ribosomal synthesis, the 57 amino acid precursor of nisin is modified by dehydratase NisB and cyclase NisC (figure 1.6.1). NisB is a 993 amino acid, 117.5 kDa dehydratase with 1 helical transmembrane domain, anchored to the membrane. [10] [46] It dehydrates serine to form dehydroalanine (Dha) and threonine to form dehydrobutyrine (Dhb), the former being more difficult to dehydrate than the latter (figure 1.6.2).

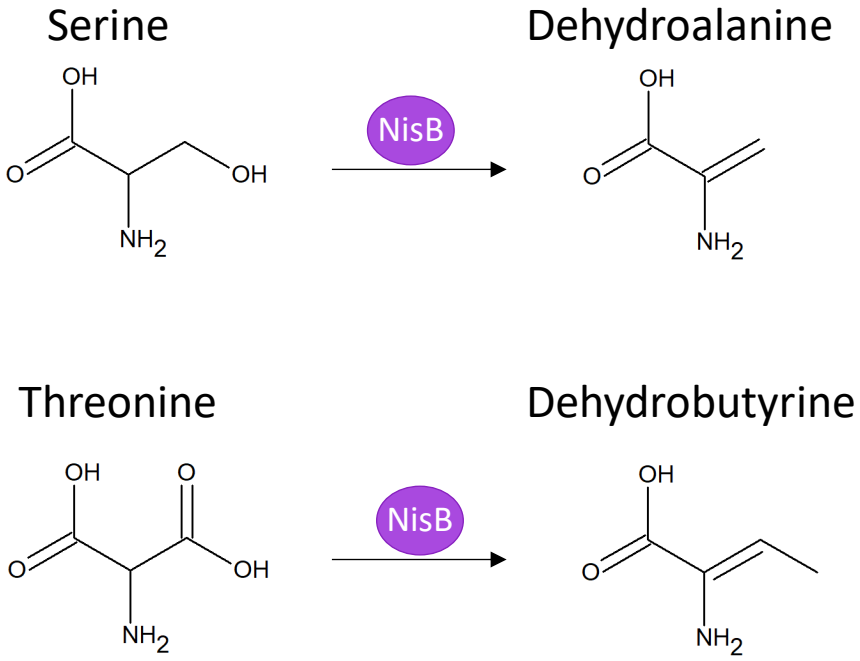

Figure 1.6.2: Dehydration of serine to form dehydroalanine and threonine to form dehydrobutyrine.

The cyclase NisC then catalyses regiospecific thioether rings between these dehydrated amino acids and cysteines. [47] This 418 residue enzyme is 47.9 kDa and capable of binding 1 zinc ion through its 3 zinc binding residues (Cys284, Cys 330 and His331), this is essential for function. [10] [48] This enzyme is enantioselective, to form these rings it is suggested that both D and L chiral residues must be present to prevent steric hindrance from inhibiting the process. [42] [47] [49] The distances between the leader peptide and potential

rings within nisin and both His212 and Asp141 of NisC are important for correct formation. When the DhaXXCys motif is present lanthionine ring formation is spontaneous; the presence of another amino acid (DhaXXXCys) impedes but does not prevent spontaneous formation. In contrast, β-methyl-lanthionine formation for the DhbXXCys motif is not spontaneous, therefore NisC is vital for the formation of rings A-E. NisB and NisC are nisin specific analogues of LanA and LanB, proteins present in other lantibiotic producing bacteria. [42] [47] [48] NisT is an ATP-binding transport protein of 600 amino acids (69.2 kDa) with 5 transmembrane helices. [10] NisT has relaxed substrate specificity and is essential for extracellular transport of this nisin precursor. A membrane complex containing 1x NisB, 2 x NisC and 2 x NisT act to dehydrate, cyclise and transport pre-nisin (figure 1.6.3). [9] [42] [50]

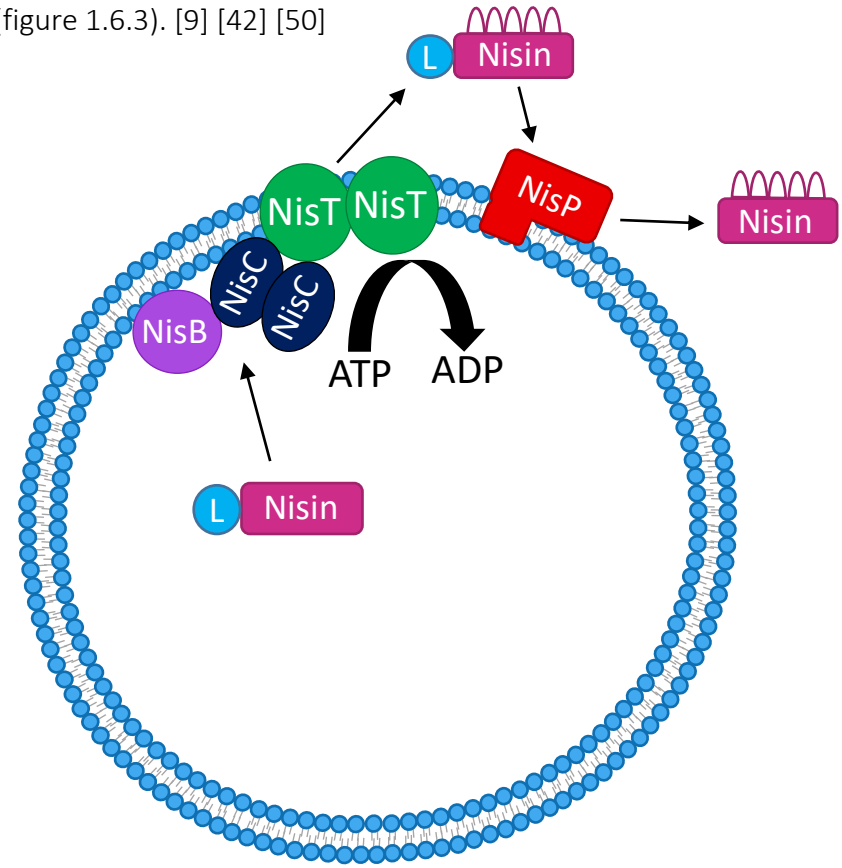

Figure 1.6.3: Overview of the proteins involved in nisin biosynthesis. Pre-nisin modified and transported by the membrane complex NisBC2T2. It is dehydrated by NisB, cyclised by NisC and transported by NisT. The leader peptide is the cleaved by NisP to produce mature nisin.

Once exported, the 57 amino acid pre-nisin is cleaved by a protease on the outer leaflet, NisP, which removes the leader peptide leaving the mature, activated nisin. NisP is a serine protease of 682 amino acids (74.8 kDa), 220 of which is a prosequence that is cleaved and acts as a secretion signal to direct NisP extracellularly. Cleavage of the leader peptide only occurs if rings A-E and the arginine at the end of leader sequence are present. [51] [52] [53]

1.7 Quorum Sensing

Nisin plays a role in quorum sensing, regulated by a two-component system that includes a sensory histidine kinase, NisK, and a response regulator, NisR. In the presence of mature nisin, the 51.3 kDa NisK undergoes autophosphorylation of the conserved His238 residue. It also contains an ATP binding domain and 2 transmembrane helices. This phosphoryl group is transferred to Asp53 of 26.7 kDa NisR, which initiates its binding to and activation of *nisA* and *nisF* (figure 1.7.1). NisR binds 2 sets of TCT repeats upstream of the *nisA* start site. *nisA* is involved in nisin biosynthesis and *nisF* in nisin self-immunity. [9] [10] [52]

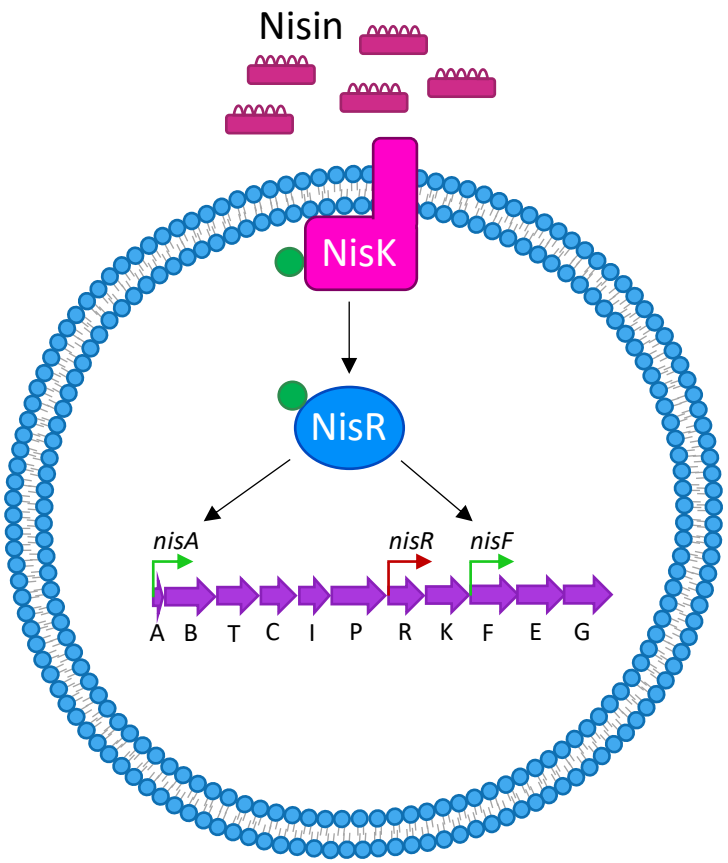

Figure 1.7.1: The two-component regulatory system involved in nisin biosynthesis and self-immunity. Nisin activates the autophosphorylation of NisK, which then phosphorylates NisR. This response regulator then activates nisA and nisF. The phosphoryl group is represented by the green circle.

Five nisin molecules are required to activate this two-component regulatory system. In contrast, *nisR* constitutively causes the expression of NisK and NisR in a nisin independent manner. Similar systems exist for the biosynthesis of other type-A(I) lantibiotics such as subtilin. The mechanism is slightly different for other class I lantibiotics that fall into the type-A(II) group such as sublancin, as described previously. [9] [42] [52]

1.8 Nisin Self-Immunity

Producer strains possess self-immunity, protecting them from the bacteriocin they synthesise. This is an important mechanism to consider in order to protect a strain selected for the production of a novel AMP.

L. lactis contains a two-tier self-protection mechanism including NisI and NisFEG. [54] The latter is an ABC efflux-type protein complex involved in ATP-dependent nisin export. Alkhatib *et al* found that ring E and the final 6 residues of nisin are required for NisFEG to bind. [55] NisE (27.6 kDa) and NisG (24.2 kDa) both contain 6 transmembrane helices that form the vital membrane transporter section of the complex. Two monomers of 24.7 kDa NisF are present in the complex, each containing an ATP binding domain (figure 1.8.1). [10] [56]

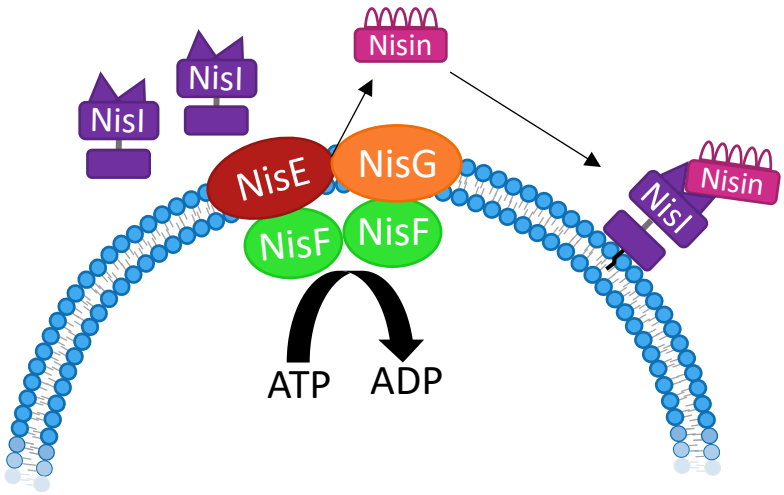

Figure 1.8.1: Nisin self-immunity mechanism, including efflux pump NisFEG and lipoprotein NisI that sequesters nisin.

NisI is a lipoprotein, which provides protection through two mechanisms. Approximately 70% of NisI undergoes cleavage of the first 19 residues, then the Cys at the new N-terminus is palmitoylated creating a membrane anchor. The remaining 30% undergoes cleavage but not lipidation, and is released extracellularly (figure 1.8.1). [57] [58] NMR data indicate that both of these forms contain an N and C terminal domain connected *via* a flexible linker. [59] The C terminal domain binds to nisin, sequestering it without causing modification or degradation. [58] Removing up to 22 residues from the C-

terminus of nisin reduces the action of NisI, causing immunity to fall to ~30%. [56] Membrane anchored NisI contains a sulphate ion in the linker region, which resembles the phosphate present in lipid II. As nisin interacts with the pyrophosphate of lipid II it is hypothesised that it interacts with NisI in a similar way. [60] The lipid-free form of NisI causes cells to cluster when the inhibitory concentration rises above 50% (IC_{50}), reducing the availability of lipid II. Once the concentration of nisin has dropped below IC_{50} the cells disperse again. [55] An orthologous mechanism, responsible for subtilin protection in *B. subtilis*, is encoded by spaI and spaFEG. This indicates that self-immunity is essential for lantibiotic producing bacteria and is widely present in nature. [61]

1.9 Antimicrobial Mechanism of Nisin

The efficiency and low toxicity of lantibiotics is underpinned by a target-selective mode of action. It has been shown that nisin and subtilin act through a lipid II and pyrophosphate-mediated mechanism. [16] *In silico* studies have revealed that there is a pattern to the phospholipids surrounding lipid II in bacterial membranes. [62] This arrangement appears to be present for longer than other mosaic patterns of the lipid bilayer resulting in a recognisable binding platform. Modelling studies of lipid II have also shown that the terminal tail groups repel each other, preventing the interaction of lipid II molecules. This may result in a similar environment for each molecule, providing an ideal site of interaction for nisin. [62]

Upon interaction with lipid II, the orientation of nisin alters from parallel to perpendicular to the membrane surface, which facilitates pore formation. [63] It has also been shown that the N-terminus and lanthionine rings A and B of nisin

bind to the pyrophosphate moiety within lipid II. [16] [64] Solution NMR data indicates that five hydrogen bonds form between the amides of rings A and B of nisin and the pyrophosphate of lipid II. [65] Extracellular pyrophosphates, such as those within lipid II, are an ideal target as they are found exclusively in the bacterial kingdom. Besides nisin, specific target recognition underpins the activity of other lantibiotics, such as mutacin 1140 and mersacidin. In fact rings A and B are conserved in other antimicrobials, such as subtilin, gallidermin, epidermin and plantaricin C indicating the importance of its role. [37]

The initial interaction of nisin and lipid II is likely to occur at a 1:1 molar ratio and may be important in cell wall inhibition. A higher order oligomeric complex is proposed to exist on membrane surfaces, in which C-terminal insertion of nisin into the membrane leads to self-association of binary complexes, possibly with the participation of another nisin molecule. It has been proposed that 8 nisin and 4 lipid II molecules participate in the formation of a membrane lytic complex with putative pore size around 2-2.5 nm (figure 1.9.1). The binding of nisin to pyrophosphate also prevent the recycling of 11PP. [37] [64] [66]

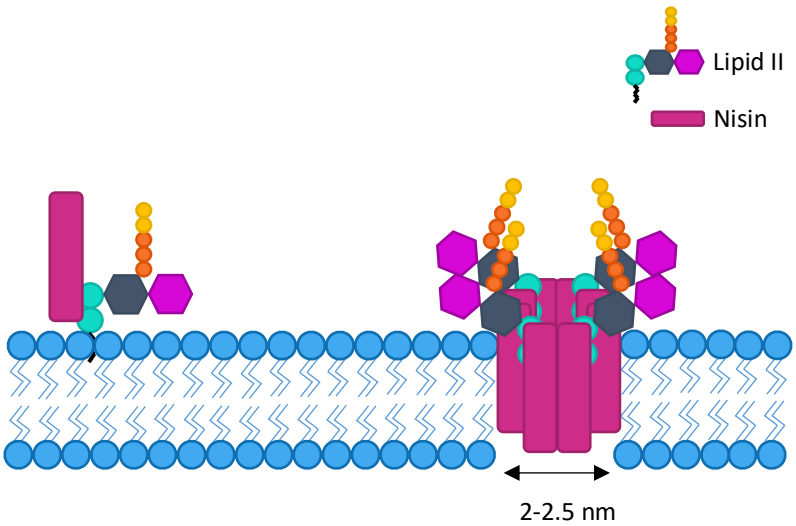

Figure 1.9.1: Mechanism of action of nisin. Nisin can sequester lipid II and prevent glycosylation (left) or 8 nisin and 4 lipid II molecules interact to form a 2-2.5 nm pore.

At the molecular level, besides the pyrophosphate, possible sites for nisin targeting on lipid II include the first isoprene and MurNAc. The role of the former has been assessed by replacement with a saturated chain, which did not affect the activity of nisin. [65]

Studies of membrane leakage in the presence of lipid I, lipid II or 11PP have shown that GlcNAc is not required for nisin-induced lysis, while MurNAc-5Pep is. An additional effect of nisin involves the sequestration of 11PP, which inhibits recycling of this vital molecule in the peptidoglycan biosynthetic pathway. [16]

1.10 Adaptations to Nisin

Gram-negative bacteria are inherently less susceptible to nisin due to their outer membrane and LPS layer. Some form of additional stress is required for nisin to have antimicrobial activity against Gram-negative bacteria, such as EDTA or temperature shock. These stresses are known to increase the permeability of the outer membrane, allowing nisin to reach lipid II within the inner membrane. Therefore the presence of an outer membrane, LPS layer and absence of stress provides decreased sensitivity to nisin. [67] [68]

In vitro studies have indicated various mechanisms utilised by Gram-positive bacteria to decrease their susceptibility to nisin. It has been found that the composition of the membrane of less sensitive bacteria was different from that of nisin sensitive strains. [69] Increasing the positive charge of the membrane by coupling D-alanine to lipids also excludes nisin. [70] Reducing the fluidity of the membrane by increasing the amount of long chain fatty acids has also been shown to increase tolerance. [71] The interaction of lipid II with PBPs prevents nisin from binding. The expression of PBP2A was discovered to be twice as high

in nisin resistant strains relative to nisin-sensitive *L. lactis*, therefore limiting the availability of lipid II. [70]

A dehydropeptide reductase found in *Bacillus sp.* causes enzymatic inactivation of nisin. Known as nisinase, this enzyme reduces the C-terminal dehyroalanyl-lysine of nisin to alanyl-lysine. [72]

A nisin resistance gene was discovered in a non-nisin producing *L. lactis* strain. It encodes a 35 kDa nisin resistance protein with serine-type peptidase activity. This enzyme proteolytically inactivates nisin by cleaving the 6 C-terminal residues, which decreases nisin's activity 100-fold. [73]

1.11 Antimicrobial Activity of Nisin

The antimicrobial activity of compounds is often measured as a MIC. This is the minimum concentration of compound required to prevent visible growth of a microorganism. [74] Nisin has MIC values as low as 0.07 μg/ml against *M. luteus* and 0.08 μg/ml against *L. lactis* MG 1614 (lacking the nisin production and associated resistance genes). [75] A higher MIC of 1.12 μg/ml has been reported against *S. aureus,* possibly resulting from the additional peptidoglycan cross-linking or lower availability of lipid II in this organism. The antimicrobial activity of nisin against *M. luteus* is mediated by the presence and ready availability of lipid II, if this is lower for *S. aureus*, due to increased crosslinking, nisin's mode of action will be limited. [37] [76]

1.12 Nisin Modifications

Many alterations of nisin have been previously attempted and characterised to determine which aspects of its structure are vital for its activity. For example, no

change in activity was observed when Dha33 and Lys34 were removed. Altering the charge of the peptide has also been attempted by swapping valine at position 32 for lysine and also for glutamic acid. The former caused little change but the latter resulted in a 4-fold decrease in activity against some species such as *Micrococcus flavus*. [77] [78]

Gallidermin and epidermin, produced by *Staphylococcus* spp., have a higher binding affinity for lipid II compared to nisin, this is thought to be due to the presence of a lysine residue at position 4. This increase in positive charge is suggested to result in an increased affinity for the phospholipids, indicating that this lysine is key for interaction. [37] [65] [79]

Field *et al* completed the systematic mutagenesis of nisin in the hopes of identifying specific mutations that will increase nisin's activity against a range of pathogens, including those most commonly found in food. In fact some mutations displayed increased activity against *L. monocytogenes*, such as M21V. [80] They also discovered that mutation of the serine residue at position 29 can lead to better activity against some Gram-positive bacteria than that of nisin. In particular the S29A mutant demonstrates increased activity against *L. monocytogenes*, *S. aureus* and *B. cereus*. [81] [82]

Breukink *et al* reported that the swapping the third thioether bond, which forms lanthionine ring C, with a disulphide bond resulted in severe reduction of activity. [83]

Nisin has been cleaved previously to produce nisin$^{1-28}$ using a nisin resistance protein found in *L. lactis*, which is involved in the proteolytic degradation of nisin. This analogue contained all 5 rings but displayed no pore formation and a

100-fold decrease in activity. It is thought that the formation of the negative charge at position 28, due to this cleavage, prevents the peptide from interacting with the negatively charged bacterial membrane. Whether this lack of interaction is due to the prevention of the analogue binding to lipid II is unknown. [73]

Nisin has also been cleaved to generate fragments of varying length. Nisin$^{1-20}$ contains ring A, B and C and displays activity 100-fold lower than that of nisin. Nisin$^{1-12}$, containing only rings A and B, is inactive. This smaller fragment is incapable of forming pores but has been shown to also prevent pore formation by competing with nisin to bind membranes. [84]

In 2014 Slootweg *et al* used chymotrypsin to cleave nisin to produce the ABC fragment, then click chemistry was utilised to add an azido functionalised dicarba-DE ring mimic. This chimera was shown to bind lipid II but no pore formation was observed. They believed this was caused by two possible changes, the first being the replacement of the sulphides of the DE ring mimic. The presence of a triazole moiety was the second change. It may be an insufficient substitution of the peptide bond between the ABC fragment and DE mimic, even though triazoles and peptide amide bonds have similar characteristics such as size, hydrogen bonding and rigidity. The ABC fragment was also shown to have a lower affinity for binding lipid II than native nisin. [85]

It has been demonstrated that nisin becomes inactive when the lanthionines are oxidised, converting the thioether linkages to sulphoxides. The histidine and methionine residues were also oxidised producing oxo-histidine and methionine sulphoxide, respectively. Even though this nisin analogue displayed no activity it

did not exhibit an antagonistic effect on the activity of unmodified nisin. It was hypothesised that the oxidation may interfere with either the ability of nisin to insert into bacterial membranes, to bind to lipid II or to prevent the assembly of larger complexes. It was demonstrated that both the interaction and the assembly of larger complexes were still evident, however binding to lipid II was prevented. Lantibiotics in the same class, such as gallidermin, have also shown loss of activity when thioether linkages are oxidised. [54]

During the study of the relationship between nisin's structure and action it was found that replacement of gly10 with a bulky residue interferes with the dehydration at position 8 and abolishes antimicrobial activity. [86]

Residue 1 seems to be crucial for activity within the class I type-A(I) lantibiotics. Deletion of tryptophan at position 1 within subtilin completely abolishes its activity. A 20-fold decrease in antimicrobial activity is also observed when subtilin is N-terminally succinylated. In contrast, loss of the final three C-terminal residues has no effect on activity. [87]

1.13 Magainin II

Numerous cationic antimicrobial peptides have been derived from various sources. For example, magainin II from the defence secretions of the African clawed frog (*Xenopus laevis*) and melittin from the venom of the honey bee (*Apis melifera*), have been identified and studied extensively. These non-lantibiotic peptides are 18-50 residues long and usually form amphiphilic α-helices upon binding to lipid membranes. [88] They disrupt bacterial membranes in a non-specific, charge-mediated way, the details of which depend on the target membrane lipid composition. A number of peptides exist within the magainin

family, including magainin I, II and PGLa. Magainin II is a 23 residue cationic peptide that adopts a rod-like alpha helical structure. It has been shown that magainin II does not form an α-helix in aqueous buffer, but only does so on addition of a hydrophobic solvent. [89] [90]

The magainin family, meaning 'shield' in Hebrew, was discovered by Michael Zasloff in 1987 when he was studying *Xenopus* ooctyes. He found that *X. laevis* remained infection free when employing sepsis-inducing operation techniques and concluded that these peptides are produced as part of its innate immune system. [91] Zasloff isolated the cDNA of magainin I and II and determined that they are produced from the same precursor. Peptides in the magainin family are synthesised and stored in the granular glands within the skin and gastric mucosal cells of the African clawed frog, with no significant production detected prior to metamorphosis. [92] [93] These antimicrobial peptides are released in response to stress or injury. Magainin II is active against various bacteria, broadening the ability of the organism to defend itself from infection. It also has activity against bacteria that have resistance to other antimicrobials, such as *Burkholderia cepacia*, which is associated with chronic opportunistic lung infections. [94] [95] Therapies have been developed involving magainin II analogues, such as a therapeutic cream Pexiganan, which is specific to bacterial membranes and active against a large range of bacteria. Even though this candidate to treat infected diabetic foot ulcers displayed promising results in phase II trials the FDA refused to approve it due to insufficient evidence of efficacy and comparatively high haemolytic activity. [94]

1.14 Antimicrobial Mechanism of Magainin II

Non-lantibiotic antimicrobials commonly kill bacteria by disrupting their plasma membranes without involving specific receptors. Often positively charged, such antimicrobial peptides rely on electrostatic interactions with negatively charged lipids in bacterial membranes and unlike lantibiotics, chirality of the AMP's residues is not a determinant of activity. Evidence suggests that magainin II causes the formation of toroidal pores, however visualisation has not been possible. Synergistic antimicrobial activity has been observed for magainin II and PGLa. [96] The former forms relatively stable pores slowly, whereas the latter creates unstable pores quickly. Combining the two leads to a 1:1 interaction, frequent stable pore formation and, therefore, increased antimicrobial activity (figure 1.14.1). [97]

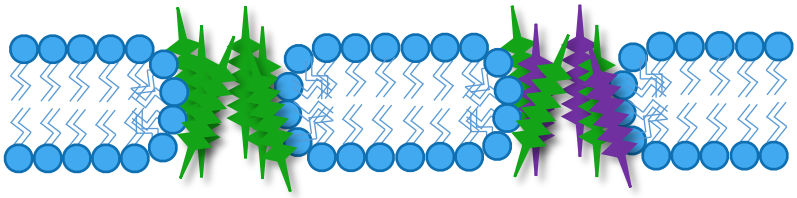

Figure 1.14.1: Toroidal pore formation by magainin II (green) and magainin II combined with PGLa (purple).

While these peptides may have good antimicrobial activity the selectivity for bacterial vs. eukaryotic cells is poor. The low haemolytic activity of magainin II can be understood considering its stronger interactions with negative phospholipids such as phosphatidyl-glycerol, -serine and cardiolipin compared to the weaker interactions it has with the zwitterionic phospholipids like phosphatidylcholine and the sphingolipid sphingomyelin. This is advantageous to eukaryotes, as their cell membranes contain more of the latter and bacterial membranes the former. [98] [99] There is also a large, inside-negative

transmembrane potential present in bacterial cells, further attracting magainin II. Magainin-induced lysis can be inhibited, to a certain degree, by cholesterol. This inhibition is thought to be the result of hydrogen bonding between the glu19 residue in magainin II and cholesterol, therefore preventing pore formation. Cholesterol is found in eukaryotic membranes but not in bacterial membranes, making the latter vulnerable to magainin-induced lysis. The role of membrane receptors in antimicrobial action has been assessed by comparing the ability of magainin II and nisin to disrupt model membranes with or without lipid II. A 100-fold increase in leakage was observed for nisin, yet no leakage was seen on addition of magainin II when lipid II was present. [83] [99] [100]

Melittin, a haemolytic toxin from the venom of the honey bee *Apis mellifera*, acts in a similar way to magainin II but is significantly more haemolytic due its ability to interact with various phospholipids causing a lack of cell selectivity. [101]

1.15 Activity of Magainin II

At a concentration of 0.98 µg/ml of magainin II applied to *M. flavus,* cell survival was still observed. This is significantly higher than the 0.011 µg/ml MIC value calculated for nisin against *M. flavus*. Magainin II has MIC values of 64 µg/ml against 90% of 10 strains of both methicillin-sensitive and methicillin-resistant *S. aureus*. The peptide has also shown MIC values of 2 µg/ml against 90% of 30 strains of *E. coli*, displaying clear activity against Gram-negative bacteria. [102] [103]

1.16 Modifications of Magainin II

The degradation of magainin II is caused by an endopeptidase, which is present in *X. laevis* and proteolytically cleaves magainin II between two lysine residues at positions 10 and 11. When treated with leaf extracts, it was found that the peptide was cleaved between residues 7 and 8 and also at the C-terminus. To produce an antimicrobial peptide that could function in plants, without being cleaved, magainin II was altered at these sites. An analogue was produced with arginine at position 7, glutamic acid at positon 8 and proline at position 23. This new peptide retained its activity and displayed resistance to cleavage. [98] [104] [105]

Magainin II can induce lysis of eukaryotic cells, despite the protective effect displayed by cholesterol and magainin II's preferential binding of negative phospholipids present in bacterial cell membranes. This occurs by binding to the negatively charged gangliosides, which act as magainin II receptors present on mammalian cells. Gangliosides contain sugar regions comprised of negatively charged sialic acid residues. It was found that an increase in these residues resulted in an increased affinity of magainin II for these gangliosides. [106]

The structure of magainin II has been altered in different ways to determine which residues are necessary for interaction and activity. Deletion of the first 3 residues has been shown to have little to no effect on the activity of the peptide. However, deletion of the lysine at position 4 results in a substantial decline in activity. Subsequent removal of residues indicated that activity was lost once the first 7 N-terminal residues were detached. By contrast, removal of any C-terminal residues abolishes activity. This is thought to be due to the reduced size

of the C-terminal end of the peptide, preventing insertion into bacterial membranes and pore formation. However the deletion could also affect the hydrophobicity, flexibility and charge of the peptide. [89] [98]

Magainin II mutants S8A and G13A lead to increased α-helical content. An increase in antimicrobial activity was also observed but with concomitant increase in haemolytic activity. It was concluded that substituting the Gly residues was key to increased activity and that subsequent substitution of Ser had no further effect on activity but did increase haemolysis. Acetylation of the N-terminus stabilises the α-helix, but at the cost of decreased activity. It was proposed that altering this free amino group resulted in a more negative overall charge, which most likely diminished magainin's ability to interact with target membranes and further indicating that activity is likely to be charge-mediated. Further studies indicated that the α-helical structure at the N-terminus was required for activity. [89] [107]

Another study involving magainin II analogues showed that C-terminal amides are more active than acids. It was also observed that the deletion of A15 or G18 improved activity but also caused an increase in haemolysis. In contrast, deletion of E19 improved activity without increasing haemolysis. This study also confirmed that deletion of residues 1-14 resulted in loss of activity. A separate study hypothesised that addition of lysine would increase the positive charge of magainin II and enhance its interaction with bacterial membranes. However, the addition of 10 lysine residues to the N-terminal end of magainin II, resulted in decreased antimicrobial activity. [98] [108]

1.17 Assessing Haemolytic Potential

Many non-lantibiotic peptides cause haemolysis due to their lack of specificity. By contrast, the receptor-specific antimicrobial action of nisin is accompanied by negligible haemolytic activity, which has secured its worldwide acceptance as a safe and efficient food additive. In addition, intestinal microflora is comparatively insensitive to nisin, which resonates with current recognition of the importance of unperturbed gut microbiome in human health.

Pandinin 2 is an α-helical 24 residue peptide found in African scorpion venom. It is a candidate for treating *Mycobacterium tuberculosis* however it is also highly haemolytic. It was hypothesised that P14 is responsible for haemolytic activity. However, P14G mutant showed no change in haemolytic activity. Two glycine residues were introduced either side of the proline and in response a reduction in both antimicrobial activity and haemolysis was observed. The reduction in both hydrophobicity and tendency to form an α-helix is believed to be the cause of this. [109]

Altering proline residues in the middle of α-helical antimicrobials has been investigated with the aim of removing the helical kink. P14 within melittin was replaced by alanine. This analogue displayed increased haemolytic and reduced antimicrobial activity. It is believed that the proline residue is a vital component in backbone flexibility allowing peptides to insert more easily into membranes and form stable pores. [110]

1.18 Synthetic Antimicrobials

Synthesis of novel antimicrobials is an interesting approach to solving the current resistance crisis. Often these compounds mimic the structure of existing antimicrobial peptides but do not contain traditional peptide structures. Many attempts have been made to chemically synthesise alternative antimicrobials. For example, peptidomimetics are a class of synthetic antimicrobials that often contain β-peptides and peptoids. [111] Nanoparticles have great potential as antimicrobial compounds due to their ability to cross the blood brain barrier. They contain cationic and hydrophobic properties to increase bacterial membrane interaction and penetration. [112] Synthetic polymers such as polymethacrylate esters also display antimicrobial activity. [113]

1.19 Membrane Acting Synthetic Antimicrobial Peptides

Previous synthetic antimicrobials often mimic the structure or sequence of existing antimicrobials. Liu *et al* evaluated the properties of a set of peptides containing arginine and tryptophan only, with up to 5 repeats. These peptides were disordered in solution but acquired structure upon interaction with phospholipids. They also found that as the number RW repeats increased, so did the antimicrobial and haemolytic activity. [114]

Isaksson *et al* also created a series of RW containing peptides with varying L and D form residues. The all L form version (LTX 109) interacts with negatively charged head groups of phospholipids to disrupt bacterial membranes. It displays activity against *S. aureus*, *E. coli*, and *P. aeruginosa*. LTX 109 is non-haemolytic at its bactericidal concentration, therefore clinical trials were

completed to determine its efficacy. This peptide was evaluated as a nasal decolonisation compound and was found to significantly reduce the bacterial load of MRSA while having no toxic effects. [115]

It was hypothesised that for an AMP to cross the bacterial membrane a helical structure could be vital. Wang *et al* designed simple peptides to generate a centrosymmetrical helical series, using the template $(y+hhh+y)_n$ – where h is a hydrophobic residue, + is a cationic residue and y is either a glycine or hydrophobic residue. They found that a glycine rich peptide with 3 repeats displayed activity against Gram negative bacteria whilst being non-haemolytic, even though the helical structure of this peptide was poor. Replacing the glycine residues with alanine resulted in a more stable helical conformation that displayed a broad spectrum of antimicrobial activity but was also haemolytic. [116]

To prevent susceptibility to proteolytic degradation, dendritic AMPs have been designed. Bruschi *et al* created a tetramer comprised of 10 amino acid monomers, linked by a lysine core with an amino valeric acid chain (SB041). Although limited antimicrobial activity against Gram-positive bacteria was demonstrated, its activity against Gram-negative bacteria was comparable to that of polymyxin B. Strong association with LPS was observed but this dendritic peptide did not block biological activity of the LPS. [117]

Daptomycin is a calcium dependent lipopeptide active against *S. aureus*. The negative residues present in daptomycin interact with Ca^{2+} reducing the net negative charge. This promotes daptomycin's interaction with and deep insertion into bacterial membranes. Makovitzki *et al* introduced aliphatic chains

of varying length to 4 residue peptides. These peptides were comprised of KXXK, where X represents L, A, G, K or E. The most potent antimicrobial was C16-KGG(K-d) and no haemolytic activity was discovered for any of the lipopeptides. They found no correlation between hydrophobicity or aliphatic chain length and antimicrobial activity. The presence of D form residues also provides some protection from degradation. These lipopeptide constructs were simple and promising. Resistance to daptomycin was observed only a year after it was approved by the FDA. Multiple resistance mechanisms have been elucidated, which vary between species of bacteria. [118] [119]

1.20 Aims

The aim of this project is to engineer chimeric antimicrobials with a lipid II dependent mode of action. We design chimeric peptides containing a novel engineered N-terminal target engaging domain, based on nisin 1-12, and magainin II as the C-terminal domain. Magainin II was selected for its pore forming ability and low haemolysis. The targeting domain is included to reduce haemolysis further by providing specific receptor-mediated action. These peptides include four cysteine residues to form two disulphide bridges that mimic nisin rings A and B. The two Cys residues involved in ring A formation are both present in L or D chiral forms, following the recommendations in Turpin *et al* 2010. [120] We will prepare, purify and characterise the properties of these novel peptides. The following aims will be completed:

- High-pressure liquid chromatography (HPLC) and mass spectrometry (MS) will be used to purify and confirm the forms of peptides.

- Molecular dynamic (MD) simulations will be used to monitor the distances between Cys residues, to predict ring formation.
- Antimicrobials activity will be assessed using agar diffusion and broth dilution activity assays.
- Haemolytic assays will be completed to evaluate toxicity.
- Interaction of the peptides with lipid II will be studied using small-angle X-ray scattering (SAXS), circular dichroism (CD) and leakage assays.
- Fluorescence microscopy will investigate the distribution of fluorescently tagged peptides across the membranes of *B. subtilis*.

The resulting properties of each design will be assessed and considered when either redesign or the development of further chimeras occurs. Once a suitable candidate has been selected a recombinant system will be designed to produce this novel AMP on an industrial scale.

Chapter 2 Materials and Methods

2.1 Peptide Synthesis

Peptides were synthesised to order by Genosphere and PGLa was purchased from Merck. Chirally-selective candidate peptides were prepared by solid phase synthesis. All N12(L/D) peptides mimic the N-terminal portion of nisin with thioether links substituted for disulphide bridges, which can be used to create macrocyclic peptides or reduced to generate linear forms. The chimeric peptides are comprised of the N12(L/D) targeting motif and a pore forming AMP, of either magainin II or melittin. See table 2.1.1 for all peptides. [120]

Table 2.1: Peptide names and sequences. PGLa was purchased from Merck and the remaining peptides were synthesised by Genosphere.

Peptide Name	Peptide Sequence
N12L	IACIA LCCPG CK
N12D	IA(d-C)IA L(d-C)CPG CK
N12LM2	IACIA LCCPG CKGIG FLHSA KKFGK AFVGE IMNS
N12DM2	IA(d-C)IA L(d-C)CPG CKGIG FLHSA KKFGK AFVGE IMNS
N12D-TAM	IA(d-C)IA L(d-C)CPG CK(K-5tamra)
N12L-TAM	IACIA LCCPG CK(K-5tamra)
Magainin II	GIGKF LHSAK KFGKA FVGEI MNS
Melittin	GIGAV LKVLT TGLPA LISWI KRKRQ Q
N12LMEL	IACIA LCCPG CKGIG AVLKV LTTGL PALIS WIKRK RQQ
PGLa	GMASK AGAIA GKIAK VALKA L

2.2 Preparation of Cyclic and Linear Forms

To evaluate the necessity of ring formation for activity and target engagement, protocols were designed to produce and separate the linear and cyclic forms.

2.2.1 Preparation of Linear N12(L/D) and N12(L/D)M2

Unpurified N12(L/D) and N12(L/D)M2 peptides (1 mg/ml) were dissolved in HPLC grade water. To reduce any disulphide bonds DTT (0.1 M) was added and

stirred for 30 minutes at room temperature. They were then centrifugated at 550 *g* for 15 minutes at room temperature and the supernatants isolated. RP HPLC and mass spectrometry were completed as described in method 3.3. HPLC fractions containing peptide were rotavapped to remove acetonitrile, lyophilised and stored at -20°C.

2.2.2 Preparation of Cyclic N12(L/D) and N12(L/D)M2

To cyclise N12(L/D)M2, the peptides were dissolved in HPLC grade water (1 mg/ml) and mixed for 20 minutes at room temperature. The pH was raised to 13 with NaOH (0.1M) and the solution stirred for 2 hours. The pH was then lowered to 7 with HCl (0.1 M) and stirred for 20 minutes at room temperature.

To cyclise N12(L/D), the peptides were dissolved in acetonitrile (25% (v/v)) with TFA (0.1% (v/v)) (1 mg/ml) and stirred for 20 minutes at room temperature. The solution was dripped into stirring Tris HCl (0.1 M pH 7) with DMSO solution (20% (v/v)) overnight using a P1 pump at room temperature.

All solutions were centrifugated at 550 *g* for 15 minutes at room temperature and the supernatants isolated. RP HPLC and mass spectrometry were completed as described in methods 3.3 and 3.4. HPLC fractions containing peptide were rotavapped to remove acetonitrile, lyophilised and stored at -20 °C.

2.3 Purification by Reverse Phase HPLC (RP-HPLC)

To separate out the various forms of the peptides RP-HPLC using a Phenomenex Gemini 250 x 10mm C18 column was used in the final purification step, with solvent A (TFA (0.1% (v/v)) in water) and solvent B (TFA (0.1% (v/v)) in acetonitrile (70% (v/v))). Injections were 3 x 2 ml using a 2ml loop for each run.

Elution was with a linear gradient from 5% to 100% of solution B over 30 minutes, measured using a UV-vis detector at 220 nm.

2.4 Mass Spectrometry

To determine the forms of the peptides present in HPLC fraction mass spectrometry (MALDI/TOF) was used. Loss of two hydrogens indicates formation of one disulphide bridge to give the semi-cyclic form. Loss of four hydrogens indicates formation of two disulphide bridges to give the cyclic form.

2.4.1 MALDI/TOF Mass Spectrometry

The sample and matrix were applied to the MALDI plate in a 1:1 ratio (matrix consisting of 5-10 mg α-cyano-4 hydroxycinnamic acid dissolved in 100 µl of acetonitrile (50% (v/v)) with TFA (0.1% (v/v))). The instrument was calibrated using using polyethylene glycol (PEG). The positive reflectron mode was utilised to detect the overall positively charged novel peptides.

2.4.2 Electrospray Ionisation Mass Spectrometry

This alternative mass spectrometry method was also used, as it provides a greater degree of accuracy for lower masses. Flow injection with methanol (70% (v/v)) is used to introduce 1 µl of each sample (~0.01 mg/ml) into the Bruker micrOTOF II where it is analysed in positive ionisation mode. Before each sample was assessed 1 µl sodium formate (2 mM) in 50:50:0.1 Methanol:Water:Formic acid solution was flowed to the source. This is used to calibrate the machine.

2.5 Purification of Nisin from Nisaplin®

Nisin A was extracted from Nisaplin®, provided by DuPont™, was dissolved in 500 ml of hydrochloric acid (10 mM). The suspension was centrifugated at 4500

g for 30 minutes at 12 °C. The supernatant was collected, ammonium sulphate crystals (0.5 M) were added and the pH adjusted to 4.0 by the addition of NaOH (1 M). A column containing Toyopearl-Butyl 650M resin was equilibrated with $(NH_4)_2SO_4$ (0.5 M) and then the supernatant was loaded on to the column which was prequilibrated in $(NH_4)_2SO_4$ (0.5 M). Deionised water was then added until A220 < 0.5 was reached, then HCl (10 mM) was applied and the nisin eluted. To separate nisin and the leader peptide the collected fraction was loaded onto a Phenomenex Gemini 250 x 10mm C18 column and RP-HPLC used with solvent A (TFA (0.1 % (v/v)) in water) and solvent B (TFA (0.1 % (v/v)) in acetonitrile (70% (v/v)). Elution was with a linear gradient from 5% to 100% of B over 30 minutes. Mass spectrometry (MALDI/TOF) was employed to detect the presence of nisin in the fractions.

2.6 Quantification by Bicinchoninic Acid (BCA) Protein Assay

To determine accurate concentrations of the peptides in solution BCA protein assays were completed as specified by Thermo Scientific using the Pierce™ BCA Protein Assay Kit. A flat-bottomed 96 well microtiter plate was used with 200 µl of working reagent and 25 µl of sample or standard per well. The plates were shaking incubated at 37 °C for 30 minutes then the absorbance was measured at 562 nm. All standards and samples were assayed in duplicate.

2.7 Microbiology

2.7.1 Sterilisation

All bacteriological protocols were performed in sterile conditions. Pipette tips, glassware, growth buffers and media were autoclaved for 15 minutes at 121 °C.

Any heat-sensitive reagents were sterilised with sterile 0.22 µm syringe filters (Sartorius stedim). Disposables such as 30 ml universals, petri dishes and syringes were supplied sterile. Lab benches were cleaned with Chemgene and wiped down with 70 % (v/v) ethanol before cellular work and growths were started. Cell work and growths were carried out in a laminar flow hood or in the presence of a gas flame. All glycerol bacterial stocks were kept at -80 °C.

2.7.2 Culturing *M. luteus*

M. luteus was cultivated by inoculating a tryptic soy agar plate with glucose (1 % (w/v)) with a loop scraping from a glycerol stock and incubating at 30 °C for 48 hours. A single colony was used to inoculate 10 ml of tryptic soy broth with glucose (1 % (w/v)). This culture was incubated at 30 °C for 24 hours at 200 rpm before 250 µl was transferred to inoculate 10 ml of fresh media and incubated for a further 24 hours under the same conditions to produce a culture containing ~10^8 colony forming units (CFU)/ml. The OD_{620} was measured in triplicate and CFU/ml calculated using a previously determined OD_{620} vs CFU/ml relationship (figure 7.2.1).

2.7.3 Agar Diffusion Activity Assay

The culture from 2.7.2 was appropriately diluted then 200 µl of *M. luteus* was spread onto tryptic soy agar (1% (w/v) plates containing glucose (1%, (w/v)) to produce a final concentration of 10^5 CFU/ml. After drying, 3 mm diameter wells were cut, 5 into each plate and the plates were dried again. The wells were loaded with 9 µl of varying concentrations of antimicrobial compounds and HPLC water as the control. Plates were refrigerated at 4°C for 24 hours then

incubated at 30°C for 48 hours and then the diameters of the zones of inhibition were recorded. [121]

2.7.3.1 Linear Regression Analysis

Both the diameters (d) and diameters squared (d^2) of 4 or 5 observed zones of inhibition were plotted against the natural logarithm of the peptide concentration in µg/ml for each repeat. Trend lines were plotted, followed by the calculation of the equation of the lines and the X intercepts. The logarithm was removed using the exponential function, this gives the MIC values in µg/ml. Each MIC value was divided by the molecular weight of the peptide and multiplied by 1000. The repeats for each peptide were then averaged to give MICs in µM. The R^2 values were also calculated for each trend line and averaged. Whichever measurement, d or d^2, has a corresponding R^2 value closer to 1 best represent the data. [121]

2.7.4 Spot On Agar Activity Assay

To evaluate the ability of the peptides to diffuse through agar, spot on agar activity assays were completed. *M. luteus* from 2.7.2 was appropriately diluted and added to warm tryptic soy agar (1.5 % (w/v)) containing glucose (1 % (w/v)) to produce a final concentration of 10^5 CFU/ml. Plates were poured and dried for 30 minutes. Varying concentrations of antimicrobial compounds (5 µl) or HPLC water as the control (5 µl) were spotted onto the agar. Plates were kept at 4°C for 24 hours, then 30°C for 48 hours. Diameters of the zones of inhibition were recorded.

2.7.5 Broth Dilution Assay

To evaluate the activity of linear and cyclic N12L against *Listeria* and *Staphylococcus*, broth dilution assays were completed at DuPont Global Food and Research Center in Brabrand, Denmark.

2.7.5.1 Preparation of Bacterial Cultures

Before each experiment, stock cultures were propagated through two consecutive growth cycles in suitable media and temperature. The overnight cultures were diluted 10-fold in saline solution to obtain working cultures. To produce vegetative cells of the bacterial strains, they were inoculated into tryptic soy broth and incubated at 30°C, pH 6 for 24 hours.

2.7.5.2 Determination of Minimum Inhibition Concentration (MIC)

The MIC assay was performed using a pipetting station (BioTek Precision: Microplate sample processor Precision™ 2000) and a semi-automated robotic assessment system, consisting of an optimized robotic chemical analysis (ORCA) robotic arm on a 3-meter track (Beckman Coulter), a Synergy HT spectrophotometer (Biotek), a Cytomat 6001 incubator (Thermo) and a Cytomat 2C incubator (Thermo). System preparation and data analysis were carried out with Microsoft Excel worksheet templates, supported by in-house written visual basic for applications (VBA) code.

Each well of a 96-well plate was then inoculated with 5 µL of an overnight culture which was 10-fold diluted in Ringer solution (Merck catalogue no. 1.15525.0001). In all experiments, controls with media only and antimicrobial in media only were included. In addition, a growth control without antimicrobial was included for each strain. The analysis was run as a kinetic assay, which

means that at time zero, after adding the antimicrobial the optical density (OD) of the bacterial culture was measured at 620 nm and then again throughout the 24-hour incubation time. The increase in OD after incubation was compared to the growth control to determine whether the tested substance had a bacteriostatic (MIC) or no effect. MIC_{90} is given as complete inhibition, meaning more than 90% inhibition compared to the growth control (positive control), which is the standard in literature. All data are presented as the mean values of duplicates or triplicates for each microorganism.

2.7.6 Haemolytic Assay

To a microtiter plate, 15 µl of peptide was added to the first well of each row, and 7.5 µl of filter sterilised phosphate-buffered saline (PBS) (NaCl (137 mM), KCl (2.7 mM), Na_2HPO_4 (10 mM), KH_2PO_4 (18 mM), pH 7.6) to all other wells. Each peptide was serially diluted by transferring 7.5 µl from the first row to the second row and mixed before repeating this for all rows. To each well 15 µl defibrinated sheep's blood (10% (v/v)) in PBS was added. The plates were incubated for 1 hour at 30°C shaking. The contents of each well were centrifugated for 10 minutes at 1000 *g*. Supernatants were sampled and OD_{540} measured using the DeNovix DS-11 Spectrophotometer. Peptides were assayed in duplicate and ODs measured in triplicate. Distilled water was used to generate 100% lysis values and PBS only included as the control.

2.8 Lipid II Synthesis

The synthesis of lipid II requires undecaprenyl monophosphate, UDP-MurNAc-pentapeptide and UDP-GluNAc. The former was purchased from LGC standards and the latter two components were isolated from *B. cereus*. The enzymatic

machinery is also required for synthesis, therefore *M. flavus* membranes were also isolated and included.

2.8.1 Preparation of the UDP-MurNAc-pentapeptide and UDP-GlucNAc

To obtain UDP-MurNAc-pentapeptide and UDP-GluNAc, 10 ml Difco 3 medium was inoculated with 50 µL of *B. cereus* glycerol stock and incubated at 30 °C, 200 rpm overnight. 4 x 500 ml Difco 3 medium were inoculated with 4 x 2 ml of the preculture and incubated at 30 °C, 200 rpm up to an OD_{620} between 0.7 and 1.0. To inhibit protein synthesis, the bacteriostatic chloramphenicol (130 mg/L) in ethanol was added and incubated for 15 minutes at 30 °C. To prevent formation of mature peptidoglycan, vancomycin (18 mg/L) in water was also added and incubated for 45 minutes at 30 °C. The cultures were centrifugated at 4500 *g*, 4 °C for 20 minutes. The cells were washed once with distilled water then suspended in 10 ml distilled water per litre of cells. Two volumes of added water (20 ml per litre of cells) was boiled, the cells added drop wise and then boiled for 15 minutes. The suspension was centrifugated at 550 *g*, 4 °C for 15 minutes in precooled SS34 tubes. The supernatant was collected and lyophilised.

2.8.2 Preparation of *Micrococcus flavus* Membrane Extracts

To achieve isolation of the membranes 40 ml TSB medium was inoculated with 200 µl *M. flavus* and incubated at 30°C, 200 rpm for 8 hours. To inoculate 2 L (4 x 500 ml) of TSB medium, 8 ml (4 x 2 ml) of the previous culture was used and incubated at 30 °C, 200 rpm overnight (final OD = 2-3). The cultures were centrifugated at 4500 *g*, 4 °C for 30 minutes and the pellets suspended in Tris-HCl ((50 mM pH 7.5) 67 ml buffer per litre culture). They were then centrifugated at 8000 *g*, 4 °C for 15 minutes. Tris-HCl (50 mM, pH 7.5) was used to resuspend

the pellet (50 ml per gram of cells). To breakdown RNA and DNA, RNAse and DNAse (0.563 mg of each per gram of cells) was dissolved in 10 ml distilled water and this solution was added to the stirring suspension. To breakdown mature peptidoglycan, lysozyme (0.02 per gram of cells) was dissolved in 10 ml distilled water, added to the suspension and stirred for 1 hour at room temperature. A solution of EDTA (0.5 M, pH 7.5) was prepared and added to the cells to produce a final concentration of 15 mM. After stirring for 15 minutes MgCl (1 M) was added (1:1 moles EDTA:MgCl) and stirred for another 15 minutes. The solution was centrifugated at 240 *g*, 4°C for 45 minutes. The supernatant was removed and then further centrifugated at 18000 g, 4°C for 30 minutes. The pellets were collected and suspended in 1-2 ml Tris-HCl (50 mM, pH7.5) and frozen in liquid nitrogen.

2.8.3 Lipid II Synthesis

Lipid II synthesis was conducted by adding the components listed below in succession.

Components: 908.75 µl of distilled water, 281.25 µl Tris:HCl (1 M, pH 8.0), 2437.5 µl 2% Triton X 100 in 100mM Tris:H_2SO_4 (pH 8.0), 37.5 µl $MgCl_2$ (1 M), 750 µl *B. cereus* extract, 85 µl of undecaprenyl monophosphate (5.67 mM) in 2% (v/v) Tween in 100 mM Tris:HCl (pH 8.0) and 1125 µl *M. flavus* membrane extract were added in succession.

The mixture was stirred for 4 hours at room temperature. 1.3 x vol of Butanol in pyridine-acetate (6 M, pH 4.2) (1:1) (2.3 ml) was then added and the solution was stirred for 10 minutes before centrifuging at 850 *g* for 10 minutes. 1.3 x vol distilled water was added to the isolated upper phase, mixed and the

centrifugation repeated. The upper phase was isolated and the butanol removed by a rotary evaporator. The resultant pellet was dissolved in $CHCl_3$:CH_3OH (1:1). Thin layer chromatography (TLC) was performed to check the presence of lipid II, using a solvent mixture containing $CHCl_3$:CH_3OH:H_2O:NH_3 (88:48:10:1). Lipid II produced from the quantitative prep was then purified using a DEAE Cellulose column. The column was prepared as instructed by Merck. [122] It was packed and equilibrated with $CHCl_3$:CH_3OH:NH_4HCO_3 (50 mM) (2:3:1) before the solution containing lipid II was added. Increasing concentrations of NH_4HCO_3 in $CHCl_3$:CH_3OH (1:2:3) were applied – 100 mM, 150 mM, 200 mM, 250 mM and 600 mM. Each concentration was added as 6 x column volumes (CV) and the final concentration as 18 x CV and fractions were collected. The fractions were then concentrated by rotary evaporation and resolubilised in $CHCl_3$:CH_3OH (1:1). TLC was performed to check the presence of lipid II, using a solvent mixture containing $CHCl_3$:CH_3OH:H_2O:NH_3 (88:48:10:1). [123]

2.9 LPS Purification

Escherichia coli BL21 was grown, the cells lysed and the LPS extracted. To achieve this, 2 x 10 ml LB containing ampicillin (286 µM) were inoculated with 1 µl *E. coli BL21* and grown overnight at 180 rpm, 37°C. 4 x 1 ml was then transferred to 4 x 500 ml LB with ampicillin (286 µM) and incubated at 37°C, 180 rpm for 6 hours or until OD_{595} reached 1.2. The cultures were centrifugated at 4000 *g* for 20 minutes. 5-6 g pellet was suspended in 20 ml distilled water and heated to 68°C. 20 ml of phenol (90% (w/v)) was heated to 68°C and added dropwise to the bacterial suspension. The suspension was stirred for 30

minutes, kept on ice for a following 15 minutes then centrifugated for 45 minutes, 1500 *g* at 10°C. The upper phase was extracted and to the remaining suspension, 20 ml distilled water was added. The suspension was then centrifugated for 45 minutes, 1500 *g* at 10°C and the upper phase kept and added to previously collected upper phase. The solution underwent dialysis to remove any phenol, and then was lyophilised. The resultant powder was dissolved in Tris-HCl-NaN_3 (0.1 M Tris, 175 mM NaCl, 0.05% (w/v) NaN_3, pH 7) at 10 mg/ml and sonicated for 10 minutes. To breakdown DNA and RNA, DNase and RNase (50 μg of both per ml of the solution) was added and incubated for 30 minutes, 37°C. To breakdown protein, proteinase K (50 μg/ml) was added and incubated at room temperature overnight. Ice-cold methanol was added at 4 x solution volume then kept on ice for 2 hours. The solution was centrifugated at 6000 *g*, 4°C for 15 minutes. The supernatant was removed and 6 ml distilled water was added to the LPS pellet. The LPS pellet was resuspended by sonication. To remove methanol the sample was dialysed, then the LPS was sedimented by centrifuging at 100000 *g*, 4°C for 6 hours. The pellet was resuspended in HPLC grade water and lyophilised. [124]

2.10 Leakage Assays

Leakage assays were completed by treating various carboxyfluorescein (CF)-loaded liposomes with the peptides or nisin and monitoring the leakage observed. The CF is self-quenching and can be detected upon release from the liposomes. These studies included liposomes comprised of synthetic 1,2-Dioleoyl-sn-glycero-3-phosphocholine (DOPC) only, DOPC with geranyl geranyl pyrophosphate, DOPC with lipid II, DOPC with smooth type *E. coli* LPS and DOPC

with rough type Ra mutant *E. coli* EH100 LPS. The aim was to record any variation in leakage due to interaction with the target present.

2.10.1 Preparation of CF-loaded Liposomes for Leakage Assay

LPS-free liposomes were produced by dissolving the above mixtures in $CHCl_3$:CH_3OH (1:1) then evaporating the solvents using a rotary evaporator to generate lipid films. For liposomes with LPS the lipid films of either DOPC or DOPG were produced prior to LPS addition. The LPS was dissolved in distilled water, incubated for 15 minutes at 56°C, vortexed for 2 minutes and kept on ice for 2 minutes. The heating, vortexing and cooling cycle was repeated twice before the LPS was added to the previously prepared lipid films, sonicated for 5 minutes and lyophilised. [124]

Lipid films were hydrated with CF (50 mM) with NaCl (50 mM) and HEPES (10 mM) (pH 7.4) and stirred for 1 hour. The solutions then underwent 5 cycles of freeze-thawing in which they were frozen with liquid nitrogen and thawed at 55°C for those without LPS and 40°C for those with LPS. All vesicle solutions were extruded through 1 µm pore size polycarbonate filters 11 times using an Avanti extruder. Excess CF was removed by gel filtration on a PD-10 column, equilibrated with NaCl (100 mM) and HEPES (10 mM) (pH 7.4) buffer.

2.10.2 Dye Release Leakage Assay

The peptide-induced leakage of CF from the vesicles was monitored by measuring the increase in fluorescence intensity at 515 nm (excitation at 490 nm). Total reaction time was 4 minutes. A cuvette containing 50 µl vesicle preparation (2-3 µM) and 1.95 ml NaCl (100 mM) and HEPES (10 mM) (pH 7.4) buffer was allowed to equilibrate for 1 min before 10 µl peptide solution was

added. The fluorescence intensity was monitored for a further 2 minutes before 20 µl of Triton X-100 (80% (v/v)) was added. The fluorescence intensity was measured for a further 1 min and maximum leakage measured as the final value. The peptide-induced CF leakage was expressed relative to the total amount of CF released after lysis of the vesicles by Triton X-100.

2.11 Fluorescence Imaging

The aim of this study was to visualise the binding patterns of the tetramethylrhodamine (TAMRA)-tagged peptides to *B. subtilis* to better understand their mechanism of action. To be able to accurately determine growth phase, a growth curve was generated by measuring the OD_{620} of *B. subtilis* over time.

2.11.1 *Bacillus subtilis* Growth Curve

B. subtilis was cultured by inoculating 4 x 10 ml LB broth and incubating at 35°C, 185 rpm overnight. To scale up, 4 x 1 ml of these cultures were added to 4 x 100 ml LB broth and incubated at 35°C, 185 rpm. OD readings were taken of each culture in triplicate at regular time intervals.

2.11.2 Vancomycin Fluorescence Assay

To aid the method development for *B. subtilis* treated with fluorescently tagged peptides, the boron-dipyrromethene (BODIPY)-vancomycin work by Tiyanont *et al* 2006 was repeated. [125] *B. subtilis* was cultured by inoculating 2 x 20 ml LB and incubating overnight at 35°C, 200 rpm. To scale up, 2 x 250 µl was transferred to 2 x 25 ml LB in 100 ml conical flasks and incubated at 35°C, 200 rpm until an OD_{620} of 0.5 was reached. For the cells to be treated with different

conditions 3 x 1 ml from one culture were centrifugated at 2100 *g* for 2 minutes, the supernatants were discarded. The pellets were resuspended:

1) 1 µl vancomycin-BODIPY in 1 ml 1X HEPES (1 µg/ml)
2) 0.5 µl vancomycin-BODIPY, 0.5 µl vancomycin in 1 ml 1X HEPES (1:1 0.5 µg/ml)
3) 1 ml 1X HEPES

These 3 samples were incubated statically for 10 minutes in the dark to prevent photobleaching. The cells were centrifugated at 2100 *g* for 2 minutes then resuspended in 1 ml HEPES. This washing step was repeated once more and then the pellet was resuspended in 800 µl HEPES. 5 µl of each prep was pipetted onto a poly-lysine slide to encourage sticking of the bacteria and limit movement during imaging. Cover slips were applied and then sealed with nail polish.

Fluorescence microscopy was completed using the Zeiss Axio Observer Elyra PS1 Super Resolution microscope (ZEISS, Oberkochen, Germany), with C-Apochromat 63x/1.2 W Corr M27 objective, HR Diode 488-200 laser, 488 nm excitation wavelength, 552 nm emission wavelength and PCO Edge camera. Super-resolution structured illuminated microscopy (SR-SIM) was used to capture 4 repeats of each image, which were averaged. All images were taken at random and processed in Fiji. [126]

2.11.3 N12(L/D) Fluorescence Assay

B. subtilis was cultured by inoculating 2 x 20 ml LB and incubating overnight at 35°C, 200 rpm. To scale up, 2 x 250 µl was transferred to 2 x 25 ml LB in 100 ml conical flasks and incubated at 35°C, 200 rpm until an OD_{620} of 0.5 was reached for log phase. For stationary phase once an OD_{620} of 0.6 was reached the

cultures were then kept at 4°C for an hour. For the cells to be treated with different conditions 5 x 1 ml from these cultures were centrifugated at 2100 *g* for 2 minutes and the supernatants were discarded. The pellets were resuspended in:

1) 1 ml HEPES with 2 µl N12D-(K-5TAMRA) in 25% MeCN (1 mg/ml stock)
2) 1 ml HEPES with 2 µl N12L-(K-5TAMRA) in 25% MeCN (1 mg/ml stock)
3) 1 ml HEPES with 1 µl N12D-(K-5TAMRA) in 25% MeCN (1 mg/ml stock) and 1 µl N12D in 25% MeCN
4) 1 ml HEPES with 1 µl N12L-(K-5TAMRA) in 25% MeCN (1 mg/ml stock) and 1 µl N12L in 25% MeCN
5) 1 ml HEPES with 1 µl 25% MeCN

These 5 samples were incubated at 35°C, 180 rpm for 30 minutes in the dark to prevent photobleaching. The cells were centrifugated at 2100 *g* for 2 minutes then resuspended in 1 ml HEPES. This washing step was completed 3 times in total, then the pellets were resuspended in 800 µl HEPES. 5 µl of each prep was pipetted onto a poly-lysine slide to encourage sticking of the bacteria and limit movement during imaging. Cover slips were applied and then sealed with nail polish.

Fluorescence microscopy was completed using the Zeiss Axio Observer LSM880 confocal laser scanning microscope (ZEISS, Oberkochen, Germany), with Plan-Apochromat 63x/1.40 Oil Ph3 M27 objective, DPSS 561-10 laser, 561 nm excitation wavelength and 579 nm emission wavelength. 2 repeats of each image were taken and averaged. All images were taken randomly and processed in Fiji. All conditions were completed 3 times. [126]

2.12 Circular Dichroism

Synchrotron Radiation Circular Dichroism (SRCD) experiments were performed at B23 Synchrotron Radiation CD Beamline at the Diamond Light Source, Oxford. A nitrogen flushed Module B end-station spectrophotometer with a bandwidth of 1.1 nm, 1 nm digital resolution, 39 min/min scan speed and an integration time of 1s was utilised. All samples and target were dissolved in water. 50 µl of sample, target or mixture was loaded into a Suprasil cell (Hellma Ltd) with a path length of 0.2 mm and far UV monitored (180-260 nm). For the samples in figure 8.2, 4 scans were completed at 20°C. For thermal melts (figure 8.3 and 8.4) the temperature was increased from 20°C to 94.9°C, incubated for 30 minutes then returned to 20.1°C. 4 scans were completed every 5°C rise and also when lowered to 20.1°C.

A buffer was also measured containing water only as a reference. This was subtracted from average CD (mdegs), concentration was accounted for then the values were converted to θ and finally Δε (molar CD) using the equations in figure 2.12.1 and CD apps. [127] [128]

$$\Delta\varepsilon = \Theta \times \frac{(0.1 \times MWR)}{(p \times conc) \times 3298.2}$$

Where:

$$\Theta = (A_{LCPL} - A_{RCPL}) \times 3298.2$$

$$p = \text{path length (mm)}$$

$$MWR = \frac{\text{Molecular weight}}{\text{Number of residues}}$$

Figure 2.12.1: Equations for calculating Δε. A_{LCPL} = absorbance of left circularly polarised light and A_{RCPL} = absorbance of right circularly polarised light.

2.13 Small Angle X-ray Scattering

To investigate the possible interaction of the peptides with Isopentenyl pyrophosphate, small angle x-ray scattering (SAXS) experiments were performed at B21 solution state SAXS beamline at the Diamond Light Source, Oxford. All peptides and target were dissolved in water (5.6 mM). 30 μl was loaded into the capillary per run at 15°C. Concentrations of peptides were verified using a BCA assay (method 2.6).

2.14 Molecular Dynamic (MD) Simulations

Models of the linear N12L and N12D peptides were built using discovery studio (DS) as extended structures. [129] The PDB files were uploaded to the quick MD simulator of CHARMM-GUI. Conditions chosen in CHARMM were consistent for all peptides; no terminal group patching, 0.15 M KCl ions applied with the Monte-Carlo placing method, a rectangular water box with edge distance of

10.0, temperature of 303.15 K (30°C) and disulphide bridges created where necessary. [130] [131] The minimization, equilibration and production runs were calculated using namd2. [132] The positions of the atoms were recorded every 1 ps for equilibration and every 2 ps during production. Production runs of 100 ns were completed consecutively for each peptide, to model each peptide for a total of 500 ns, with the output from the previous run as the input for the next. All simulations were analysed using VMD. [133] The distances between Cys3-7, Cys3-8, Cys7-11 and Cys8-11 were calculated in VMD over 500 frames using the radial pair distribution function, with the maximum distance set at 25 Å. Root mean squared deviation (RMSD) values were calculated using the RMSD visualizer tool.

Chapter 3 Peptide Structure, Preparation, Purification and Molecular Dynamic Simulations

3.1 Peptide Structure

When designing the chimeric peptides current antimicrobials and their method of action was considered. The aim of this work is to create antimicrobials with specific target engagement alone and also in combination with a pore forming domain. Nisin's broad spectrum of activity and target specificity is widely documented. With this in mind the target engagement portion of the chimeric peptides was designed. The first 12 residues where modelled on nisin1-12. Dehydrated residues were excluded and replaced, to prevent susceptibility to proteolytic degradation. Dhb (position 2) and Dha (position 5) were swapped for Ala. Abu (position 8) was replaced with Cys to facilitate the formation of two disulphide bridges instead of lanthionine rings – cys3-7 and cys8-11 form rings A and B (Figure 3.1.1). Following recommendations in Turpin *et al* 2010, Cys3 and Cys7 were included both, either in the L or D forms. This gives two possible conformations for interaction with lipid II, the desired target. [120]

As discussed previously, magainin II is an effective pore forming antimicrobial but is also haemolytic. We aim to impart magainin II with a targeting motif, which should also reduce its haemolytic activity.

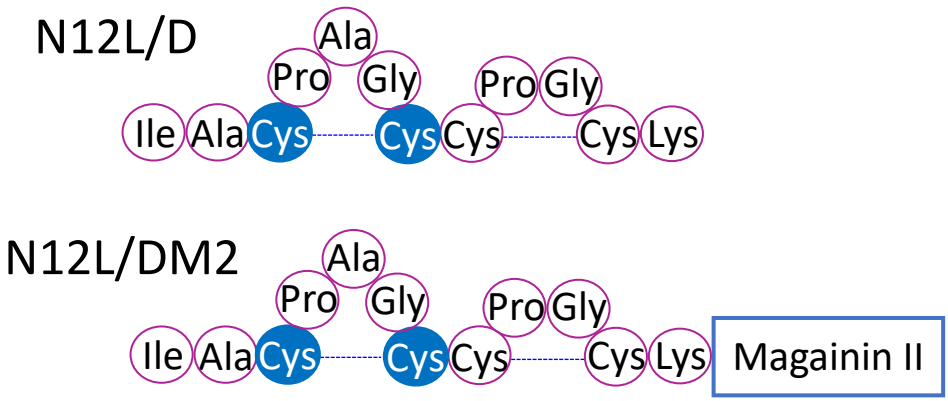

Figure 3.1.1: Overview of the peptide structures. Cys3 and 7 (blue) are either both L or D forms. Blue dashed lines represent the disulphide bridges, these are present in cyclic forms and absent for linear forms.

It is hypothesised that the first two rings of nisin are essential for target engagement. [65] In line with this our aim was to study the properties of all peptides in their linear and cyclic forms. Figure 3.1.2 displays the mechanism of conversion between linear and cyclic forms.

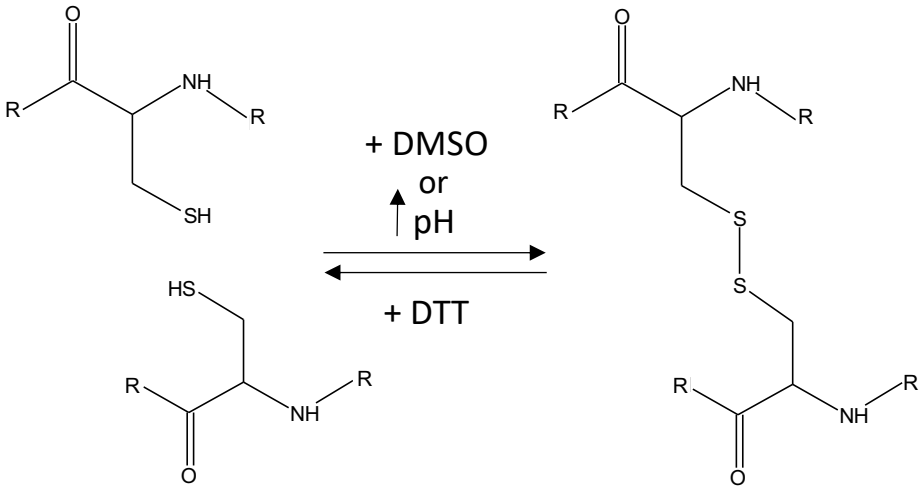

Figure 3.1.2: Reduction and oxidation to form and break disulphide bonds, respectively. Details in methods 2.2.1 and 2.2.2.

3.2 Peptide Purification

After the desired configuration (linear or cyclic) was achieved, the product was purified using reverse phase (RP) HPLC. The peptides were loaded onto a C18 column and eluted under an increasing acetonitrile gradient. Different forms of the peptides are retained for varying times, due to varying degree of hydrophobic interaction; this allows separation (Figure 3.2.1).

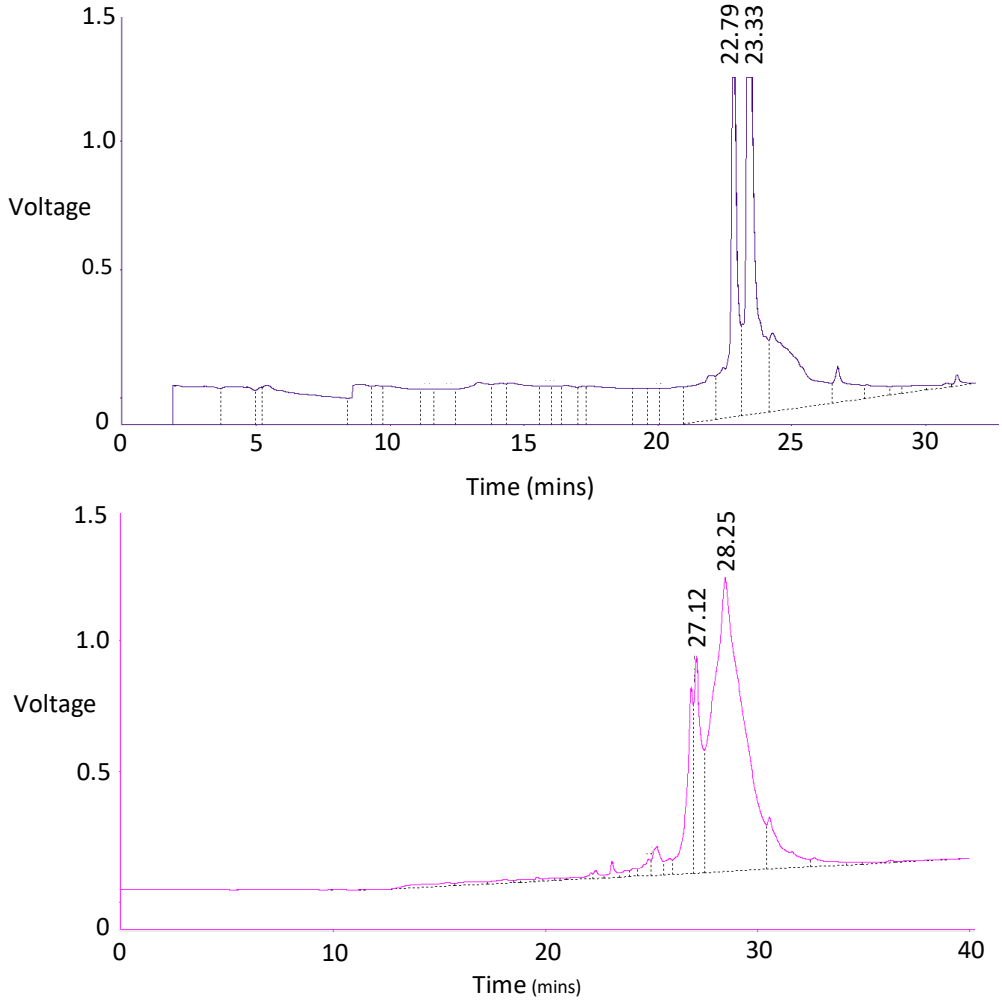

Figure 3.2.1: HPLC chromatograms displaying the retention times and multiple peaks of N12L cyclic (top) and N12LM2 cyclic (bottom). Peaks at 22.79 (top) and 27.12 (bottom) contain semi-cyclic peptide. Peaks 23.33 (top) and 28.25 (bottom) contain cyclic peptide.

The two large peaks of the N12L cyclic chromatogram (figure 3.2.1) at 22.79 and 23.33 minutes contained semi-cyclic and cyclic N12L respectively. The shoulder

seen at ~24 minutes contained the dimeric form. The longer chimeric peptides display a similar pattern of variation corresponding to retention time. The linear form is the first to elute, then as the acetonitrile percentage increases the semi-cyclic, cyclic and finally dimeric forms are eluted.

Both N12LM2 and N12DM2 have longer retention times in general. The semi-cyclic fraction was eluted at 27.12 and cyclic fraction at 28.25 (figure 3.2.1). The stronger the hydrophobic interaction with the C18 column, the higher the percentage of acetonitrile required for elution. To determine the forms of the peptides present in the fractions MALDI mass spec was completed (examples in figure 3.2.2 and figure 3.2.3).

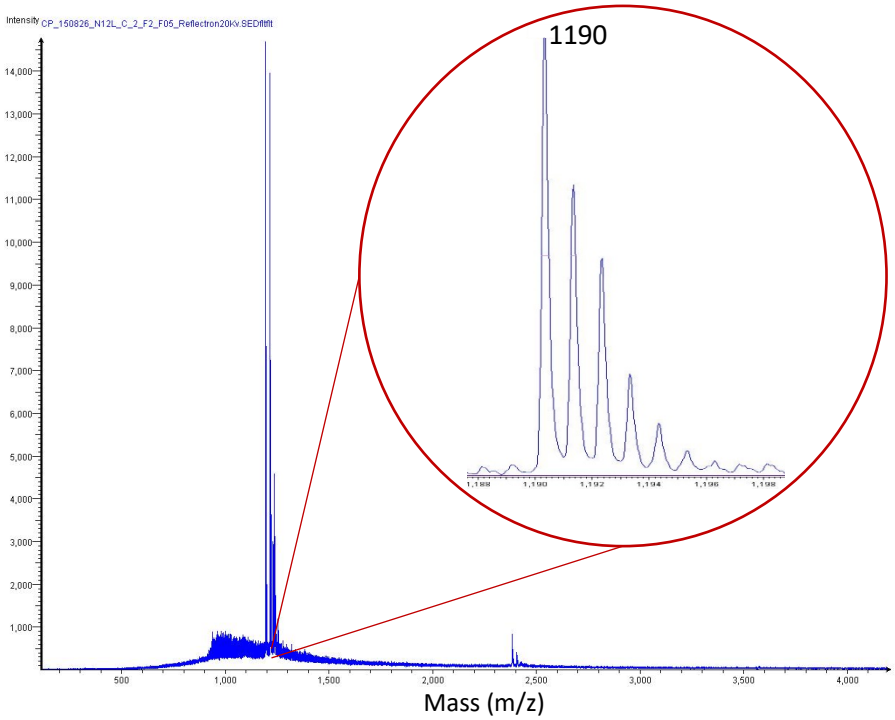

Figure 3.2.2: MALDI mass spectra of N12L cyclic containing fraction. 1190 indicates formation of two disulphide bridges, the mass distribution here of 1191, 1192, 1193 and 1194 indicates proton adducts.

For peptides N12L and N12D, 1190, 1192 and 1194 Da values indicate that the peptide is cyclic, semi-cyclic and linear, respectively, as the formation of a disulphide bridge results in the loss of two hydrogen atoms. Figure 3.2.2 displays an example of good cyclisation and separation. A small peak indicating the presence of the dimeric form can be seen at 2380. This is commonly found in fractions containing the cyclic form, for both the short N12L/D and long N12L/DM2 peptides, due to the overlapping retention times. Full separation is tricky and often fractions contain multiple forms (figure 3.2.3).

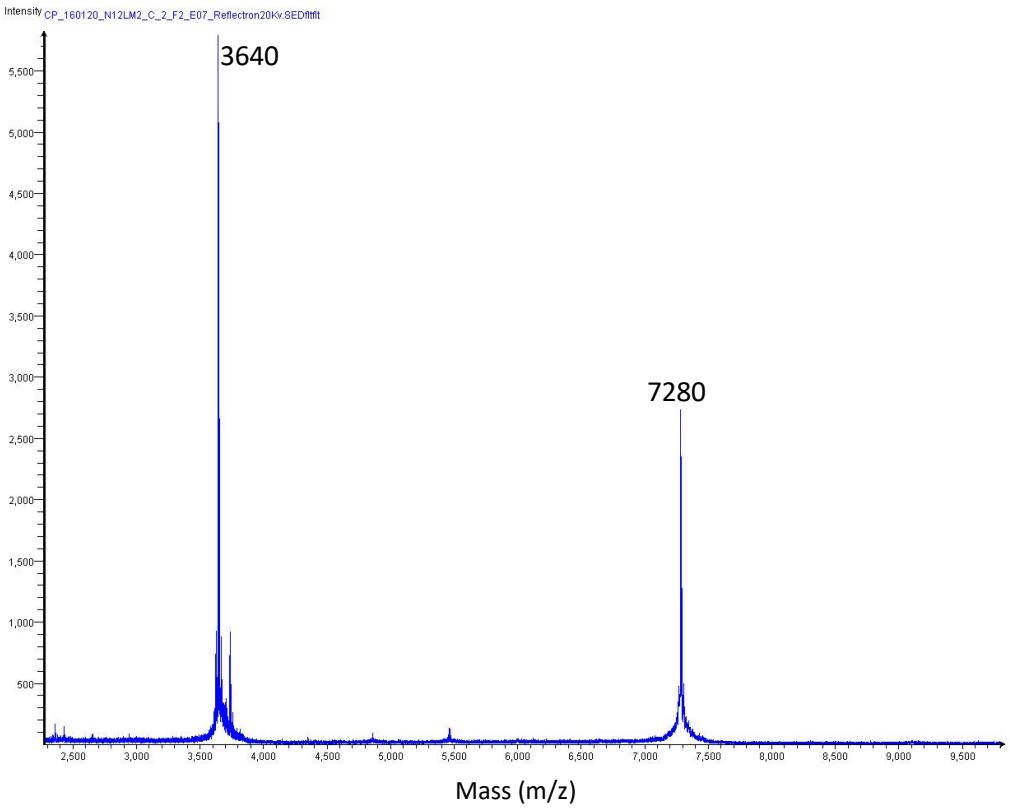

Figure 3.2.3: MALDI mass spectra of N12LM2 HPLC fraction. Cyclic and dimeric forms can be seen at 3640 and 7280 respectively.

For peptides N12LM2 and N12DM2 3639, 3641 and 3643 Da values indicate that the peptide is cyclic, semi-cyclic and linear, respectively. A significant peak can be seen at 7280 Da, which indicates an abundance of the dimeric form.

Unfortunately, many purification attempts yielded fractions containing multiple forms of the peptides. However, this was only observed in samples which underwent cyclisation, those that were linearised with DTT only displayed the linear form. Fractions with mixtures of either semi-cyclic and cyclic or cyclic and dimeric forms often occurred. Using alternative columns, such as C12 and C8, displayed similar separation issues.

The cyclisation conditions were altered to attempt to reduce incomplete ring closure. For N12D/LM2 the pH was raised for various time intervals ranging from 1 to 48 hours. We observed that raising the pH for more than 2 hours only increased the dimer content and had no effect on the semi-cyclic to cyclic ratio (method 2.4). Raising the pH for less than 2 hours resulted in increased formation of semi-cyclic peptide.

Many attempts were made to eliminate DMSO from the cyclisation process due to its increased viscosity and the challenges that causes for HPLC pressure and detection. These include raising the pH for varying time periods, similar to the N12L/DM2 cyclisation technique, and using solid phase extraction with C18 columns to concentrate peptide and remove DMSO. The former resulted in no cyclic peptide for either N12L or N12D. The latter did produce some cyclic N12L, however the yields were less than 1%. No alternative method resulted in the production of the monomeric cyclic form with improved yields for N12L. In fact, no suitable method was found that could produce the cyclic monomeric form of N12D.

We observed that the longer any peptide solution was left at 4°C prior to HPLC the more dimers were present. This suggests that thiol groups of cysteines

present in other monomers are attacking the existing disulphide bridges of cyclic or semi-cyclic monomers, causing disulphide rearrangement or shuffling and increased dimerization.

3.3 Molecular Dynamic (MD) Simulations

Previous MD simulations indicated that N12D would cyclise to form rings A (Cys3-7) and B (Cys8-11). It was also suggested that N12L favours formation of ring B (Cys8-11) followed by ring A (Cys3-7). [120] Many issues were encountered when attempting ring closure and purification for N12D. Complete ring closure for N12L was challenging but mostly successful. To better understand the persistent issues encountered during disulphide formation and purification MD simulations were performed.

Determining the proximity of two thiol groups required for the formation of a disulphide is complex. A range of factors can influence this distance including the properties of the surrounding amino acids and the environmental pH. [134] Although there is no standard proximity requirement for the thiol groups to form a disulphide bridge the likelihood of formation can be evaluated.

In silico experiments were completed to monitor the distance in angstroms between Cys3 and Cys7 for ring A and Cys8 and Cys11 for ring B over 500ns. This allows the investigation into the ability of N12L and N12D to form two disulphide bridges. The distance between SH groups was calculated in each frame using the radial distribution function (RDF) in visual molecular dynamics (VMD). [135]

The overall trends of these recorded distances will give an indication of the probability of ring formation. Turpin *et al* 2010 suggested that a disulphide bridge was likely to form if the distance observed between SH groups was less

than 5.5 Å. For all following simulations the percentage of frames where the distance is less than 5.5 Å is calculated.

Figure 3.3.1 shows that the distance for linear N12L Cys8-11 is clustered at lower values than Cys3-7. The percentage of frames with distances smaller than 5.5 Å is 4.8 % for Cys3-7 and 13.3 % for Cys8-11 (table 3.3.1). The greatest distance seen for Cys3-7 is approximately 19 Å, whereas ~16 Å is observed for Cys8-11.

A similar trend is observed for linear N12D, though the difference is more pronounced (figure 3.3.2). The percentage of frames with distances smaller than 5.5 Å is 0.4 % for Cys3-7 and 23.9 % for Cys8-11 (table 3.3.1). The greatest distance seen for Cys3-7 is ~19 Å, whereas ~15 Å is observed for Cys8-11. The modal and second modal distances observed for Cys3-7 of linear N12D occurred in 1.5 % of frames, indicating that the distance was 13.1 Å as often as it was 6.8 Å. Table 3.3.1 shows that the modal and second modal distances for N12D Cys8-11 were much lower.

Interestingly ring B (Cys8-11) appears more likely to form than ring A (Cys3-7) due to the increased proximity of the thiol groups. This is demonstrated for both linear N12L and N12D.

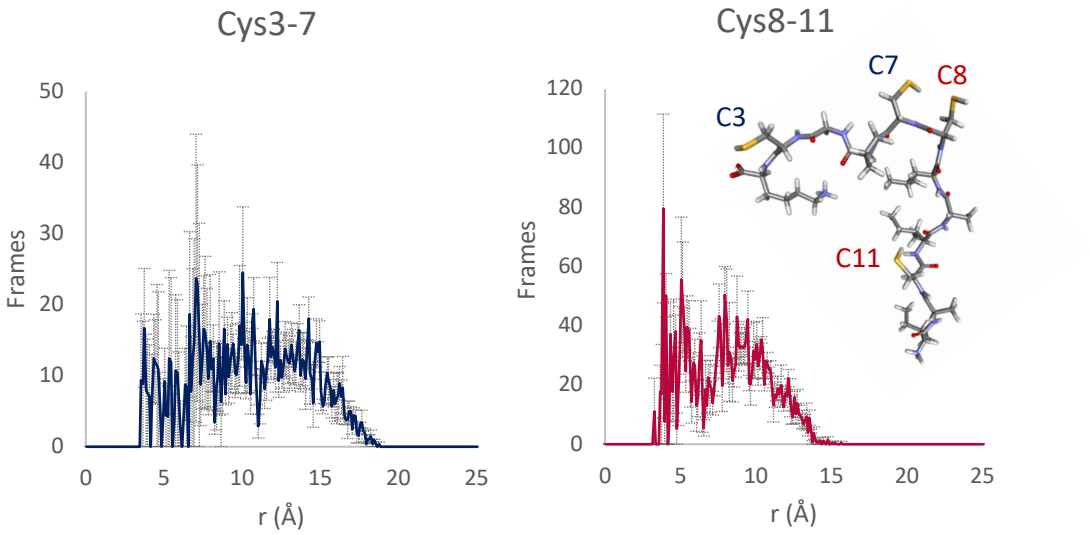

Figure 3.3.1: : Average distance in angstroms of SH groups of Cys3-7 (blue) and Cys8-11 (red) of linear N12L from 300 ns MD simulation; error bars show standard error. The structure of linear N12L after a 500 ns MD simulation is also included.

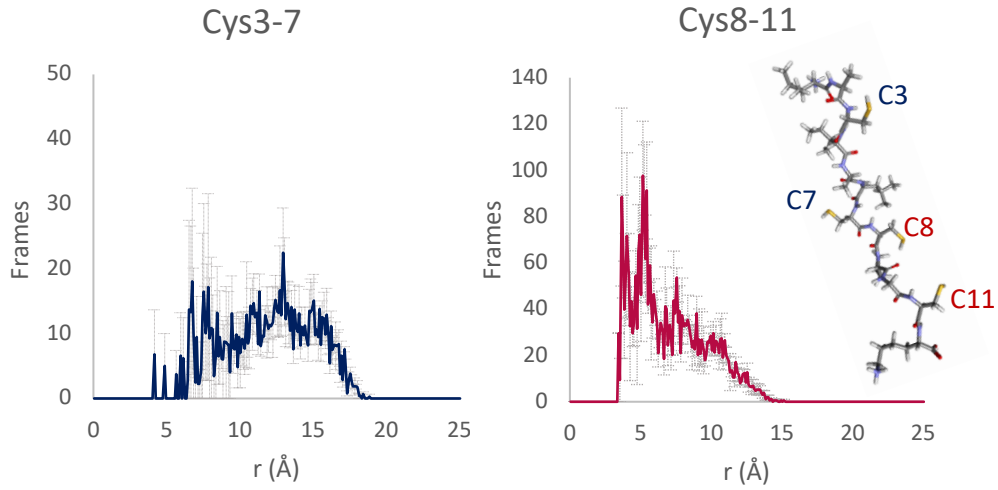

Figure 3.3.2: Average distance in angstroms of SH groups of Cys3-7 (blue) and Cys8-11 (red) of linear N12D from 300 ns MD simulation; error bars show standard error. The structure of linear N12D after a 500 ns MD simulation is also included.

Table 3.1: Distances between SH groups of Cys3-7 and Cys8-11 calculated using the RDF, including the modal, second modal and percentage of frames with distance less than 5.5 Å.

		Modal Distance (Å)	**2nd Modal Distance (Å)**	**% Frames S-S Distance < 5.5 (Å)**
N12L L	Cys3-7	10.1	7.1	4.8
	Cys8-11	3.9	5.1	13.3
N12D L	Cys3-7	6.8	13.1	0.4
	Cys8-11	5.2	3.7	23.9

Ring B is more likely to form than ring A for both linear peptides (figures 3.3.1 and 3.3.2). Formation of ring A is then dependent on the structural properties of the semi-cyclic form. To investigate further, simulations were completed with the structural constraint of ring B being formed, to give an insight into the effect of ring B on the formation of ring A.

Semi-cyclic N12L displays a percentage of frames with a distance between SH groups less than 5.5 Å for Cys3-7 of 9.5 %. The corresponding percentage occurrence for semi-cyclic N12D is 6.9 % (figure 3.3.3). The modal and second modal distances observed for Cys3-7 of semi-cyclic N12D are greater than those for N12L. Both values for semi-cyclic N12L are less than 5.5 Å, whereas those for N12D are both greater than 5.5 Å (table 3.3.2).

This shows that formation of ring A after the initial closure of ring B is likely to occur for N12L, but unlikely for N12D. This is consistent with experimental findings as the N12L has been detected in its cyclic form and N12D has not.

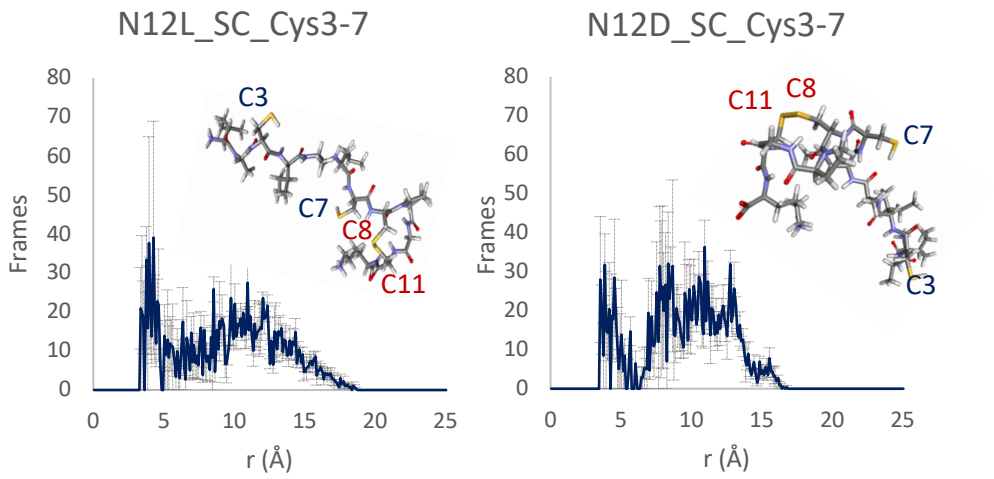

Figure 3.3.3: Average distance in angstroms of SH groups of Cys3-7 for N12L (left) and N12D (right) when ring B (Cys8-11) is closed from 300 ns MD simulations; error bars show standard error. The structures of semi-cyclised ring B containing N12L and N12D after 500 ns MD simulations are also included.

Table 3.2: Distances between SH groups of Cys3-7 calculated using the RDF, including the modal, second modal and percentage of frames with distance less than 5.5 Å for both N12L and N12D when ring B (Cys8-11) is present.

		Modal Distance (Å)	**2nd Modal Distance (Å)**	**% Frames S-S Distance < 5.5 (Å)**
N12L	Cys3-7	4.3	4.0	9.5
N12D		11.0	8.4	6.9

To complete the computational study the effects of the formation of ring B when ring A had formed first were assessed.

For semi-cyclic N12L the modal and second modal distances were both greater than 5.5 Å. The percentage of frames with a distance of less than 5.5 Å for Cys8-11 is 13.6 %. Semi-cyclic N12D displays a corresponding percentage of 11.1 %. The modal distance for N12D Cys8-11 is less than 5.5 Å, but the second modal distance is greater than this value.

These data suggest that if ring A formed for N12D subsequent formation of ring B would be possible. However, the initial formation of ring A is unlikely for N12D causing the formation of fully cyclic N12D to also be unlikely, which supports experimental findings. No cyclic N12D has been observed during purification, yet the semi-cyclic form is abundant.

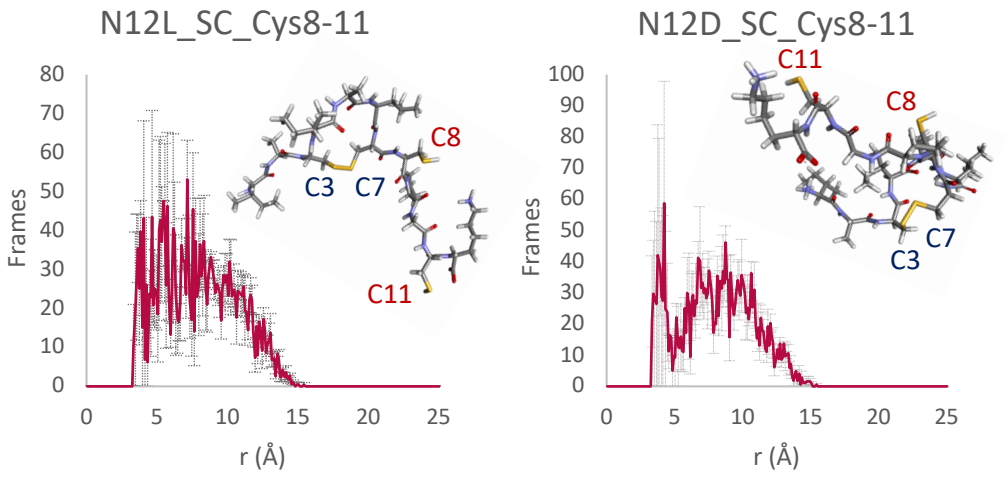

Figure 3.3.4: Average distance in angstroms of SH groups of Cys8-11 for N12L (left) and N12D (right) when ring A (Cys3-7) is closed from 300 ns MD simulations; error bars show standard error. The structures of semi-cyclised ring A containing N12L and N12D after 500 ns MD simulations are also included.

Table 3.3: Distances between SH groups of Cys8-11 calculated using the RDF, including the modal, second modal and percentage of frames with distance less than 5.5 Å for both N12L and N12D when ring A (Cys3-7) is present.

		Modal Distance (Å)	**2nd Modal Distance (Å)**	**% Frames S-S Distance < 5.5 (Å)**
N12L	Cys8-11	7.2	5.5	13.6
N12D		4.3	8.8	11.1

These preferred combinations, Cys3-7 and Cys8-11, are not the only possible pairs for ring formation. It is possible that Cys3-8 or Cys7-11 form alternative rings. To evaluate this the RDF was used to calculate the distances for these combinations.

All modal values for this data set are less than 5.5 Å (figure 3.3.5, figure 3.3.6 and table 3.3.4). For both linear N12L and N12D alternate ring B (Cys7-11) is more likely to form than alternate ring A (Cys3-8).

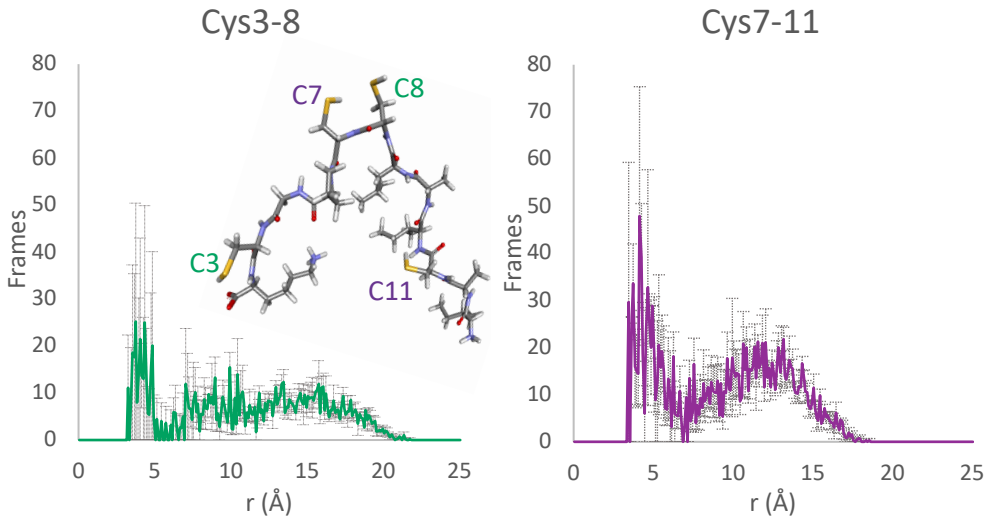

Figure 3.3.5: Average distance in angstroms of SH groups of Cys3-8 (green) and Cys7-11 (purple) of linear N12L from 300 ns MD simulation; error bars show standard error. The structure of linear N12L after a 500 ns MD simulation is also included.

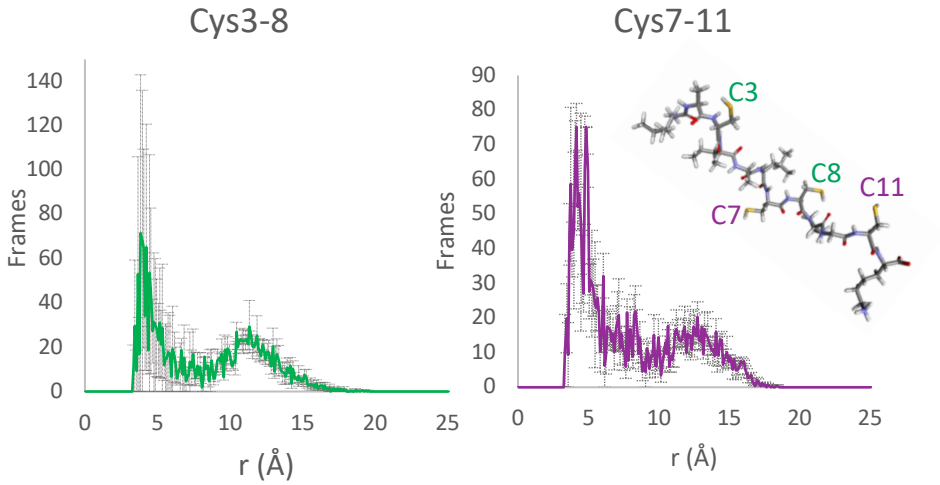

Figure 3.3.6: Average distance in angstroms of SH groups of Cys3-8 (green) and Cys7-11 (purple) of linear N12D from 300 ns MD simulation; error bars show standard error. The structure of linear N12D after a 500 ns MD simulation is also included.

Table 3.4: Distances between SH groups of Cys3-8 and Cys7-11 calculated using the RDF, including the modal, second modal and percentage of frames with distance less than 5.5 Å.

		Modal Distance (Å)	**2nd Modal Distance (Å)**	**% Frames S-S Distance < 5.5 (Å)**
N12L L	Cys3-8	3.8	4.4	7.8
	Cys7-11	4.2	4.3	12.4
N12D L	Cys3-8	3.9	4.0	18.9
	Cys7-11	4.2	4.9	22.7

To asses further cyclisation, simulations were completed with the alternate Cys7-11 ring closed for both peptides, to assess the probability of Cys3-8 forming.

All modal distances for the SH groups of Cys7-11 are less than 5.5 Å (figure 3.3.7 and table 3.3.5). The percentage of frames with a distance less than 5.5 Å is 27.1 % for N12L and 16.0 % for N12D. This suggests that formation of alternate ring B followed by alternate ring A is feasible for both N12L and N12D.

When cyclisation of N12D is attempted experimentally precipitation is observed and mass spectrometry shows that the peptide is semi-cyclic, dimeric and sometimes trimeric. It seems that although full cyclisation is possible with the alternate rings it causes N12D to become insoluble.

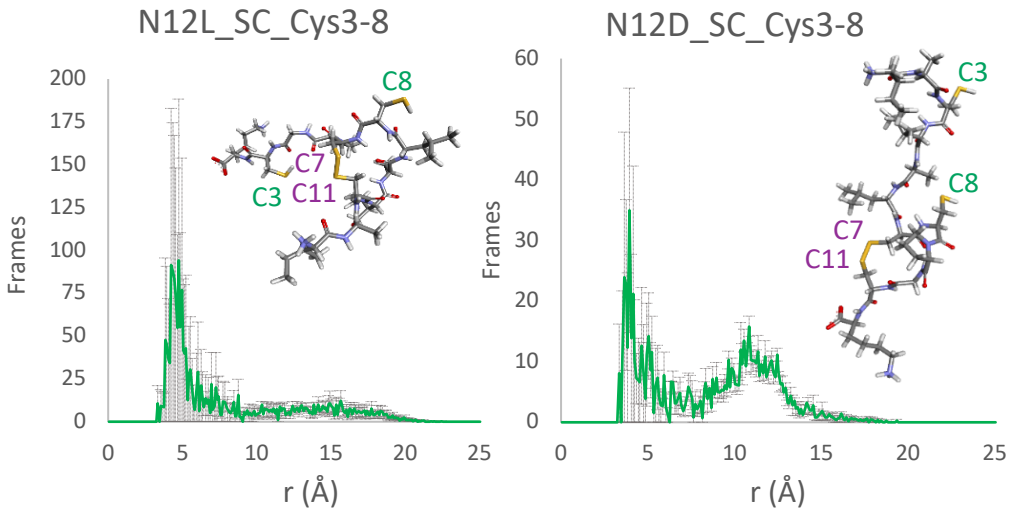

Figure 3.3.7: Average distance in angstroms of SH groups of Cys3-8 for N12L (left) and N12D (right) when alternate ring B (Cys7-11) is closed from 300 ns MD simulations; error bars show standard error. The structures of semi-cyclised ring B containing N12L and N12D after 500 ns MD simulations are also included.

Table 3.5: Distances between SH groups of Cys3-8 calculated using the RDF, including the modal, second modal and percentage of frames with distance less than 5.5 Å for both N12L and N12D when alternate ring B (Cys7-11) is present.

		Modal Distance (Å)	**2nd Modal Distance (Å)**	**% Frames S-S Distance < 5.5 (Å)**
N12L	Cys3-8	4.8	4.3	27.1
N12D		4.0	3.7	16.0

To complete the data set alternate ring A (Cys3-8) was formed and the RDF used to measure the distances between Cys7-11.

The distribution of distances observed for the SH groups of Cys7-11 for N12L and N12D vary significantly (figure 3.3.8). The modal distances for N12D are both less than 5.5 Å, whereas those for N12L are both greater than 5.5 Å (table 3.3.6). The percentage of frames with a distance less than 5.5 Å is 30.2 % for N12D and only 0.4 % for N12L.

If N12D forms alternate ring A (Cys3-8) it is very probable that alternate ring B (Cys7-11) will also form. In contrast, formation of alternate ring A (Cys3-8) then B (Cys7-11) is very unlikely for N12L.

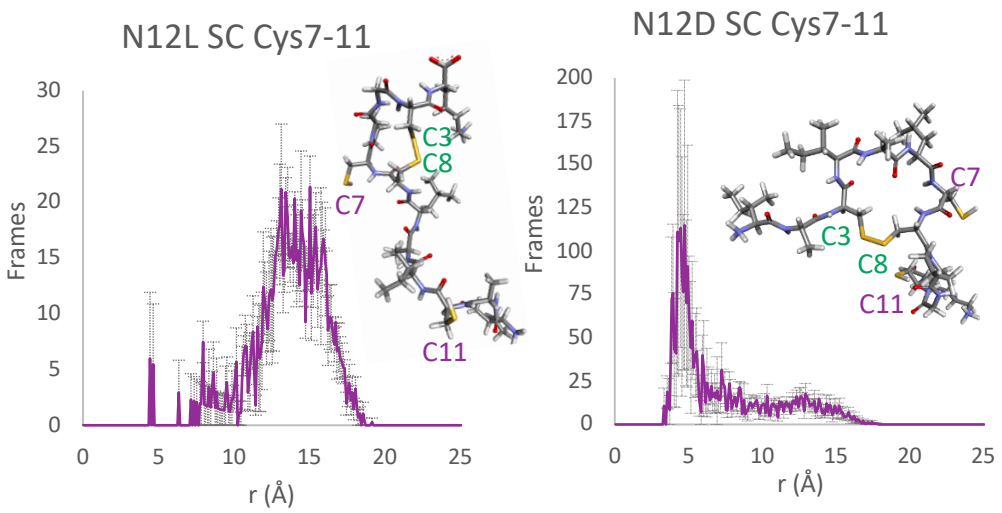

Figure 3.3.8: Average distance in angstroms of SH groups of Cys7-11 for N12L (left) and N12D (right) when alternate ring A (Cys3-8) is closed from 300 ns MD simulations; error bars show standard error. The structures of semi-cyclised ring A containing N12L and N12D after 500 ns MD simulations are also included.

Table 3.6: Distances between SH groups of Cys7-11 calculated using the RDF, including the modal, second modal and percentage of frames with distance less than 5.5 Å for both N12L and N12D when alternate ring A (Cys3-8) is present.

		Modal Distance (Å)	**2nd Modal Distance (Å)**	**% Frames S-S Distance < 5.5 (Å)**
N12L	Cys7-11	15.1	13.2	0.4
N12D		4.0	3.7	30.2

Overall these *in silico* simulations show that N12L is most likely to form ring B (Cys8-11) followed by ring A (Cys3-7) or alternate ring B (Cys7-11) followed by alternate ring A (Cys3-8). For N12L, the percentage of frames with a distance

less than 5.5 Å for Cys8-11 and Cys7-11 are 13.3 % and 12.4 %, demonstrating that cyclisation of N12L could be with either rings.

For N12D formation of ring B (Cys8-11) is possible but subsequent formation of ring A (Cys3-7) is unlikely. The initial formation of alternate rings A (Cys3-8) or B (Cys7-11) is probable and the subsequent cyclisation of their remaining rings is also possible. However, cyclic N12D has not been observed experimentally due to the change in solubility. The cyclisation of this peptide may result in its insolubility, which prevents purification by HPLC.

Chapter 4 Antimicrobial Activity against Gram-positive Bacteria

Multiple methods exist for analysing antimicrobial action against bacteria including agar diffusion, broth dilution and spot on lawn assays. Agar diffusion can be performed using discs containing varying concentrations of candidate antimicrobials. A spot on lawn agar assay was attempted but the peptides did not diffuse through the 1.5 % agar (method 2.7.4). As *M. luteus* is widely used for establishing initial antimicrobial activity of compounds, agar diffusion activity assays were completed. This method involved punching holes in agar plates treated with *M. luteus,* then filling these wells with peptide solutions of varying concentrations. *M. luteus* is a Gram-positive bacteria sensitive to many antimicrobials and especially to nisin. All agar diffusion activity assays involved this species to assess activity of the peptides against a more susceptible strain before testing any others. Broth dilution MIC assays against *Listeria* and *Staphylococcus* were completed at DuPont, Brabrand. Similar assays were attempted at the University of Nottingham against *M. luteus*, however the inoculum was too high, which prevented accurate absorbance readings.

4.1 Agar Diffusion Activity Assays

In order to be able to use a consistent bacterial concentration for these assays the correlation between optical density and CFU were investigated for *M. luteus* (figure 4.1.1).

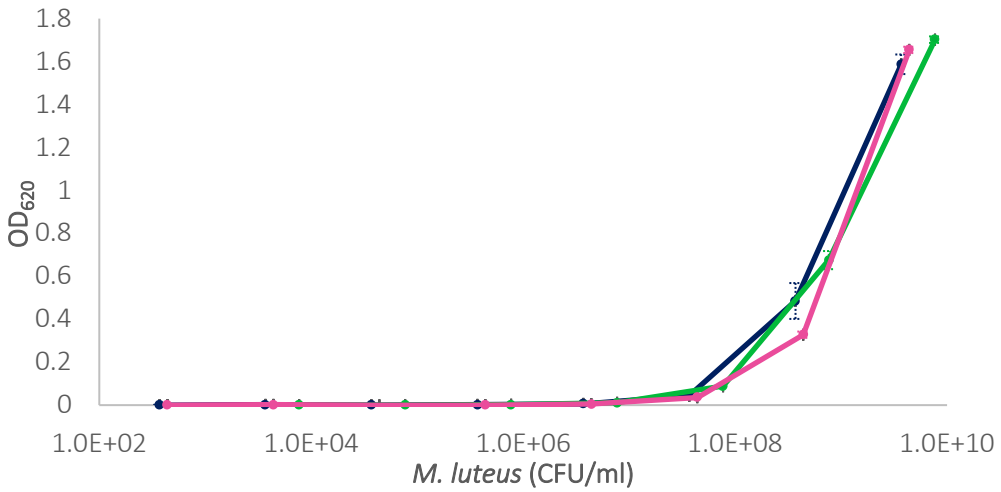

Figure 4.1.1: Correlation between OD_{620} and CFU/ml counts for M. luteus. Three cultures were analysed and their ODs measured in triplicate. Error bars display standard error.

Using these data *M. luteus* was grown to 10^8 CFU/ml then diluted to a final concentration of 10^6 CFU/ml for the agar diffusion activity assays. Results from the well diffusion assay are shown in table 4.1.1; of the tested peptides nisin, magainin II and cyclic N12L were the only ones showing activity against *M. luteus*.

Table 4.1: Diameter of inhibition zones caused by varying concentrations of antimicrobial peptides against M. luteus.

	Average Zone Diameter (mm)				
Estimated Concentration of Antimicrobial (mg/ml)	0.5	0.1	0.05	0.01	0.005
Nisin	29	24.3	22.3	14.7	12.8
Estimated Concentration of Antimicrobial (mg/ml)	1.5	1.0	0.8	0.6	
Magainin II	13.5	10.8	8.8	4.3	
N12L L	0	0	0	0	
N12L C	17.5	15.7	14.7	13.3	
N12D L	0	0	0	0	
N12LM2 L	0	0	0	0	
N12DM2 L	0	0	0	0	
PGLa	6	0	0	0	

PGLa, an AMP belonging to the magainin family, was included to assess its sole antimicrobial activity. As it can augment the activity of magainin II, PGLa will be introduced in combination with the other AMPs to evaluate any possible synergism or antagonism. Nisin has a high bactericidal activity against *M. luteus* and was used at lower concentrations to provide reasonably sized zones of inhibition.

Weighing out such small amounts of electrostatic peptide can potentially introduce error, therefore concentration must be accurately determined. The peptides assayed that displayed no activity may be at lower concentrations than estimated (table 4.1.1). In order to be able to calculate the accurate concentration of the peptides the ODs of BSA at specific concentrations were measured and a trend established (figure 4.1.2 and table 4.1.2).

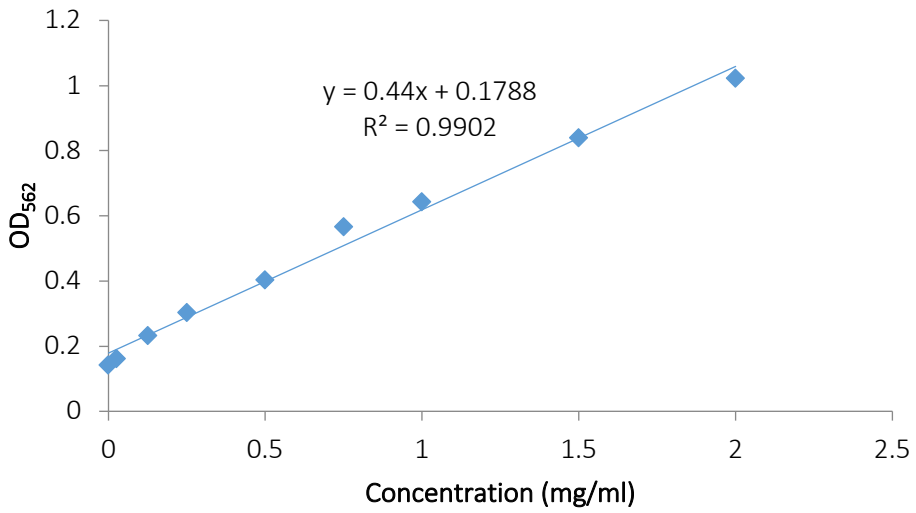

Figure 4.1.2: Correlation between BSA concentration and optical density used to calculate peptide concentrations in table 4.1.2. Standards were assayed in duplicate with OD_{562} measured.

The correlation was then used to calculate the actual concentration of the different antimicrobial peptides and the results showed that the concentrations were incorrect for all peptides (table 4.1.2).

Table 4.2: Actual concentrations of antimicrobials used in these activity assays, determined using a BCA assay. Peptides were assayed in duplicate and measured at OD_{562}.

Peptide	Actual Concentration (mg/ml)	Estimated Concentration (mg/ml)
Nisin	0.2	0.5
Magainin II	1.4	1.5
N12L L	2.7	1.5
N12L C	0.9	1.5
N12D L	4.7	1.5
N12LM2 L	5.2	1.5
N12DM2 L	1.1	1.5
PGLa	1.1	1.5

The results showed that the concentration of nisin was estimated to be 0.5 mg/ml but the actual concentration was 0.2 mg/ml, which was 0.3 mg/ml lower than predicted and linear N12DM2 and PGLa were 0.4 mg/ml lower. The

difference in concentration of cyclic N12L was considerable at 0.6 mg/ml lower than expected. Magainin II was the most accurate at 0.1 mg/ml lower than predicted. Linear N12L, N12D and N12LM2 were 1.2, 3.2 and 3.7 mg/ml more concentrated, respectively.

The concentrations of the inactive peptides were not lower than those that are active. This indicates that low concentration is not the reason why no activity was observed. To be able to calculate MIC values for these active peptides the values in table 4.1.2 were used to plot accurate concentrations in figure 4.1.3 and 4.1.4.

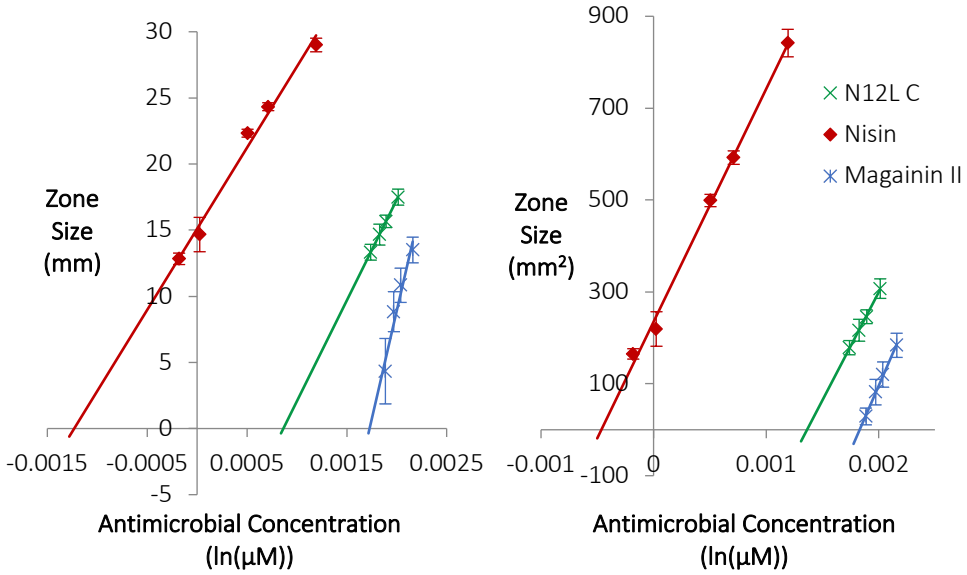

Figure 4.1.3: The zones of inhibition measured as diameter (left) and diameter squared (right) are plotted against the corrected antimicrobial concentration. Error bars display standard error. These data include 2 assays with triplicate repeats in each.

Using the diameter to calculate the MIC assumes free diffusion of the peptide, whereas diameter squared accounts for dissipative diffusion. [121] Whichever R^2 value is closer to 1 best describes the data and the corresponding MIC is the most accurate, in this case accounting for diffusion is essential. Linear regression was used to calculate the MIC values (method 2.7.3.1).

Interestingly the µM MIC for cyclic N12L is less than half that for magainin II and the MIC as µg/ml is 4.8 times lower (table 4.1.3). The MIC for nisin is comparable to published values against *M. luteus* of 0.07 µg/ml. [75]

Table 4.3: MICs were calculated using the slope and intercept from activity graphs (figure 4.1.3). The best representations of the data are those with R^2 values closer to 1, their corresponding concentrations are highlighted in yellow. MICs are included as both µM and µg/ml values due to the differences in molecular mass.

	R^2 / d	MIC (µM)	MIC (µg/ml)	R^2 / d^2	MIC (µM)	MIC (µg/ml)
Nisin	0.962	0.00347	0.0116	0.976	0.0437	0.147
Magainin II	0.909	129	318	0.938	190	468
N12L C	0.920	15.9	18.9	0.925	81.7	97.2

Agar diffusion activity studies were then completed with the peptides in combination with PGLa. Magainin II causes the formation of relatively stable pores slowly and PGLa forms unstable pores quickly. Together these antimicrobials associate to form a 1:1 complex and cause the formation of stable membrane pores. [96] Overall this synergy results in a lower MIC than that of magainin II or PGLa alone. As our two chimeric peptides include a magainin II domain we evaluated the peptides in combination with PGLa against *M. luteus,* using the well diffusion assay, to determine any possible synergy (table 4.1.4).

Table 4.4: Diameter of zones caused by varying concentrations of antimicrobial peptides against M. luteus. All antimicrobials were applied in a 1:1 w/w ratio with PGLa.

	Average zone diameter (mm)				
Estimated Concentration of total Antimicrobial (mg/ml)	**0.25**	**0.05**	**0.025**	**0.005**	**0.0025**
Nisin	27.7	22.8	20.2	9.8	0
Estimated Concentration of total Antimicrobial (mg/ml)	**0.75**	**0.5**	**0.4**	**0.3**	
Magainin II	20.7	19.2	16.2	13.5	
N12L L	0	0	0	0	
N12L C	17.5	16.2	15.0	13.7	
N12D L	0	0	0	0	
N12LM2 L	8.8	5.2	0	0	
N12DM2 L	10.3	7.5	6.3	2.7	

Similar to the previous assay, nisin, magainin II and cyclic N12L were active. Activity is observed for linear N12DM2 and N12LM2 when combined with PGLa (table 4.1.4). The actual concentrations present in table 4.1.2 were used to plot the results accurately (figure 4.1.4) and linear regression was used to calculate the MICs (table 4.1.5).

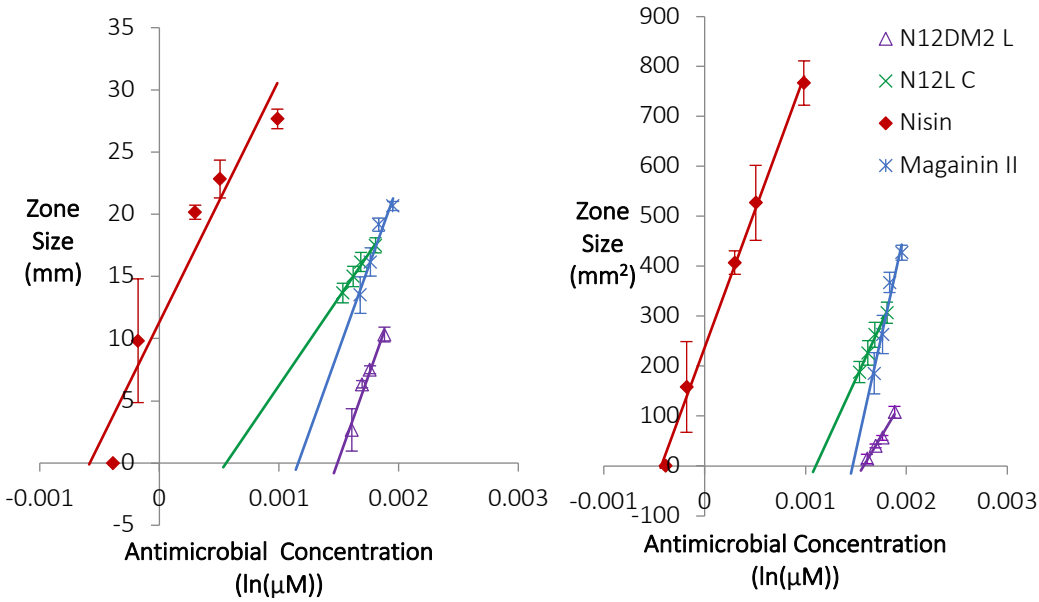

Figure 4.1.4: The zones of inhibition measured as diameter (left) and diameter squared (right) are plotted against the corrected antimicrobial concentration. Error bars display standard error. These data include 2 assays with triplicate repeats in each.

Similar to the previous assay, accounting for diffusion yields the most accurate MIC values. The MIC values are directly comparable with those in table 4.1.3. It would be ideal to create isobolograms for these peptides and PGLa to determine any antagonism or synergism. Unfortunately, the MIC value for PGLa could not be calculated from the activity trials, this could have been achieved if the starting concentration was higher. Instead the MICs of the AMPs were calculated assuming PGLa was not present. The final concentrations of each peptide became half of that present in the original activity assay without PGLa. As seen previously magainin II and PGLa demonstrate synergism. [96] In line with this the MIC for magainin II improved upon inclusion of PGLa, it became 129.8 µM (320.1 µg/ml) lower than that without PGLa (table 4.1.5).

The MIC for cyclic N12L in the presence of PGLa was 35.8 µM lower than for cyclic N12L alone. This could indicate a degree of synergism; however, it is more likely that issues with diffusion cause this variation. Inhibition zones observed were 17.5-13.3 mm for cyclic N12L alone and 17.5-13.7 mm in combination with PGLa. The latter assay contained concentrations of cyclic N12L half of those in the former assay. This suggests that diffusion of the peptide may be limited, leading to similar zone size.

In contrast, nisin has an MIC 0.027 µM (0.092 µg/ml) higher with PGLa. There may be a degree of competition between these AMPs. PGLa interacts non-specifically with the membrane, if it interacts at a site in which lipid II is present it could prevent nisin from interacting. A degree of electrostatic repulsion may also contribute to the increase in MIC, as PGLa has a +4 charge and nisin has a net charge between +3 and +5, depending on the pH, due to the His residues.

Table 4.5: MICs were calculated using the slope and intercept from activity graphs (figure 4.1.4). The best representations of the data are those with R^2 values closer to 1, their corresponding concentrations are highlighted in yellow. MICs are included as both µM and µg/ml values due to the differences in molecular mass and are calculated assuming PGLa isn't present.

	R^2 d	MIC (µM)	MIC (µg/ml)	R^2 d^2	MIC (µM)	MIC (µg/ml)
Nisin	0.914	0.0396	0.133	0.942	0.0710	0.238
Magainin II	0.911	23.4	57.6	0.924	59.7	147
N12L C	0.889	12.5	14.9	0.902	45.9	54.6
N12DM2 L	0.895	38.6	141	0.937	77.9	284

The most remarkable effect was that observed for linear N12LM2 and N12DM2. The former, previously inactive, demonstrated activity at the two highest concentrations (table 4.1.4), unfortunately 3 data points are required to accurately calculate an MIC. Linear N12DM2 with PGLa displayed activity across the entire concentration range. The activity is not due to PGLa alone, as it has been shown to be almost inactive at this concentration (table 4.1.1). This suggests that PGLa works synergistically with both linear N12DM2 and N12LM2, perhaps through a similar mechanism as to that with magainin II.

The concentrations of linear N12L present are 3 times higher than the corresponding cyclic N12L concentrations. As shown in figure 4.1.5 the linear form is completely inactive, even at 2.7 mg/ml, whereas the cyclic form produces clear zones of inhibition at 0.4-0.2 mg/ml. As mentioned previously the zones are of similar diameters for this range of concentrations, which indicates an issue with diffusion.

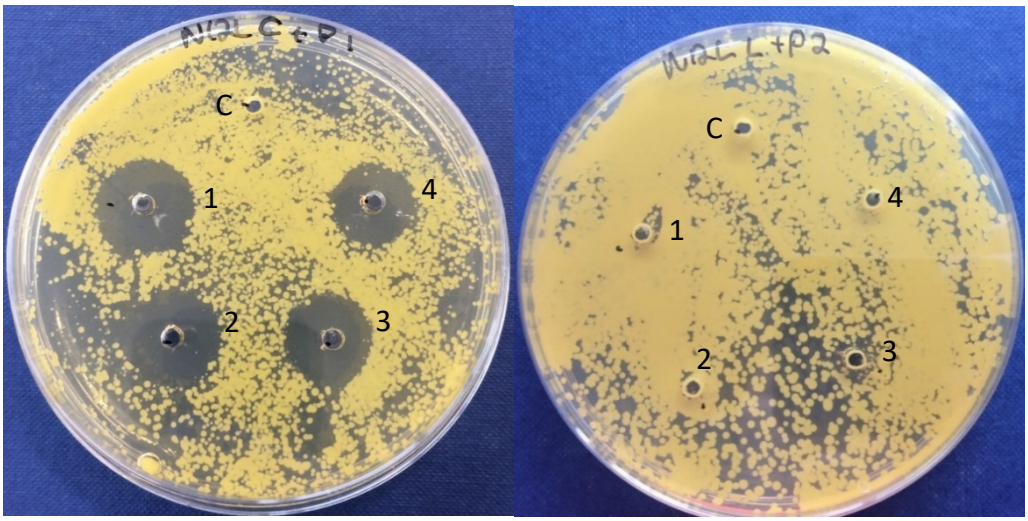

Figure 4.1.5: Images taken of agar plates with M. luteus and treated with cyclic N12L (left) and linear N12L (right), in the presence of PGLa. HPLC water was present in wells labelled 'C' as a control. The peptide applied in wells 1-4 was highest to lowest in concentration.

4.2 Broth Dilution Assays against *Listeria* and *Staphylococcus*

Broth dilution assays were completed with foodborne pathogenic bacteria to determine how broad the inhibition spectrum of N12L is.

Staphylococcus epidermis, two strains of *S. aureus* and three strains of *L. monocytogenes* were treated with two concentrations (1.5 and 0.75 mg/ml) of linear and cyclic N12L. The microtiter plate was filled according to table 4.2.1.

Table 4.6: Layout of microtiter plate for broth dilution assay. Strains 1-3 were L. monocytogenes, strains 4-5 were S. aureus and strain 6 was S. epidermis. Dilutions 1 and 2 contained peptide at 1.5 and 0.75 mg/ml, respectively.

	Cyclic N12L					
	1	2	3	4	5	6
A	Media Blank					
B	STRAIN 1 DIL 1	STRAIN 1 DIL 2	STRAIN 4 DIL 1	STRAIN 4 DIL 2	STRAIN 1 CTRL	STRAIN 4 CTRL
C						
D	STRAIN 2 DIL 1	STRAIN 2 DIL 2	STRAIN 5 DIL 1	STRAIN 5 DIL 2	STRAIN 2 CTRL	STRAIN 5 CTRL
E						
F	STRAIN 3 DIL 1	STRAIN 3 DIL 2	STRAIN 6 DIL 1	STRAIN 6 DIL 2	STRAIN 3 CTRL	STRAIN 6 CTRL
G						
H	Media Blank					
	Linear N12L					
	7	8	9	10	11	12
A	Media Blank					
B	STRAIN 1 DIL 1	STRAIN 1 DIL 2	STRAIN 4 DIL 1	STRAIN 4 DIL 2	STRAIN 1 CTRL	STRAIN 4 CTRL
C						
D	STRAIN 2 DIL 1	STRAIN 2 DIL 2	STRAIN 5 DIL 1	STRAIN 5 DIL 2	STRAIN 2 CTRL	STRAIN 5 CTRL
E						
F	STRAIN 3 DIL 1	STRAIN 3 DIL 2	STRAIN 6 DIL 1	STRAIN 6 DIL 2	STRAIN 3 CTRL	STRAIN 6 CTRL
G						
H	Media Blank					

As can be seen in figure 4.2.1, linear N12L displayed no inhibition against *L. monocytogenes*, and only moderate or no inhibition against *Staphylococcus* spp. In contrast, cyclic N12L showed full inhibition against all three strains of *L. monocytogenes* tested at the higher concentration (1.5 mg/ml). The lower concentration (0.75 mg/ml) increased the lag phase for two out of three *Listeria* strains. *L. monocytogenes* strain 2 was more sensitive to cyclic N12L and full inhibition is displayed at both concentrations. This is in line with the inhibition observed when nisin is applied.

Cyclic N12L also completely inhibited the growth of *S. aureus* at the higher concentration and supressed growth at the lower concentration. *S. epidermis* was fully inhibited at both concentrations.

Figure 4.2.1: OD_{620} measured every hour for 24 hours. Microtiter plate layout as shown in table 4.2.1. Green = complete inhibition, yellow = moderate inhibition, red = no inhibition and dashed purple = inconclusive.

These activity trials show that cyclic N12L is active against *M. luteus*, *Staphylococcus* spp. and *L. monocytogenes*. Linear N12L is mostly inactive, but some inhibition is seen against *S. aureus* and *S. epidermis*. The agar diffusion activity assays suggest that the target domain of linear N12LM2 and N12DM2 hinders activity, which is somewhat recovered upon the addition of PGLa. It is likely that the targeting domains of these peptides are interacting with possible membrane targets and this prevents the magainin II domain from forming pores.

Chapter 5 Haemolytic Activity of Chimeric Peptides

It is vital to assess the haemolytic properties of antimicrobial candidates that are intended for use therapeutically or for food preservation. As the chimeric peptides contain the pore forming component magainin II, analysing their haemolytic activity is essential. The N12(L/D) domain may assist bacterial targeting and it is important to evaluate the effect this has upon addition to red blood cells (RBCs).

5.1 Haemolytic Assay Development

Otvos *et al* 2005 reported haemolysis of human RBCs when treated with 160 µM magainin II. The starting concentrations for this study were calculated based on this, we used defibrinated sheep's blood instead of human RBCs. [136] Approximately 200 µM (0.5 mg/ml) magainin II and 175 µM (0.5 mg/ml) melittin were trialled against defibrinated sheep's blood. Since no lysis was observed in the presence of magainin II at the highest concentration, the concentration was increased further to 4.1 mM, then to 8.1 mM and finally 16.2 mM (figure 5.1.1).

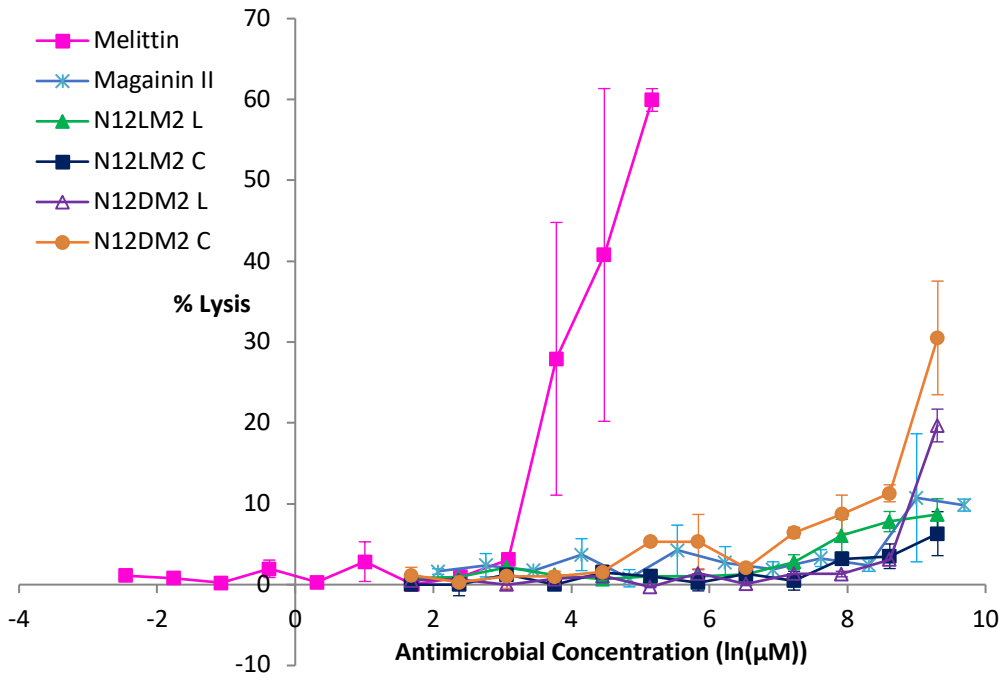

Figure 5.1.1: Percentage lysis of defibrinated sheep's blood observed against the natural logarithm of antimicrobial applied. 100% lysis was determined by the addition of distilled water to blood cells; lysis caused by AMP present was measured as a percentage of this values. Assay completed with duplicate repeats measured in triplicate. Error bars display standard error.

The highest percentage haemolysis was caused by melittin and reaches 59.9% at 175 µM. Haemolytic activity observed when cyclic and linear N12DM2 were present at 11.0 mM was 30.5% and 19.7%, respectively. Magainin II displayed haemolysis of 9.8% at 16.2 mM, slightly higher than the 8.7% and 6.3% observed for linear N12LM2 and cyclic N12LM2 at 11.0 mM, respectively. These lytic percentages are reported with concentrations of peptides and magainin II at 40 mg/ml. Magainin II displays antimicrobial activity at 1.5 mg/ml (table 4.1.1). If the peptide concentrations required for antimicrobial activity are lower than 40 mg/ml they will achieve the aim of being active, but not haemolytic. All peptides are more than two orders of magnitude less haemolytic than melittin. Nisin is

not a haemolytic AMP, it was considered for these trials however is not soluble at comparable concentrations.

The difference between N12LM2 and N12DM2 is one of chirality. In N12LM2 Cys3 and Cys7 are in the L form, whereas N12DM2 contains D form Cys3 and Cys7. This difference in conformation may cause the variation in haemolytic percentages when added to sheep RBCs. Both linear and cyclic N12DM2 displayed slightly higher haemolytic activity than magainin II, whereas both linear and cyclic N12LM2 demonstrated lower haemolysis. In general, haemolytic percentages for the peptides were similar to magainin II and considerably lower than those observed when treated with melittin (figure 5.1.1). This study, however, may not reflect the haemolytic nature of the peptides when applied to RBCs from various species and in particular humans. The phosphatidylcholine (PC) content in sheep RBCs is 1.6% compared to the ~40% present in human RBCs. Other phospholipids in RBC membranes, such as phosphatidyl- ethanolamine and serine, are present at similar percentages in both species. This significant difference in PC may affect the interaction of the peptides with the RBC membranes. Despite this, these results are very promising. Any candidate peptide displaying antimicrobial activity against a broad spectrum of bacteria will undergo thorough haemolysis testing against human RBCs and any other relevant species before being considered for industrial application. [137]

Chapter 6 Target Engagement

The current understanding is that nisin acts in a lipid II-dependent way. Nisin has been shown to bind lipid II primarily through the pyrophosphate region, with an additional nisin binding the MurNAc motif. [16] [36] The new epitopes were designed to engage lipid II as well. To investigate this, we employed several techniques to determine the specific interaction of the novel peptides with lipid II and its components, including small angle x-ray scattering, circular dichroism and vesicle leakage.

6.1 Small Angle X-ray Scattering (SAXS)

SAXS involves x-rays being passed through a sample, then measuring the degree of scattering of these x-rays. The resultant varying angle correlates to the size and shape of the particle in solution. This technique is used to determine the structure of particles in solution and can also be used to assess target interaction. The idea is to dock the peptides to the target *in silico* then fit the corresponding scattering profiles. The model that best fits the scattering profile determines if interaction is occurring.

All peptides and target are soluble in water until they are mixed. Figure 6.1.1 (E) shows substantial precipitation, indicating that cyclic N12LM2 and isopentenyl pyrophosphate (I-PP) interact causing a decrease in solubility. Slight precipitation is displayed with linear N12L and I-PP, this can be seen in figure 6.1.1 (D). As precipitation occurred it was not possible to generate scattering profiles and assess the behaviour of these peptides with I-PP in solution using

SAXS, although due to the precipitation it is clear that cyclic N12LM2 interacts with I-PP. It is also possible that linear N12L interacts with I-PP to some extent.

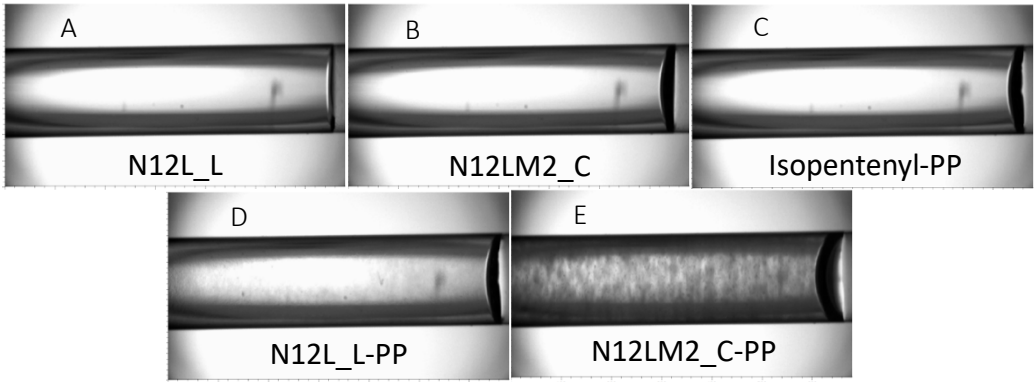

Figure 6.1.1: Images of capillary with samples injected for SAXS. Capillaries contain 30 µl of sample (5.6 mM). Linear N12L (A), cyclic N12LM2 (B), isopentenyl pyrophosphate (C), linear N12L with isopentenyl pyrophosphate (D) and cyclic N12LM2 with isopentenyl pyrophosphate (E).

6.2 Circular Dichroism (CD)

CD is a powerful biophysical tool. It can be used to determine target engagement of smaller peptides. The peptide and target CD profiles can be measured independently, then used to calculate the predicted spectra for non-interacting species. These spectra can then be compared to the actual recorded spectra of the mixed samples; variation indicates binding. Circularly polarised light is utilised to measure CD. A source of monochromatic linearly polarised light is passed through a dynamic quarter-wave plate to produce left and right-handed polarised light (L-CPL and R-CPL). These are then passed through a circularly dichroic sample. The difference in absorption of L- and R-CPL results in elliptically polarised light, which is measured as circular dichroism (figure 6.2.1). CD can be expressed in absorbance units and equations allow conversion (figure 2.13.1). CD is measured over a range of wavelengths, typically 180-260 nm (far-UV). This method has applications including secondary structure determination, assessment of thermal stability of proteins and analysis of target interaction. [138] [139]

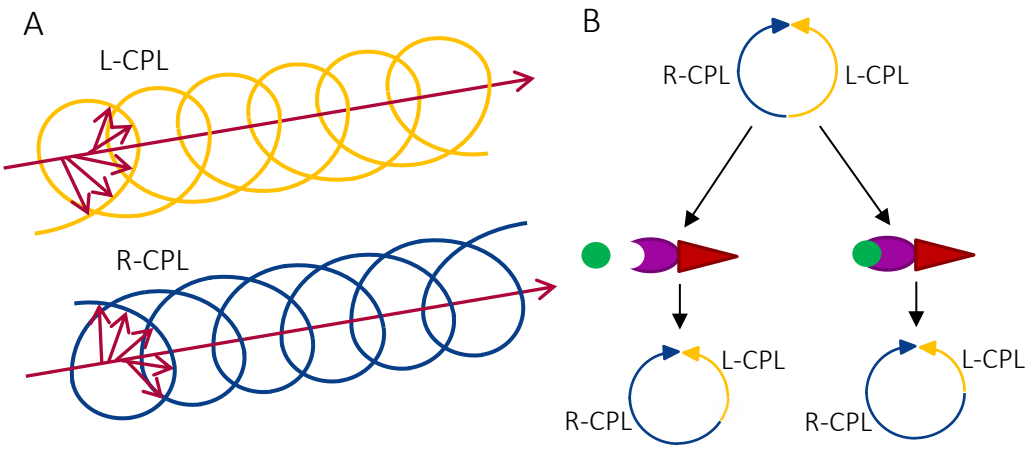

Figure 6.2.1: Basic principles of CD. Left and right-handed circularly polarised light (A). An example is also included of both interaction and no interaction and the differing effect on CD (B). Example includes schematic of a peptide, divided into target engaging (purple) and pore forming (red) domains, and the target MurNAc-dipeptide (green).

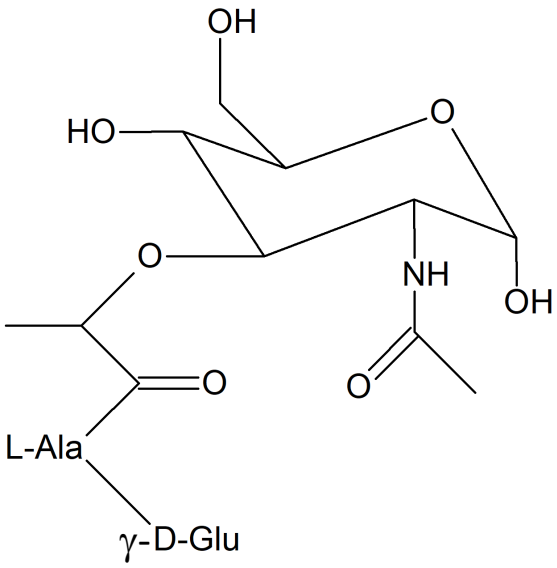

Figure 6.2.2: Structure of MurNAc-dipeptide.

MurNAc-dipeptide is a structure present in lipid II (figure 6.2.2). We hypothesise that the target domain of the peptides interacts with lipid II. MD simulations have shown that nisin interacts with the pyrophosphate and MurNAc domains of lipid II. [36] To further assess the novel peptides' interaction with specific domains of lipid II, interaction with MurNAc-dipeptide was monitored using this technique. To determine if interaction is occurring, the actual CD of the sample

containing target and peptide must be compared to the predicted CD of these components being present with no interaction (figure 6.2.1). Therefore, the CD of each component was measured in isolation and the data combined to give a predicted spectra, this is compared with the spectra when mixed (figure 6.2.3).

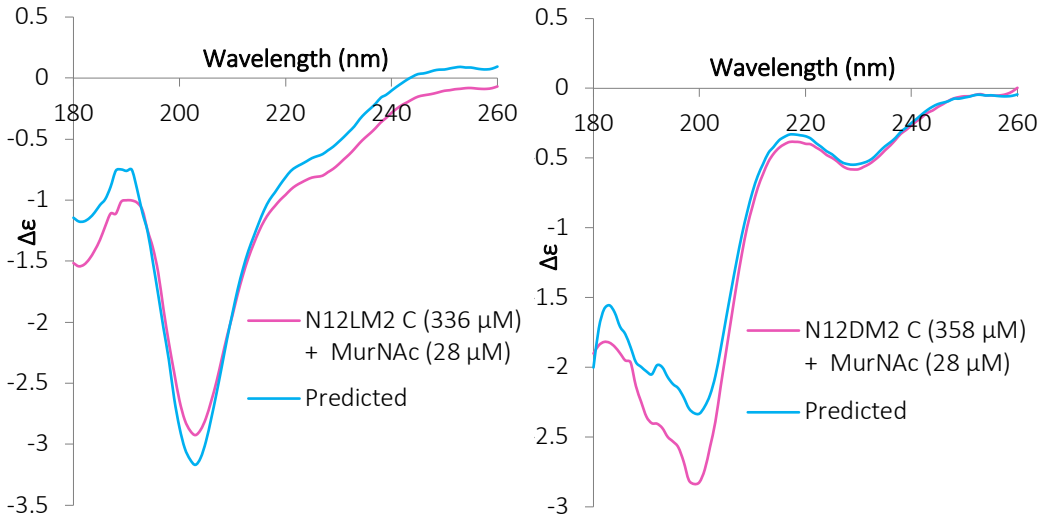

Figure 6.2.3: The Δε of both actual and predicted samples containing cyclic N12LM2 + MuNAc-dipeptide (left) and N12DM2 + MurNAc-dipeptide (right), in water at 20°C.

A significant difference is seen at ~200 nm for cyclic N12DM2 in the presence of MurNAc-dipeptide, suggesting interaction is occurring. In contrast cyclic N12LM2 with target follows the predicted spectra closely. As an increase in thermal stability can indicate binding, thermal melts of the components were completed.

To predict thermal stability CD spectra for a mixture of non-interacting peptide and target, the components were assessed individually over a temperature range (figure 6.2.4). The spectra for MurNAc-dipeptide alter significantly when 90°C (light blue) is reached, becomes disordered at 94°C (red) and remains disordered once the temperature was returned to 20.1°C (green). This indicates

that MurNAc-dipeptide is not stable at 94°C and does not regain its structure if cooled to 20.1°C.

This is not the case for both peptides. Cyclic N12LM2 remained very stable over the entire temperature range. Cyclic N12DM2 displayed some fluctuation at ~200 nm and below, but ultimately once returned to 20.1°C demonstrated a similar CD to that observed at the starting temperature of 20°C. This shows that the peptides are thermally stable and MurNAc-dipeptide is not.

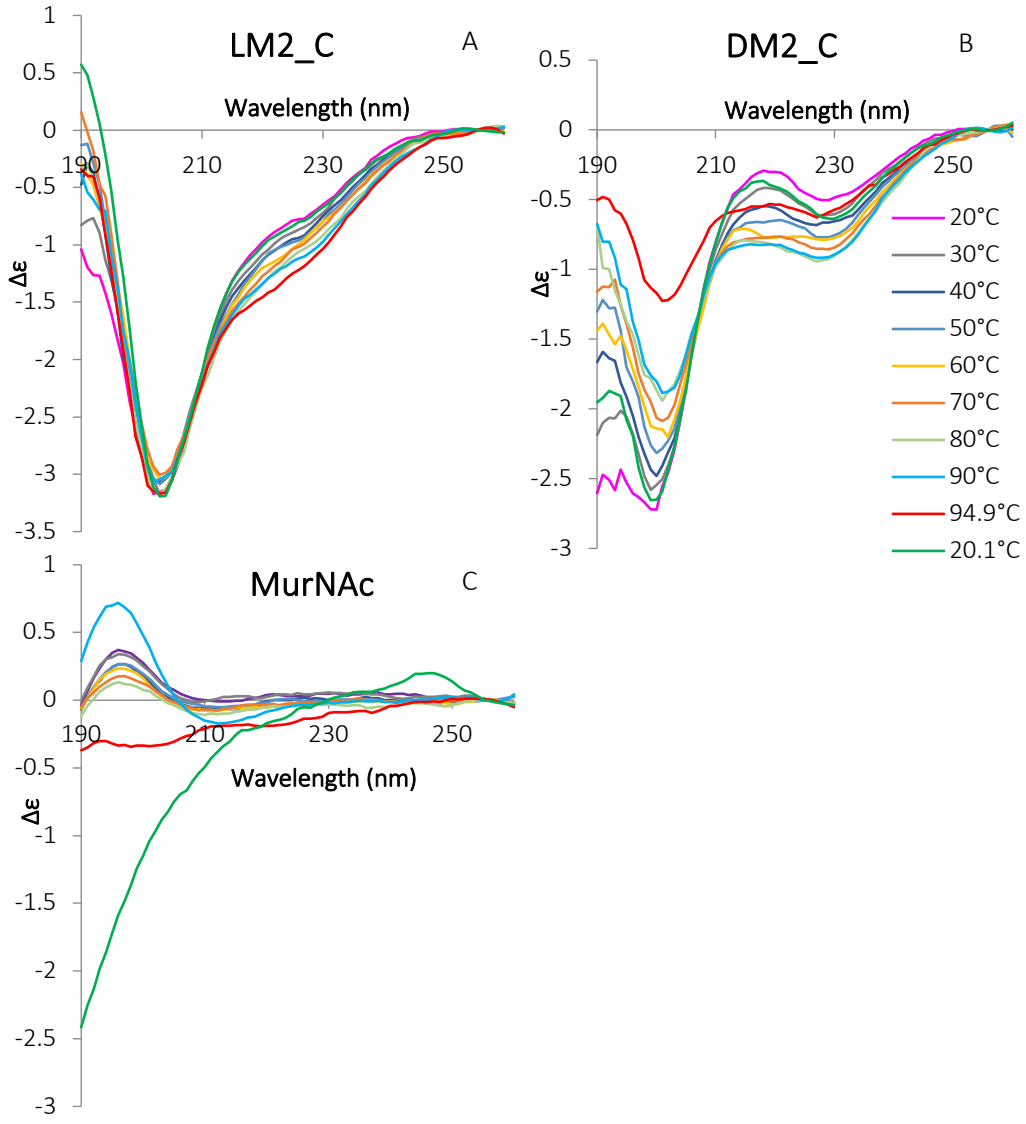

Figure 6.2.4: The Δε of cyclic N12LM2 (A), cyclic N12DM2 (B) and MurNAc-dipeptide (C) at various temperatures.

Actual spectra show that cyclic N12LM2 with target appears to be more stable over the entire temperature range than cyclic N12DM2 with target (figure 6.2.5). However, the former also seems to follow the predicted spectra for no interaction, except for 20.1°C. In this case it is most likely that the target becomes disordered as seen in figure 6.2.4 (C). Some evaporation of the sample was also observed once the cell was recovered, which may explain this difference.

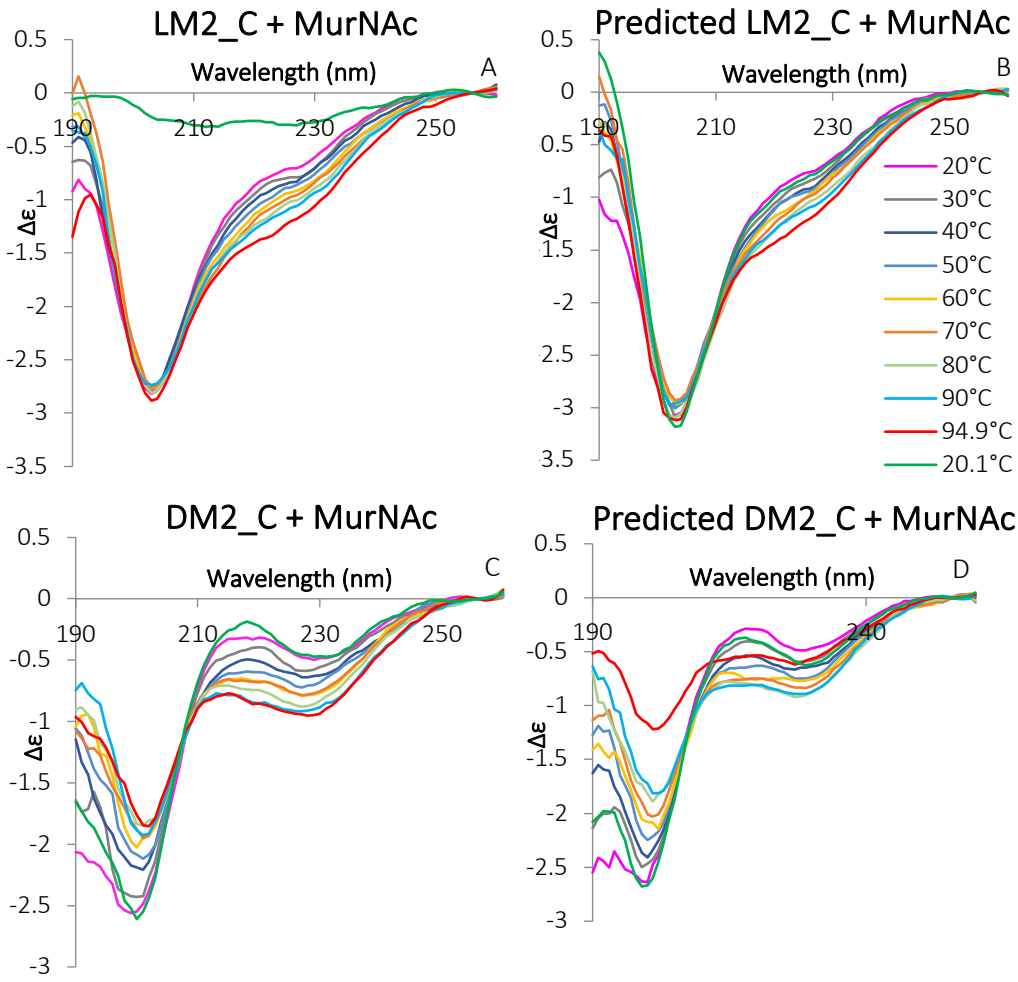

Figure 6.2.5: Thermal melts of cyclic N12LM2 + MurNAc-dipeptide (A) and cyclic N12DM2 + MurNAc-dipeptide (C) with corresponding predicted thermal stability spectras (B and D).

Cyclic N12DM2 with MurNAc-dipeptide seems to be more stable than predicted at ~200 nm especially at the highest temperature (figure 6.2.5). This indicates that the probable interaction helps to stabilise the target.

6.3 Carboxyfluorescein Leakage

Carboxyfluorescein containing vesicles can be used to evaluate the membrane lytic properties of compounds. These vesicles can be comprised of varying lipid compositions and carefully selected membrane anchored targets, in order to investigate specific hypotheses. In this case, geranyl geranyl pyrophosphate (GGPP) and lipid II were added to vesicles comprised of DOPC. This allows the evaluation of the necessity of pyrophosphate or MurNAc-dipeptide for interaction, as the latter is present in lipid II but not GGPP (figure 6.3.1).

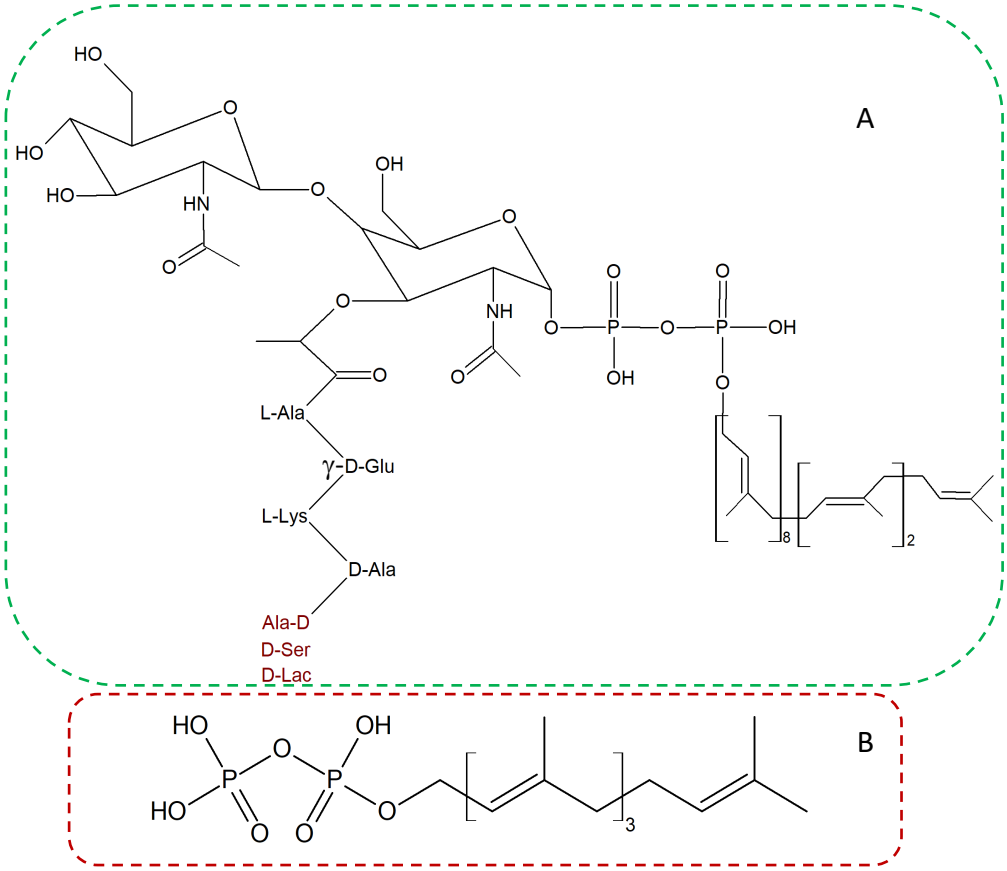

Figure 6.3.1: Structure of lipid II (A) and geranyl geranyl pyrophosphate (B).

This preliminary data displays an interesting trend. Previous published data indicates that nisin causes increased leakage when lipid II is present, which is confirmed see figure 6.3.2. [140]

Interestingly an inverse relationship is displayed when applying cyclic N12DM2. There is a significant decrease in leakage when lipid II is present, indicating that the peptide is interacting with lipid II. This interaction then impacts on the ability of the AMP to insert into the membrane. This decrease in leakage is not observed in the presence of GGPP, suggesting that cyclic N12DM2 does not interact with the pyrophosphate in the same way.

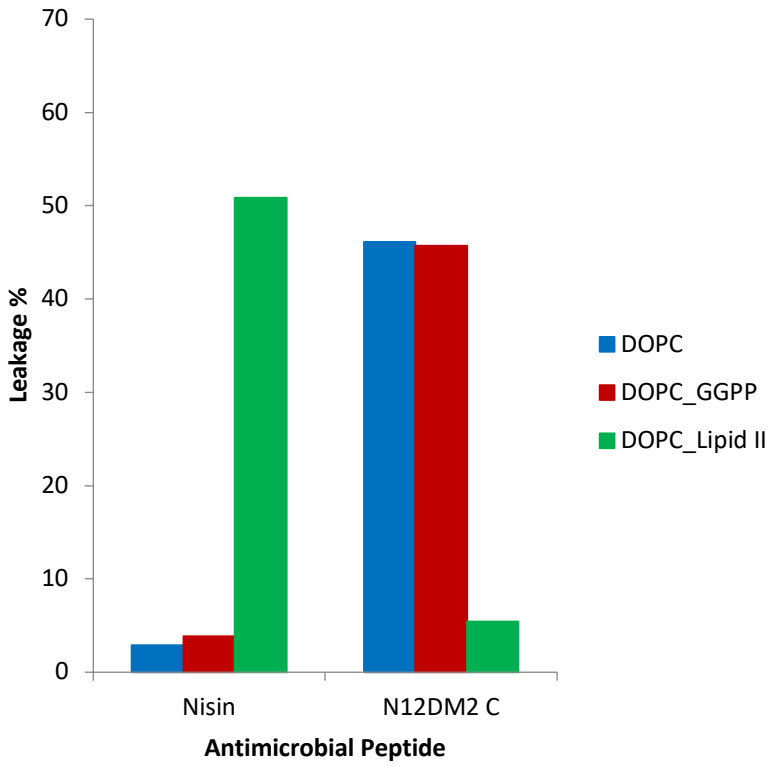

Figure 6.3.2: Percentage CF release from vesicles when AMP is applied. 100 % leakage is determined by treating vesicles with 80 % triton-X100. Vesicles consisted of 1,2-Dioleoyl-sn-glycero-3-phosphocholine (DOPC), DOPC and 2 % geranylgeranyl pyrophosphate (GGPP) or DOPC and 2 % lipid II.

The capillary images from the SAXS beamline indicate that cyclic N12LM2 and possibly linear N12L interact with I-PP. The target engaging section of cyclic N12LM2 may be interacting with the pyrophosphate to cause insolubility. The varying levels of insolubility observed demonstrates that full cyclisation of N12L may be essential for substantial interaction. The CD data shows thermally stable interaction of cyclic N12DM2 with MurNAc-dipeptide, whereas cyclic N12LM2 does not. The leakage data suggests that cyclic N12DM2 does not interact with pyrophosphate but does interact with lipid II. This supports the CD findings that cyclic N12DM2 interacts with the MurNAc-dipeptide domain of lipid II. Upon interaction, the activity of the peptide is hindered and significantly reduced leakage is observed. In conclusion, the chiral forms of Cys3 and Cys7 are integral to the mechanism of interaction. Cyclic N12L containing peptides display interaction with pyrophosphate but not with MurNAc-dipeptide. Whereas cyclic N12DM2 displays interaction with MurNAc-dipeptide but not with pyrophosphate.

Chapter 7 Fluorescence Microscopy of *B. subtilis* treated with Fluorescently-Tagged Compounds

Fluorescence microscopy allows the excitation of specific fluorophores and monitors the light emitted. This technique can be used to excite and monitor the emission of multiple fluorophores present. It was employed here to investigate the distribution of fluorescently-tagged peptides when added to *B. subtilis*.

The basic arrangement of components in a fluorescence microscope is shown in figure 7.1. In confocal microscopy a laser is the light source. A filter is used to allow only the excitation wavelength from the laser through to the sample. The dichroic mirror then reflects the filtered excitation laser light through the objective to the sample. The objective acts to focus the light onto the sample, where excitation of the sample occurs. The specific fluorophore present enters the excited state and emits light at the emission wavelength, as it returns to its ground state. The emitted light passes back through the objective and the dichroic mirror. Due to the differing wavelengths, the emission light is not reflected. The light then passes through an emission filter which allows only the emission wavelength to pass through to the detector. This prevents any reflected excitation light from reaching the detector and obscuring the image. [138]

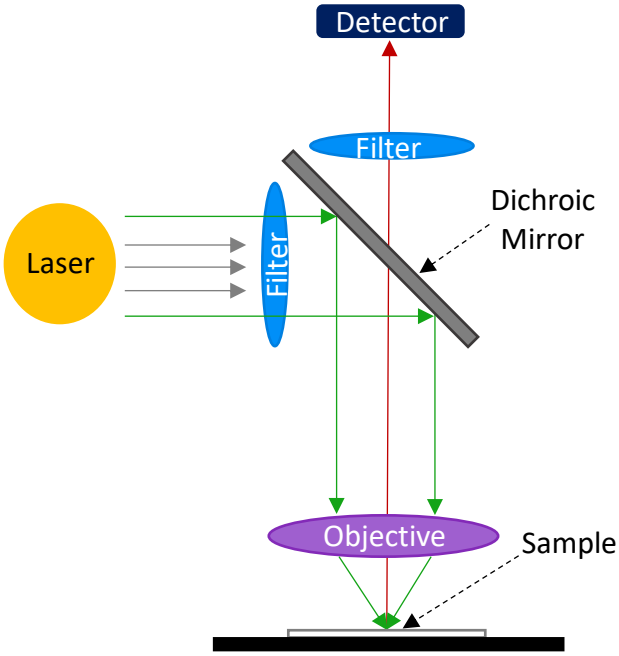

Figure 6.3.1: Configuration of a fluorescence microscope.

7.1 Method Validation: BODIPY-Vancomycin Fluorescence

Fluorescent tagging of AMPs and antibiotics, like vancomycin, has been used previously to visualise their interaction with bacteria. Specifically, the interaction of fluorescently tagged (FT) vancomycin with *B. subtilis* has been assessed. Tiyanont *et al* 2006 found that when the bacteria were treated with 1:1 vancomycin and BODIPY-vancomycin staining of the septa was more substantial and some helical wall staining was observed. [125] Hasper *et al* 2006 also treated *B. subtilis* with a FT-vancomycin and observed a similar binding pattern. [141] Daniel and Errington 2003 evaluated the changes in localisation of fluorescence through the cell cycle of *B. subtilis*. These images showed clear accumulation of the FT-vancomycin at septa during division. [142]

We hypothesise that our antimicrobial peptides interact with lipid II through a mechanism similar to that of nisin. Although vancomycin interacts with lipid II through a differing mechanism its thoroughly documented use in fluorescence microscopy makes it an ideal candidate for validating a protocol for these studies. Using the methods detailed in Daniel and Errington 2003, Hasper *et al* 2006 and Tiyanont *et al* 2006 a new protocol was developed to assess the binding of the novel peptides to *B. subtilis*.

The vancomycin experiment displayed the same interaction pattern as shown in the previous experiments. [125] [141] [143] [144] Clear labelling of the septa can be seen, indicating the accumulation of BODIPY-vancomycin here. Slight helical wall staining is also displayed (figure 7.1.1).

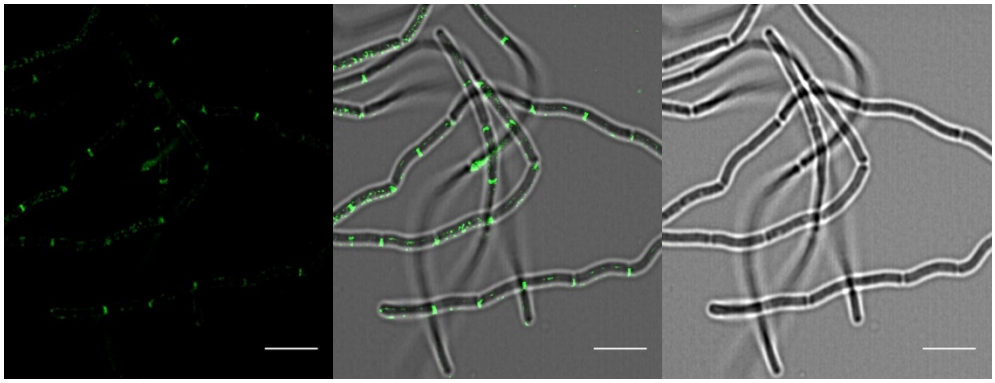

Figure 7.1.1: B. subtilis treated with vancomycin and BODIPY-vancomycin (1:1). Images displayed are fluorescence only (left) composite (middle), and phase contrast (right). Scale bars represent 5 µM.

7.2 TAMRA-tagged Peptide Fluorescence

Fluorescently tagged versions of the short N12L and N12D peptides were generated in order to visualise their distribution when added to *B. subtilis*. An additional lysine was added to the C-terminus for the TAMRA tag to attach to, leaving the lysine in position 12 free to engage the target (table 2.1.1). To determine the forms of these TAMRA-tagged peptides used in this assay electrospray mass spectrometry was completed. This method provides mass values accurate up to four decimal places (figure 7.2.1). These data indicate that both tagged N12L and N12D are in the semi-cyclic state, although the specific cysteines involved in this ring formation are unknown.

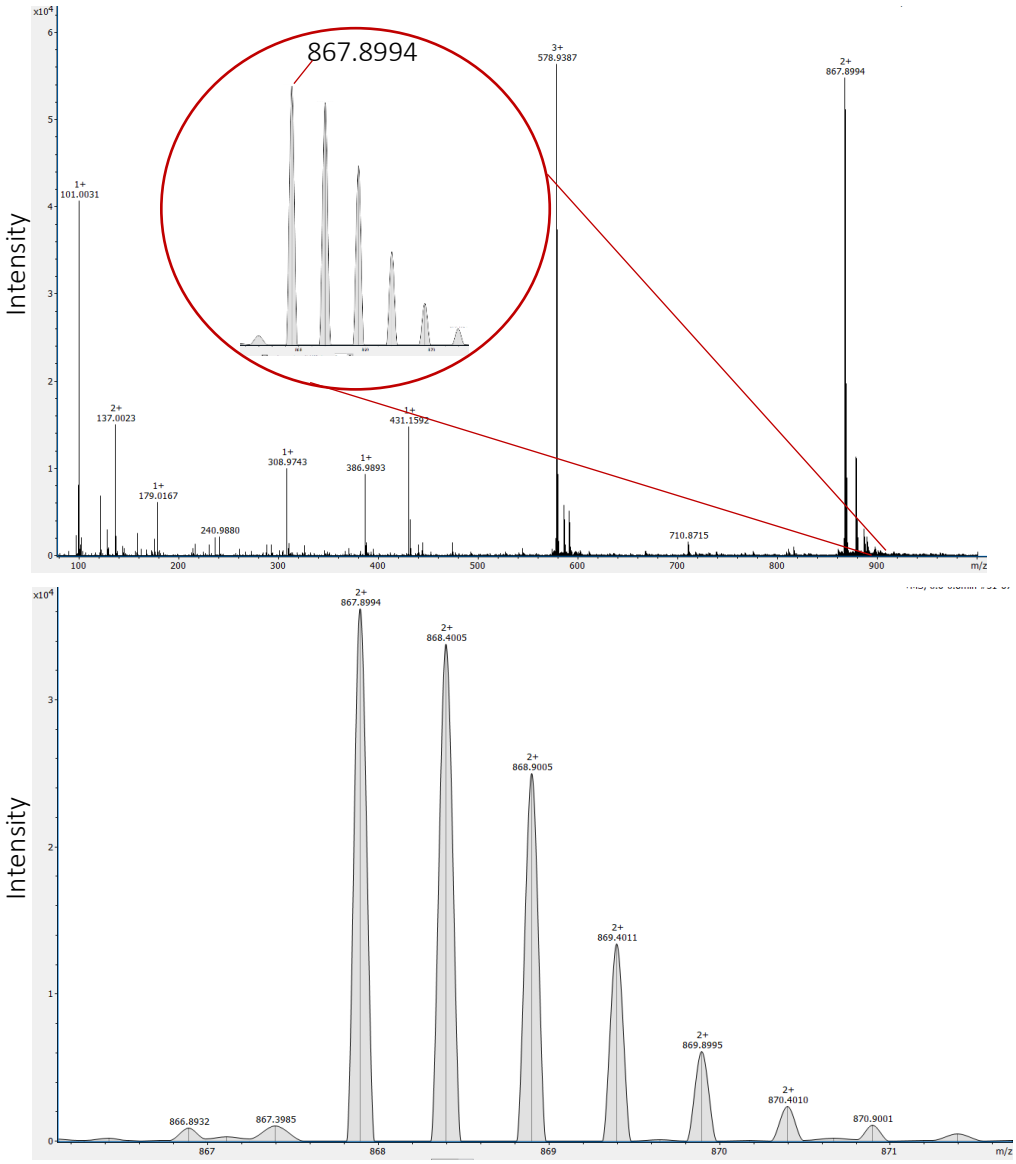

Figure 7.2.1: ESI spectra. N12D-TAM broad and zoomed (top), zoomed only for N12L-TAM (bottom).

B. subtilis is a safe Gram-positive, rod-shaped species ideal for microscopy studies. In order to visualise varying growth phases of *B. subtilis* when treated with fluorescently tagged peptide, the optical density of the bacteria was measured over 8.5 hours. This allows for accurate determination of the growth phase of the *B. subtilis* used in each assay.

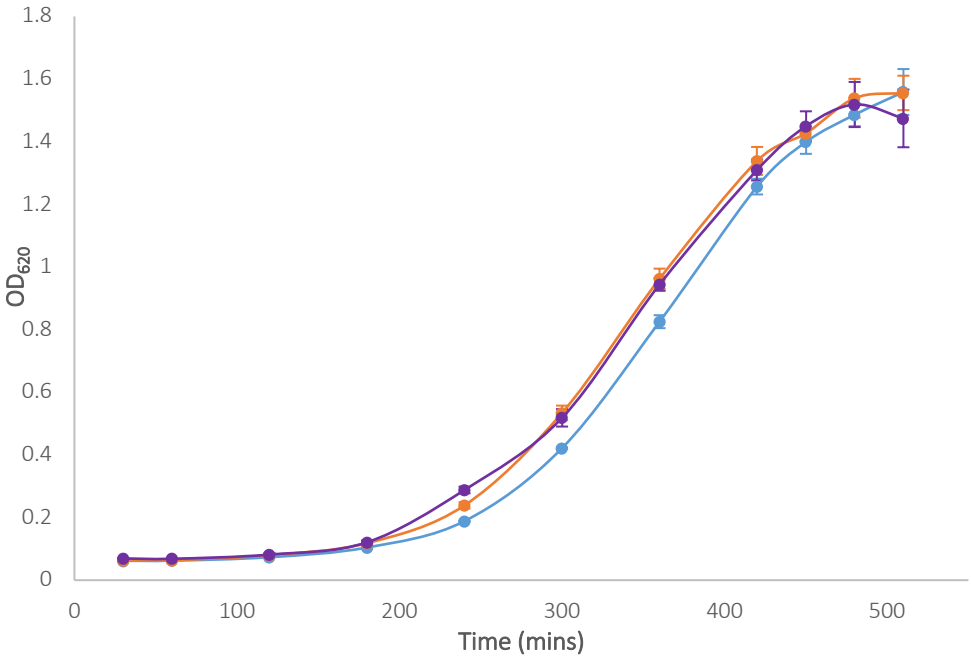

Figure 7.2.2: Growth curves for B. subtilis at 35°C. Three cultures were monitored over 8.5 hours, OD measured in triplicate.

In line with the BODIPY-vancomycin experiment the bacteria were treated in early log phase. The method designed for BODIPY-vancomycin visualisation was optimised with respect to the TAMRA tag. The best results were observed when the incubation time was increased from 10 minutes to 30 minutes and also by introducing an extra wash step.

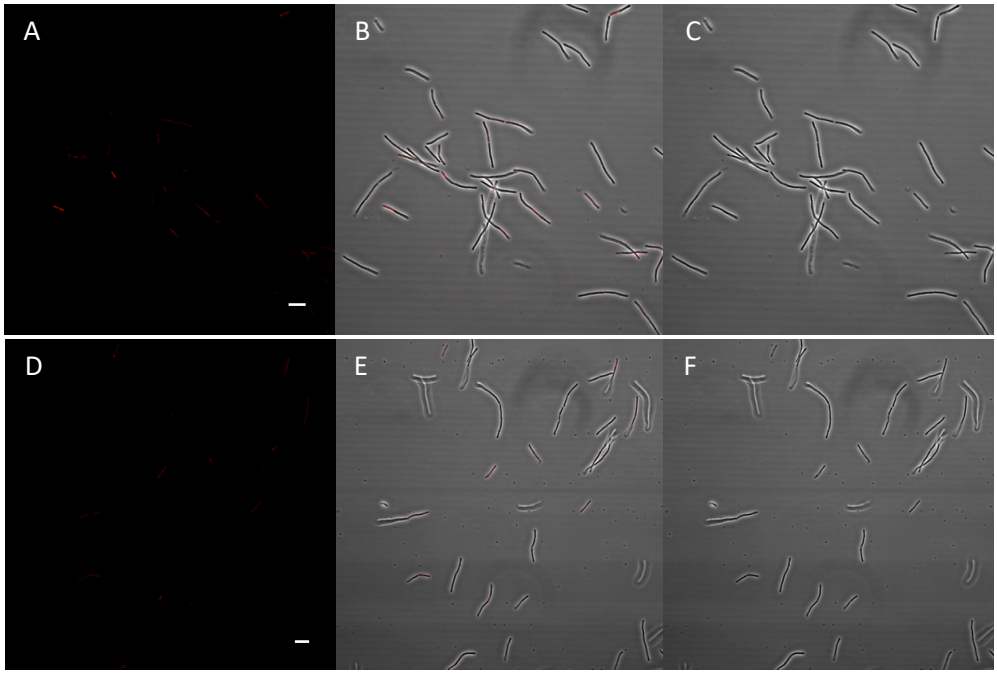

Figure 7.2.3: B. subtilis in log phase treated with N12L-TAM (top) and N12D-TAM (bottom). Images displayed are fluorescence only (A and D) composite (B and E), and phase contrast (C and F). Scale bars represent 10 µM.

BODIPY-vancomycin treated log phase bacteria have been shown to increase binding at the septa in the presence of non-tagged vancomycin (figure 7.1.1). Therefore, log phase *B. subtilis* were also treated with TAMRA tagged and non-TAMRA tagged peptide (1:1). This enabled the assessment and comparison of binding patterns.

Cells treated with N12L-TAM and N12D-TAM displayed some fluorescence. Often, an entire bacterium becomes bound by TAMRA tagged peptide, although not all bacteria in a spindle become labelled and the location of the labelled one is not specific at this magnification (figure 7.2.3 (B) and (E)). This may indicate a degree of self-association. A decrease in fluorescence in cells treated with N12D-TAM and N12D (1:1) resulted in almost no fluorescence in log phase (figure 7.2.4 (E)), whereas for corresponding N12L (1:1) similar levels of fluorescence are observed as for N12L-TAM only treatment (figure 7.2.4 (B) and

figure 7.2.3 (B)). To determine if this interaction is growth phase dependent stationary phase *B. subtilis* were also treated with the same peptides (figure 7.2.4 and figure 7.2.5).

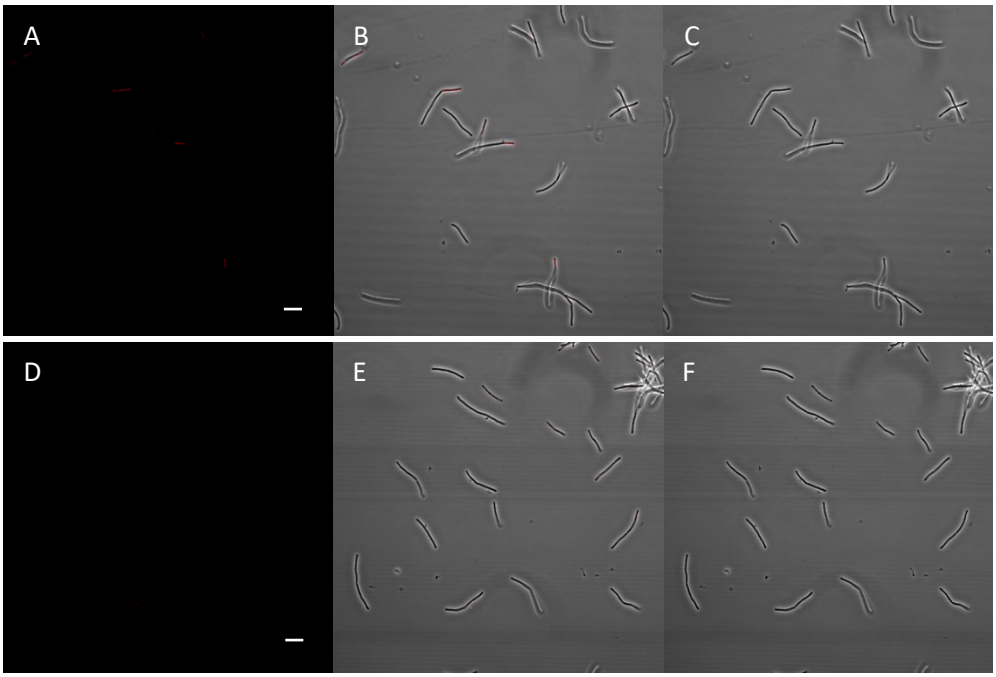

Figure 7.2.4: B. subtilis in log phase treated with TAMRA tagged and non-TAMRA tagged peptide (1:1) N12L-TAM (top) and N12D-TAM (bottom). Images displayed are fluorescence only (A and D) composite (B and E), and phase contrast (C and F). Scale bars represent 10 µM.

A similar pattern of fluorescence is seen for stationary phase *B. subtilis*. N12D-TAM and N12L-TAM (figure 7.2.5) show similar fluorescence distribution and intensity. When treated with N12L-TAM or N12D-TAM only the whole bacterium became labelled but entire spindles did not. However, in contrast to the labelling observed in log phase the fluorescence displayed for almost every treatment combination in stationary phase is substantially increased.

Interestingly 1:1 addition of N12L-TAM and N12L (figure 7.2.6) resulted in a significant reduction of fluorescence compared to N12L-TAM only treatment. This suggest that TAMRA tagged and non-TAMRA tagged peptide may compete to bind available pyrophosphate. The TAMRA tag could reduce target affinity by

contributing to steric hindrance. The comparable N12D images show that binding of N12D-TAM still occurs in the presence of non-tagged N12D, although the fluorescence observed is reduced (figure 7.2.6).

Perhaps a similar mode of interaction occurs in both log and stationary phase, but there is significantly less target availability in log phase for N12D. Application of N12L-TAM and N12L (1:1) to bacteria in log and stationary phase resulted in comparable levels of fluorescence (figure 7.2.4 (B) and figure 7.2.6 (B)). However, as the levels of fluorescence demonstrated in stationary phase for this treatment are already so low any further reduction in log phase would be very difficult to determine. In contrast treatment for N12L-TAM displayed noticeably reduced fluorescence when the cells where in log phase. This could be rationalised if there is a degree of target availability dependent on the growth phase for N12L, but not to the same extent as observed for N12D.

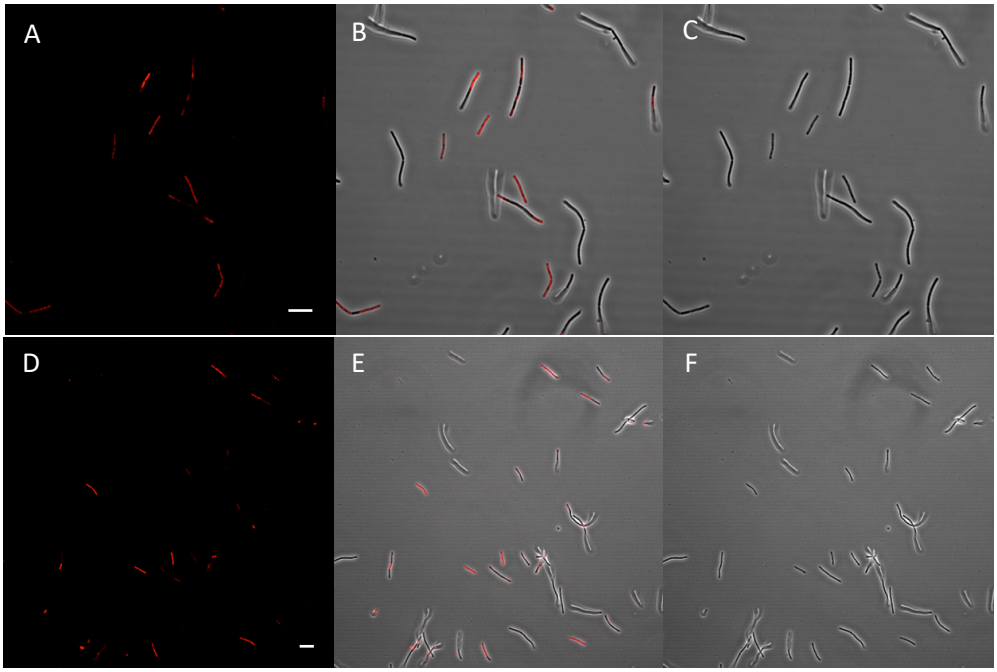

Figure 7.2.5: B. subtilis in stationary phase treated with N12L-TAM (top) and N12D-TAM (bottom). Images displayed are fluorescence only (A and D) composite (B and E), and phase contrast (C and F). Scale bars represent 10 µM.

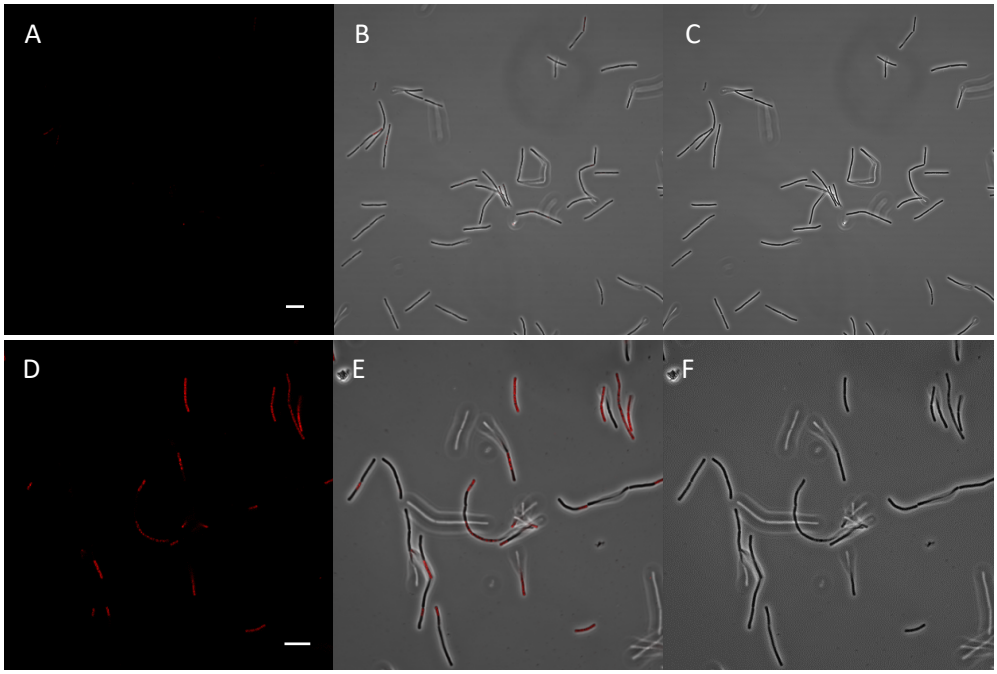

Figure 7.2.6: B. subtilis in stationary phase treated with TAMRA tagged and non-TAMRA tagged peptide (1:1). N12L-TAM (top) and N12D-TAM (bottom). Images displayed are fluorescence only (A and D) composite (B and E), and phase contrast (C and F). Scale bars represent 10 µM.

In contrast to the distribution of BODIPY-vancomycin, the TAMRA-tagged peptides did not show septal localisation under any conditions. Both of these semi-cyclic peptides were confirmed to bind *B. subtilis*, although most likely with varying targets. Increased interaction occurs for N12D-TAM when bacteria are in stationary phase, indicating that there is a degree of growth phase dependence. The fluorescence pattern displayed when bacteria are treated with N12D-TAM and N12D (1:1) is similar to that of N12D-TAM only for both growth phases. This suggests that the target of interaction is abundant and competitive binding is not an issue, whereas the opposite is observed for N12L. The target engagement studies indicate that N12L binds pyrophosphates and N12D binds MurNAc-dipeptide, which explains the variable patterns of binding observed in fluorescence microscopy.

Chapter 8 Discussion

The main aim of this work was to create a new platform for the development of novel AMPs inspired by those that occur in nature. Ideally, these novel peptides will have broad spectrum antimicrobial activity and low toxicity. The strategy involved designing a targeting motif modelled on nisin's first 12 residues, with the pore forming magainin II attached at the C terminus. We have characterised many properties of these peptides and gained insight into their mechanisms of interaction.

8.1 Preparation of Peptides and MD Simulations

The first two thioether rings of nisin are necessary for binding lipid II. We took an approach to assess the necessity of ring formation within these peptides. Preparation and purification of the linear and cyclic forms of all peptides was attempted. We encountered issues with the formation of cyclic monomers, with fractions often containing semi-cyclic, dimeric and trimeric forms. Monomeric cyclic N12D proved impossible to form experimentally. MD simulations revealed that for this linear peptide ring B (Cys8-11) or alternate rings A (Cys3-8) or B (Cys7-11) are the most likely to initially interact due to the proximity of the cysteines. Complete cyclisation of N12D with both alternate rings A and B is possible. Even though the formation of ring B is probable the following formation of ring A (Cys3-7) is not likely. The linear and semi-cyclic forms of N12D are soluble but attempts to fully cyclise resulted in precipitation and mass spectrometry indicated the presence of semi-cyclic, dimeric and trimeric peptide. It seems that increased ring formation leads to increased insolubility.

Cyclic monomers of N12DM2 could be purified. This shows that the solubility of the magainin II domain counteracts the lower solubility of the N12D domain when cyclisation occurs. It is likely that ring closure of N12DM2 results in the formation of alternate rings A and B.

The properties of N12L are less complex. Purification of the cyclic monomer was achieved and simulation data shows that two different conformations are possible. Either the formation of rings A (Cys3-7) and B (Cys8-11) or alternate rings A (Cys3-8) and B (7-11).

8.2 Antimicrobial Activity of N12L Containing Peptides

Agar diffusion activity assays proved that cyclic N12L is active against *M. luteus*, whereas its linear form is completely inactive. This trend is also observed for the broth dilution assays. At 1.5 mg/ml cyclic N12L showed complete inhibition against all three strains of *L. monocytogenes*. The lower concentration (0.75 mg/ml) of cyclic N12L caused complete inhibition of one strain and increased the lag phase of the other two. Linear N12L displayed no inhibition of *L. monocytogenes.* Cyclic N12L displayed full inhibition of both *S. aureus* strains at the higher concentration and moderate inhibition at the lower concentration. This cyclic peptide also demonstrated complete inhibition of *S. epidermis* at both concentrations. For linear N12L, moderate or no inhibition was observed when applied to *Staphylococcus* spp.

The agar diffusion assays also show that N12L demonstrates better activity than magainin II against *M. luteus*. It is also possible that this peptide has an even lower MIC against *M. luteus* but is limited by diffusion. The zones of inhibition formed were similar in size for a range of concentrations. This trend was seen

with peptide alone and when combined with PGLa. For treatment with PGLa, concentrations of cyclic N12L were half those used in the former assay, yet zone sizes where similar. This resulted in an MIC value of 45.9 μM, almost half the MIC value for cyclic N12L treatment alone.

8.3 Target Interaction of N12L Containing Peptides

As nisin interacts with lipid II via the pyrophosphate domain we completed experiments to determine if the mechanism of interaction was similar for this targeting motif. The cyclic form of N12LM2 has been shown to interact with I-PP by resulting in precipitation when mixed. The antimicrobial activity of N12L is dependent on completion of ring formation. However, some precipitation is observed when linear N12L is mixed with I-PP. It is possible that the interaction of linear N12L with I-PP is transient or weaker than when the peptide is cyclised. This would explain the inactivity of linear N12L.

To determine if there is a secondary site of interaction CD experiments were completed with cyclic N12LM2 and MurNAc-dipeptide, another lipid II component. It was shown that this peptide does not interact with MurNAc-dipeptide.

The fluorescence microscopy studies between *B. subtilis* and semi-cyclic N12L clearly showed that the peptide interacts with *B. subtilis* in the stationary phase. A similar pattern of fluorescence was observed in log phase, but overall fluorescence is less. This indicates that the target of interaction is more abundant when cells are in stationary phase. Treatment of the cells with N12L-TAM and N12L (1:1) resulted in reduced fluorescence, suggesting a degree of competitive binding.

Interestingly, both linear and cyclic N12LM2 are less haemolytic than magainin II, showing that addition of a targeting domain with all L form cysteines to magainin II reduces its haemolytic activity. In contrast, linear and cyclic N12DM2 display increased haemolytic activity, although still much lower than that of melittin.

8.4 Target Interaction of N12D Containing Peptides

The mechanism of interaction for the D form cysteine containing peptides differs from that of the L form containing peptides. The CD study revealed that cyclic N12DM2 interacts with MurNAc-dipeptide and that this interaction is thermally stable. Interestingly leakage assays showed considerable leakage for both DOPC and DOPC_GGPP containing vesicles when treated with cyclic N12DM2, this indicates that the presence of a pyrophosphate on the membrane surface has no effect on leakage. When vesicles were comprised of DOPC and lipid II molecules there was significantly reduced leakage upon treatment with cyclic N12DM2. The opposite trend is observed with nisin, increased leakage is observed only when lipid II is present. This confirms that cyclic N12DM2 interacts with the MurNAc-dipeptide domain of lipid II and that this binding prevents the peptide from inserting into the membrane.

This mechanism of interaction is consistent with the activity data. Linear N12DM2 is shown to be inactive against *M. luteus*, revealing that this peptide is most likely binding MurNAc-dipeptide in its linear form as well as its cyclic form.

8.5 Fluorescence Microscopy of N12D-TAM

The fluorescence microscopy with semi-cyclic N12D displayed a similar trend as semi-cyclic N12L. Extensive binding of *B. subtilis* was observed in stationary phase and, to a lesser extent, cells in log phase. When treated with N12D-TAM and N12D (1:1) no change in fluorescence was observed, signifying that for this peptide competitive binding is not an issue.

Increased cross-linking of muropeptides occurs in stationary phase, this may have some bearing on the increased binding of N12D-TAM. [145] It is difficult to understand the specific reasons for increased interaction in stationary phase. For example, one possibility involves autolytic enzymes that are responsible for recycling peptidoglycan. It has been shown that during vegetative growth peptidoglycan turnover occurs at over 50 % during each generation and results in fragments being recycled or released into the medium and that this recycling is essential for the survival of stationary phase *B. subtilis.* [146] [147] This process could have some effect on the binding of N12D-TAM.

8.6 Pore Formation of Magainin II

When linear N12DM2 was combined with PGLa activity against *M. luteus* was displayed. Treating the bacteria with a combination of magainin II and PGLa shows a similar trend that is well-documented. [96] It seems that PGLa helps to overcome the interaction of linear N12DM2 with MurNAc-dipeptide that is causing the inactivity. PGLa interacts with the magainin II domain of the peptide and aids membrane insertion. Increased activity is also observed when PGLa is combined with linear N12LM2. Alone this peptide is inactive however

combination with PGLa results in some activity against *M. luteus* at the two highest concentrations.

We have shown that adding a targeting domain to magainin II hinders its activity. Research into the mechanism of action revealed that magainin II is hypothesised to act as an antiparallel dimer, to induce the formation of toroidal pores. [148] [97] Although visualisation of these toroidal pores has not been possible, indirect experimental evidence and *in silico* modelling supports this theory. [97] [149] The MD simulations involved monitoring the formation of pores when either magainin II or melittin was added to lipid bilayers. For the formation of a magainin II induced toroidal pore, as many as 17-18 monomers were found to associate. These simulations have shown the formation of a small pore that becomes larger as more magainin II monomers aggregate and expand the pore. In contrast, melittin induced pores contained 4-6 monomers and no further aggregation or expansion was displayed. [149]

Addition of an N-terminal targeting domain, present in N12L/DM2, prevents the theorised antiparallel association of magainin II monomers and subsequent pore formation. PGLa and magainin II form and act through a 1:1 association. [150] Inclusion of PGLa in this activity study appears to overcome this factor and functions as a substitute for the N terminally membrane inserting magainin II.

It is possible to attach the targeting domain, N12L, to an alternate antimicrobial that has a pore forming mechanism of action. We designed a new chimeric AMP containing N12L and melittin (table 2.1.1). We have obtained the semi-cyclic form when aiming to linearise or cyclise. This is a promising new chimeric AMP; it is worth developing a reliable purification technique in order to assess

antimicrobial activity of its specific forms. The mechanism of action of melittin has been shown to require less monomers for pore formation than magainin II and does not act through an antiparallel mechanism.

8.7 Future Directions

A key achievement of this study was the identification of cyclic N12L as a viable and effective antimicrobial. We have shown that, like the first two rings of nisin, this peptide interacts with pyrophosphates. N12L also requires ring closure to be active.

The process by which N12L is cyclised currently involves DMSO and small scale HPLC. The chemicals involved in cyclisation and purification are similar to those required for purification of other short AMP, such as teixobactin. [32] It may be possible to develop an alternate cyclisation protocol not relying on DMSO that permits upscaling of production. *L. lactis* produces NisC, which cyclises nisin (figure 1.6.1). [42] This would be an ideal mechanism for N12L ring closure if a suitable enzyme could be produced.

We have shown that the chimeric peptides have low haemolytic activity. It is very unlikely that cyclic N12L has any haemolytic activity, due to its small size and similarity to nisin, which is non-haemolytic. Although cyclic N12LM2 shows clear interaction with pyrophosphate, target engagement studies could be completed to assess the specific binding of cyclic N12L. It would also be ideal to assess the binding patterns of TAMRA-tagged cyclic and linear N12L to *B. subtilis* and their antimicrobial activity against *M. luteus*. This may give an insight into the inactivity of linear N12L.

We have shown that nisin interacts with LPS causing destabilisation of the outer membrane. [124] Analysing any possible interaction of cyclic N12L and LPS would be interesting, given that our targeting motif is based on nisin.

Chapter 9 Conclusion

Despite several challenges, including the production of a reliable purification process, this work has yielded insightful information about the properties of these novel peptides. In particular, cyclic N12L has great potential as an antimicrobial. Table 9.1 provides an overview of the properties determined in this work. Although no candidate peptide displayed comparable activity to nisin, this work can be used to inform the creation of alternative chimeras.

We have shown that it is feasible to engineer new antimicrobials based on the structure of existing AMPs, supporting the pursuit of novel compound design using this method.

Table 9.1: Overview of the properties of each peptide.

	Agar Diffusion Activity			Interaction		Leakage			Microscopy *(B. subtilis)*	
Peptides	Activity	Activity + PGLa	Haemolytic Activity	I-PP	MurNAc-dipeptide	DOPC	DOPC + GG-PP	DOPC + Lipid II	Log phase	Stationary phase
N12L L	Inactive	Inactive	-	Inc	-	-	-	-	-	-
N12L SC	-	-	-	-	-	-	-	-	Slight	Intermediate
N12L C	Active	Active	-	-	-	-	-	-	-	-
N12D L	Inactive	Inactive	-	-	-	-	-	-	-	-
N12D SC	-	-	-	-	-	-	-	-	Intermediate	Extensive
N12D C	-	-	-	-	-	-	-	-	-	-
N12LM2 L	Inactive	Active	< MagII	-	-	-	-	-	-	-
N12LM2 C	-	-	< MagII	Yes	No	-	-	-	-	-
N12DM2 L	Inactive	Active	> MagII	-	-	-	-	-	-	-
N12DM2 C	-	-	> MagII	-	Yes	High %	High %	Very low %	-	-

Bibliography

[1] J. O'Neill, "Tackling Drug-Resistant Infections Globally: Final Report and Recommendations," 2016.

[2] World Health Organisation, "Antimicrobial Resistance." [Online]. Available: https://www.who.int/antimicrobial-resistance/global-action-plan/database/en/. [Accessed: 16-Jan-2019].

[3] BBC, "Antibiotic Resistance Plan to Fight 'Urgent' Global Threat," 2019. .

[4] M. C. Erickson and M. P. Doyle, "The Challenges of Eliminating or Substituting Antimicrobial Preservatives in Foods," *Annu. Rev. Food Sci. Technol.*, vol. 8, no. 1, pp. 371–390, 2017.

[5] F. S. Agency, "EU Approved Additives and E Numbers," 2018. [Online]. Available: https://www.food.gov.uk/business-guidance/eu-approved-additives-and-e-numbers. [Accessed: 05-Nov-2018].

[6] J. C. Pederson, "Natamycin as a Funicide in Agar Media," *Am. Soc. Microbiol.*, vol. 58, no. 3, pp. 1064–1066, 1992.

[7] R. Coico, "Gram Staining," *Curr. Protoc. Microbiol.*, vol. Appendix 3, no. Appendix 3C, 2005.

[8] C. H. Hsu *et al.*, "Structural and DNA-binding studies on the bovine antimicrobial peptide, indolicidin: Evidence for multiple conformations involved in binding to membranes and DNA," *Nucleic Acids Res.*, vol. 33, no. 13, pp. 4053–4064, 2005.

[9] C. Chatterjee, M. Paul, L. Xie, and W. a van der Donk, "Biosynthesis and mode of action of lantibiotics.," *Chem. Rev.*, vol. 105, no. 2, pp. 633–84, 2005.

[10] A. Bateman *et al.*, "UniProt: The universal protein knowledgebase," *Nucleic Acids Res.*, vol. 45, no. D1, pp. D158–D169, 2017.

[11] D. Mengin-Lecreulx, L. Texier, M. Rousseau, and J. Van Heijenoort, "The murG gene of Escherichia coli codes for the UDP-N-acetylglucosamine:N-acetylmuramyl-(pentapeptide) pyrophosphoryl-undecaprenol N-acetylglucosamine transferase involved in the membrane steps of peptidoglycan synthesis," *J. Bacteriol.*, vol. 173, no. 15, pp. 4625–4636, 1991.

[12] A. M. Michaelis and Z. Gitai, "Dynamic polar sequestration of excess MurG may regulate enzymatic function," *J. Bacteriol.*, vol. 192, no. 18, pp. 4597–4605, 2010.

[13] E. V. D. B. Der Laan *et al.*, "Membrane Interaction of the Glycosyltransferase MurG: a SpecialRole for Cardiolipin," *J. Bacteriol.*, vol. 185, no. 13, pp. 1–7, 2003.

[14] N. Ruiz, "Lipid flippases for bacterial peptidoglycan biosynthesis," *Lipid Insights*, vol. 2015, pp. 21–31, 2015.

[15] D. J. Scheffers and M. B. Tol, "LipidII: Just Another Brick in the Wall?," *PLoS Pathog.*, vol. 11, no. 12, pp. 1–12, 2015.

[16] B. B. Bonev, E. Breukink, E. Swiezewska, B. De Kruijff, and A. Watts, "Targeting extracellular pyrophosphates underpins the high selectivity of nisin.," *FASEB J.*, vol. 18, no. 15, pp. 1862–9, 2004.

[17] J. van Heijenoort, "Peptidoglycan Hydrolases of *Escherichia coli*," *Microbiol. Mol. Biol. Rev.*, vol. 75, no. 4, pp. 636–663, 2011.

[18] P. Macheboeuf, C. Contreras-Martel, V. Job, O. Dideberg, and A. Dessen,

"Penicillin binding proteins: Key players in bacterial cell cycle and drug resistance processes," *FEMS Microbiol. Rev.*, vol. 30, no. 5, pp. 673–691, 2006.

[19] M. Banzhaf *et al.*, "Cooperativity of peptidoglycan synthases active in bacterial cell elongation," *Mol. Microbiol.*, vol. 85, no. 1, pp. 179–194, 2012.

[20] C. Paradis-bleau *et al.*, "Lipoprotein cofactors located in the outer membrane activate bacterial cell wall polymerases," *Cell*, vol. 143, no. 7, pp. 1110–1120, 2010.

[21] E. Sauvage and M. Terrak, "Glycosyltransferases and Transpeptidases/Penicillin-Binding Proteins: Valuable Targets for New Antibacterials," *Antibiotics*, vol. 5, no. 1, p. 12, 2016.

[22] W. Vollmer, B. Joris, P. Charlier, and S. Foster, "Bacterial peptidoglycan (murein) hydrolases," *FEMS Microbiol. Rev.*, vol. 32, no. 2, pp. 259–286, 2008.

[23] K. Bush, "A resurgence of β-lactamase inhibitor combinations effective against multidrug-resistant Gram-negative pathogens," *Int. J. Antimicrob. Agents*, vol. 46, no. 5, pp. 483–493, 2015.

[24] B. Ostash and S. Walker, "Moenomycin family antibiotics: chemical synthesis, biosynthesis, biological activity," *Nat. Prod. Rep.*, vol. 27, no. 11, pp. 1594–1617, 2010.

[25] D. L. Higgins *et al.*, "Telavancin , a Multifunctional Lipoglycopeptide , Disrupts both Cell Wall Synthesis and Cell Membrane Integrity in Methicillin-Resistant *Staphylococcus aureus*," *Antimi*, vol. 49, no. 3, pp.

1127–1134, 2005.

[26] H. Jeong, Y. M. Sim, H. J. Kim, Y.-J. Lee, S.-K. Lim, and S.-J. Lee, “Genome Sequences of *Amycolatopsis orientalis* subsp. *orientalis* Strains DSM 43388 and DSM 46075,” vol. 1, no. 4, pp. 1–2, 2013.

[27] D. H. Williams and B. Bardsley, “The vancomycin group of antibiotics and the fight against resistant bacteria,” *Angew. Chemie - Int. Ed.*, vol. 38, no. 9, pp. 1172–1193, 1999.

[28] D. Munch and H. G. Sahl, “Structural variations of the cell wall precursor lipid II in Gram-positive bacteria - Impact on binding and efficacy of antimicrobial peptides,” *Biochim. Biophys. Acta - Biomembr.*, vol. 1848, no. 11, pp. 3062–3071, 2015.

[29] N. J. Economou, S. Cocklin, and P. J. Loll, “High-resolution crystal structure reveals molecular details of target recognition by bacitracin,” *Proc. Natl. Acad. Sci.*, vol. 110, no. 35, pp. 14207–14212, 2013.

[30] FDA, “U.S. Food and Drug Administration (FDA).,” *U.S. Food and Drug Administration*, 2008. [Online]. Available: http://mendeley.csuc.cat/fitxers/35abd0eb4108a5f34d4dc9d0348e4c30. [Accessed: 05-Nov-2018].

[31] A. P. Zavascki, L. Z. Goldani, J. Li, and R. L. Nation, “Polymyxin B for the treatment of multidrug-resistant pathogens: A critical review,” *J. Antimicrob. Chemother.*, vol. 60, no. 6, pp. 1206–1215, 2007.

[32] L. L. Ling *et al.*, “A new antibiotic kills pathogens without detectable resistance,” *Nature*, vol. 517, pp. 455–459, 2015.

[33] H. Yang, K. H. Chen, and J. S. Nowick, “Elucidation of the Teixobactin

Pharmacophore," *ACS Chem. Biol.*, vol. 11, no. 7, pp. 1823–1826, 2016.

[34] A. Parmar *et al.*, "Efficient total syntheses and biological activities of two teixobactin analogues," *Chem. Commun.*, vol. 52, no. 36, pp. 6060–6063, 2016.

[35] A. Essig *et al.*, "Copsin, a novel peptide-based fungal antibiotic interfering with the peptidoglycan synthesis," *J. Biol. Chem.*, vol. 289, no. 50, pp. 34953–34964, 2014.

[36] S. Mulholland, E. R. Turpin, B. B. Bonev, and J. D. Hirst, "Docking and molecular dynamics simulations of the ternary complex nisin2:lipid II," *Nat. Publ. Gr.*, no. August 2015, pp. 1–11, 2016.

[37] S. M. Asaduzzaman, T. Bashar, and R. Noor, "Lantibiotics : A Candidate for Future Generation of Antibiotics," *Stamford J. Microbiol.*, vol. 1, no. 1, 2011.

[38] K. Altena, A. Guder, C. Cramer, and G. Bierbaum, "Biosynthesis of the lantibiotic mersacidin: Organization of a type B lantibiotic gene cluster," *Appl. Environ. Microbiol.*, vol. 66, no. 6, pp. 2565–2571, 2000.

[39] D. Hatziioanou *et al.*, "Discovery of a novel lantibiotic nisin O from *Blautia obeum* A2-162, isolated from the human gastrointestinal tract," *Microbiol. (United Kingdom)*, vol. 163, no. 9, pp. 1292–1305, 2017.

[40] C. Piper, C. Hill, P. D. Cotter, and R. P. Ross, "Bioengineering of a Nisin A-producing *Lactococcus lactis* to create isogenic strains producing the natural variants Nisin F, Q and Z," *Microb. Biotechnol.*, vol. 4, no. 3, pp. 375–382, 2011.

[41] J. W. M. Mulders, I. J. Boerrigter, H. S. Rollema, R. J. Siezen, and W. M. De

Vos, “Identification and characterization of the lantibiotic nisin Z, a natural nisin variant,” *Eur. J. Biochem.*, vol. 201, pp. 581–584, 1991.

[42] C.-I. Cheigh and Y.-R. Pyun, “Nisin biosynthesis and its properties.,” *Biotechnol. Lett.*, vol. 27, no. 21, pp. 1641–8, Nov. 2005.

[43] A. Bartoloni *et al.*, “In-Vitro Activity of Nisin Against Clinical Isolates of *Clostridium difficile*,” *J. Chemother.*, vol. 16, no. 2, pp. 119–121, 2004.

[44] A. H. Ali, T. W. Hale, R. S. Urban, H. V Werner, and R. D. Smalligan, “NISIN and *Clostridium difficile*: A Potentially Effective Treatment for an Increasingly Problematic Disease,” *Am. J. Gastroenterol.*, vol. 108, no. 4, p. 625, 2012.

[45] R. Gough *et al.*, “Oral delivery of nisin in resistant starch based matrices alters the gut microbiota in mice,” *Front. Microbiol.*, vol. 9, no. Jun, 2018.

[46] G. Engelke, Z. Gutowski-Eckel, M. Hammelmann, and K. D. Entian, “Biosynthesis of the lantibiotic nisin: Genomic organization and membrane localization of the NisB protein,” *Appl. Environ. Microbiol.*, vol. 58, no. 11, pp. 3730–3743, 1992.

[47] R. Rink, L. D. Kluskens, A. Kuipers, A. J. M. Driessen, O. P. Kuipers, and G. N. Moll, “NisC, the cyclase of the lantibiotic nisin, can catalyze cyclization of designed nonlantibiotic peptides.,” *Biochemistry*, vol. 46, no. 45, pp. 13179–89, 2007.

[48] B. Li and W. A. Van Der Donk, “Identification of essential catalytic residues of the cyclase NisC involved in the biosynthesis of nisin,” *J. Biol. Chem.*, vol. 282, no. 29, pp. 21169–21175, 2007.

[49] M. A. Ortega, Y. Hao, Q. Zhang, M. C. Walker, W. A. van der Donk, and S.

K. Nair, “Structure and mechanism of the tRNA-dependent lantibiotic dehydratase NisB,” *Nature*, 2014.

[50] M. L. S. Complex, K. Siegers, S. Heinzmann, and K. Entian, “Biosynthesis of Lantibiotic Nisin,” vol. 271, no. 21, pp. 12294–12301, 1996.

[51] J. R. Van der Meer, J. Polman, M. M. Beerthuyzen, R. J. Siezen, O. P. Kuipers, and W. M. De Vos, “Characterization of the *Lactococcus lactis* nisin A operon genes nisP, encoding a subtilisin-like serine protease involved in precursor processing, and nisR, encoding a regulatory protein involved in nisin biosynthesis,” *J. Bacteriol.*, vol. 175, no. 9, pp. 2578–2588, 1993.

[52] O. P. Kuipers, M. M. Beerthuyzen, R. J. Siezen, and W. M. De Vos, “Characterization of the nisin gene cluster nisABTCIPR of *Lactococcus lactis* Requirement of expression of the nisA and nisI genes for development of immunity,” *Eur. J. Biochem.*, vol. 216, no. 1, pp. 281–291, 1993.

[53] A. Kuipers *et al.*, “NisT, the transporter of the lantibiotic nisin, can transport fully modified, dehydrated, and unmodified prenisin and fusions of the leader peptide with non-lantibiotic peptides,” *J. Biol. Chem.*, vol. 279, no. 21, pp. 22176–22182, 2004.

[54] S. Wilson-Stanford, A. Kalli, K. Håkansson, J. Kastrantas, R. S. Orugunty, and L. Smith, “Oxidation of lanthionines renders the lantibiotic nisin inactive.,” *Appl. Environ. Microbiol.*, vol. 75, no. 5, pp. 1381–7, 2009.

[55] Z. Alkhatib *et al.*, “The C-terminus of nisin is important for the ABC transporter NisFEG to confer immunity in *Lactococcus lactis*,”

Microbiologyopen, vol. 3, no. 5, pp. 752–763, 2014.

[56] T. Stein, S. Heinzmann, I. Solovieva, and K. D. Entian, "Function of *Lactococcus lactis* nisin immunity genes nisI and nisFEG after coordinated expression in the surrogate host *Bacillus subtilis*," *J. Biol. Chem.*, vol. 278, no. 1, pp. 89–94, 2003.

[57] M. Qiao, T. Immonen, O. Koponen, and P. E. J. Saris, "The cellular location and effect on nisin immunity of the NisI protein from *Lactococcus lactis* N8 expressed in Escherichia coli and *L. lactis*," *FEMS Microbiol. Lett.*, vol. 131, no. 1, pp. 75–80, 1995.

[58] T. M. Takala and P. E. J. Saris, "C terminus of NisI provides specificity to nisin," *Microbiology*, vol. 152, no. 12, pp. 3543–3549, 2006.

[59] C. Hacker *et al.*, "NMR Resonance Assignments of the Lantibiotic Immunity Protein NisI from *Lactococcus lactis*," *Biomol. NMR Assign.*, vol. 9, no. 2, pp. 293–297, 2015.

[60] J. H. Jeong and S. C. Ha, "Crystal structure of NisI in a Lipid-Free Form, the Nisin Immunity Protein, from *Lactococcus lactis*," *Antimicrob. Agents Chemother.*, pp. 1–12, 2018.

[61] T. Stein, S. Heinzmann, S. Düsterhus, S. Borchert, and K. D. Entian, "Expression and functional analysis of the subtilin immunity genes spaIFEG in the subtilin-sensitive host *Bacillus subtilis* MO1099," *J. Bacteriol.*, vol. 187, no. 3, pp. 822–828, 2005.

[62] A. Chugunov, D. Pyrkova, D. Nolde, A. Polyansky, V. Pentkovsky, and R. Efremov, "Lipid-II forms potential 'landing terrain' for lantibiotics in simulated bacterial membrane.," *Sci. Rep.*, vol. 3, p. 1678, 2013.

[63] H. E. Van Heusden, B. De Kruijff, and E. Breukink, “Lipid II induces a transmembrane orientation of the pore-forming peptide lantibiotic nisin,” *Biochemistry*, vol. 41, pp. 12171–12178, 2002.

[64] R. a. G. Harmsen, N. Ghalit, J. Kemmink, E. Breukink, R. M. J. Liskamp, and D. T. S. Rijkers, “A conformationally constrained fused tricyclic nisin AB-ring system mimic toward an improved pyrophosphate binder of lipid II,” *Tetrahedron*, vol. 70, no. 42, pp. 7691–7699, 2014.

[65] S.-T. D. Hsu *et al.*, “The nisin-lipid II complex reveals a pyrophosphate cage that provides a blueprint for novel antibiotics.,” *Nat. Struct. Mol. Biol.*, vol. 11, no. 10, pp. 963–7, 2004.

[66] H. E. Hasper, B. de Kruijff, and E. Breukink, “Assembly and stability of nisin-lipid II pores.,” *Biochemistry*, vol. 43, no. 36, pp. 11567–75, 2004.

[67] K. A. Stevens, B. W. Sheldon, N. A. Klapes, and T. R. Klaenhammer, “Nisin treatment for inactivation of *Salmonella* species and other gram-negative bacteria,” *Appl. Environ. Microbiol.*, vol. 57, no. 12, pp. 3613–3615, 1991.

[68] I. S. Boziaris and M. R. Adams, “Temperature shock, injury and transient sensitivity to nisin in Gram negatives,” *J. Appl. Microbiol.*, vol. 91, no. 4, pp. 715–724, 2001.

[69] E. A. Davies, M. B. Falahee, and M. R. Adams, “Involvement of the cell envelope of *Listeria monocytogenes* in the acquisition of nisin resistance,” *J. Appl. Bacteriol.*, vol. 81, no. 2, pp. 139–146, 1996.

[70] N. E. Kramer, S. A. F. T. Van Hijum, J. Knol, O. P. Kuipers, and J. Kok, “Transcriptome Analysis Reveals Mechanisms by Which *Lactococcus*

lactis Acquires Nisin Resistance Transcriptome Analysis Reveals Mechanisms by Which *Lactococcus lactis* Acquires Nisin Resistance," *Antimicrob. Agents Chemother.,* vol. 50, no. 5, pp. 1753–1761, 2006.

[71] X. Ming and M. A. Daeschel, "Nisin Resistance of Foodborne Bacteria and the Specific Resistance Responses of *Listeria monocytogenes* Scott A," *J. Food Prot.*, vol. 56, no. 11, pp. 944–948, 1993.

[72] B. Jarvis, "Enzymic Reduction of the C-Terminal Dehydroalanyl-lysine Sequence in Nisin," *Biochemistry*, vol. 119, no. 56, p. 1967, 1970.

[73] Z. Sun, J. Zhong, X. Liang, J. Liu, X. Chen, and L. Huan, "Novel mechanism for nisin resistance via proteolytic degradation of nisin by the nisin resistance protein NSR.," *Antimicrob. Agents Chemother.*, vol. 53, no. 5, pp. 1964–73, 2009.

[74] J. M. Andrews, "Determination of Minimum inhibitory Concentrations," *J. Antimicrob. Chemother.*, vol. 48, pp. 5–16, 2001.

[75] W. C. Chan *et al.*, "Structure-activity relationships in the peptide antibiotic nisin: Antibacterial activity of fragments of nisin," *FEBS Lett.*, vol. 390, no. 2, pp. 129–132, 1996.

[76] E. Breukink, "Use of the Cell Wall Precursor Lipid II by a Pore-Forming Peptide Antibiotic," *Science.*, vol. 286, no. 5448, pp. 2361–2364, 1999.

[77] W. C. Chan, B. W. Bycroft, L.-Y. Lian, and G. C. K. Roberts, "Isolation and characterisation of two degradation products derived from the peptide antibiotic nisin," *FEBS Lett.*, vol. 252, no. 1–2, pp. 29–36, 1989.

[78] I. Wiedemann *et al.*, "Specific binding of nisin to the peptidoglycan precursor lipid II combines pore formation and inhibition of cell wall

biosynthesis for potent antibiotic activity.," *J. Biol. Chem.*, vol. 276, no. 3, pp. 1772–9, 2001.

[79] I. Wiedemann and T. Böttiger, "Lipid II-based antimicrobial activity of the lantibiotic plantaricin C," *Appl. Environ. Microbiol*, vol. 72, no. 4, pp. 2809–2814, 2006.

[80] D. Field, P. M. O. Connor, P. D. Cotter, C. Hill, and R. P. Ross, "The generation of nisin variants with enhanced activity against specific Gram-positive pathogens," *Mol. Microbiol.*, vol. 69, no. May, pp. 218–230, 2008.

[81] D. Field *et al.*, "Bioengineered Nisin A Derivatives with Enhanced Activity against Both Gram Positive and Gram Negative Pathogens," *PLoS One*, vol. 7, no. 10, 2012.

[82] D. Field *et al.*, "Studies with bioengineered Nisin peptides highlight the broad-spectrum potency of Nisin V," *Microb. Biotechnol.*, vol. 3, no. 4, pp. 473–486, 2010.

[83] E. Breukink, I. Wiedemann, C. Van Kraaij, O. P. Kuipers, H. G. Sahl, and B. De Kruijff, "Use of the cell wail precursor lipid II by a pore-forming peptide antibiotic," *Science.*, vol. 286, no. 5448, pp. 2361–2364, 1999.

[84] W. C. Chan *et al.*, "Structure-activity relationships in the peptide antibiotic nisin : role of dehydroalanine 5 . These include : Structure-Activity Relationships in the Peptide Antibiotic Nisin : Role of Dehydroalanine 5," *Appl. Environ. Microbiol.*, vol. 62, no. 8, pp. 2966–2969, 1996.

[85] J. C. Slootweg, N. Peters, H. L. C. Quarles van Ufford, E. Breukink, R. M. J. Liskamp, and D. T. S. Rijkers, "Semi-synthesis of biologically active nisin hybrids composed of the native lanthionine ABC-fragment and a cross-

stapled synthetic DE-fragment.," *Bioorg. Med. Chem.*, vol. 22, no. 19, pp. 5345–53, 2014.

[86] R. Rink *et al.*, "Dissection and modulation of the four distinct activities of nisin by mutagenesis of rings A and B and by C-terminal truncation," *Appl. Environ. Microbiol.*, vol. 73, no. 18, pp. 5809–5816, 2007.

[87] J. Parisot, S. Carey, E. Breukink, W. C. Chan, A. Narbad, and B. Bonev, "Molecular mechanism of target recognition by subtilin, a class I lanthionine antibiotic.," *Antimicrob. Agents Chemother.*, vol. 52, no. 2, pp. 612–8, 2008.

[88] S. Ludtke, K. He, and H. Huang, "Membrane thinning caused by magainin 2," *Biochemistry*, vol. 34, no. 51, pp. 16764–16769, 1995.

[89] H. Chen, J. Brown, J. Morell, and C. Huang, "Synthetic magainin analogues with improved antimicrobial activity," *Febs Lett.*, vol. 236, no. 2, pp. 462–466, 1988.

[90] B. Bechinger, M. Zasloff, and S. J. Opella, "Structure and orientation of the antibiotic peptide magainin in membranes by solid-state nuclear magnetic resonance spectroscopy.," *Protein Sci.*, vol. 2, no. 12, pp. 2077–84, 1993.

[91] M. Zasloff, "Magainins, a class of antimicrobial peptides from Xenopus skin: isolation, characterization of two active forms, and partial cDNA sequence of a precursor," *Proc. Natl. Acad. Sci.*, vol. 84, no. August, pp. 5449–5453, 1987.

[92] D. S. Reilly, N. Tomassini, and M. Zasloff, "Expression of Magainin Antimicrobial Peptide Genes in the Developing Granular Glands of

Xenopus Skin and Induction by Thyroid Hormone," *Dev. Biol.*, vol. 162, pp. 123–133, 1994.

[93] K. S. Moore *et al.*, "A novel peptide-producing cell in *Xenopus*: multinucleated gastric mucosal cell strikingly similar to the granular gland of the skin.," *J. Histochem. Cytochem.*, vol. 40, no. 3, pp. 367–378, 1992.

[94] A. Moore, "The big and small of drug discovery. Biotech versus pharma: advantages and drawbacks in drug development.," *EMBO Rep.*, vol. 4, no. 2, pp. 114–117, 2003.

[95] J. E. Thwaite *et al.*, "The cationic peptide magainin II is antimicrobial for *Burkholderia cepacia*-complex strains.," *J. Med. Microbiol.*, vol. 58, no. Pt 7, pp. 923–9, 2009.

[96] K. Matsuzaki *et al.*, "Mechanism of synergism between antimicrobial peptides magainin 2 and PGLa," *Biochemistry*, vol. 37, no. 43, pp. 15144–15153, 1998.

[97] U. Ros and A. J. García-Sáez, "More Than a Pore: The Interplay of Pore-Forming Proteins and Lipid Membranes," *J. Membr. Biol.*, vol. 248, no. 3, pp. 545–561, 2015.

[98] W. L. Maloy and U. P. Kari, "Structure-activity studies on magainins and other host defense peptides.," *Biopolymers*, vol. 37, no. 2, pp. 105–22, 1995.

[99] K. Matsuzaki, K. Sugishita, N. Fujii, and K. Miyajima, "Molecular basis for membrane selectivity of an antimicrobial peptide, magainin 2.," *Biochemistry*, vol. 34, no. 10, pp. 3423–3429, 1995.

[100] E. M. Tytler, G. M. Anantharamaiah, D. E. Walker, V. K. Mishra, M. N.

Palgunachari, and J. P. Segrest, “Molecular basis for prokaryotic specificity of magainin-induced lysis.,” *Biochemistry*, vol. 34, no. 13, pp. 4393–401, 1995.

[101] T. Unger, Z. Oren, and Y. Shai, “The effect of cyclization of magainin 2 and melittin analogues on structure, function, and model membrane interactions: implication to their mode of action.,” *Biochemistry*, vol. 40, no. 21, pp. 6388–97, 2001.

[102] Y. Zhou and Y. Peng, “Synergistic effect of clinically used antibiotics and peptide antibiotics against gram-positive and gram-negative bacteria,” *Exp. Ther. Med.*, vol. 6, pp. 1000–1004, 2013.

[103] L. Lins, P. Ducarme, E. Breukink, and R. Brasseur, “Computational study of nisin interaction with model membrane.,” *Biochim. Biophys. Acta*, vol. 1420, no. 1–2, pp. 111–120, 1999.

[104] M. Giovannini, L. Poulter, B. Gibson, and D. Williams, “Biosynthesis and degradation of peptides derived from *Xenopus laevis* prohormones.,” *Biochem. J*, vol. 243, pp. 113–120, 1987.

[105] N. M. Resnick, W. L. Maloy, H. R. Guy, and M. Zasloff, “A novel endopeptidase from *Xenopus* that recognizes α-helical secondary structure,” *Cell*, vol. 66, no. 3, pp. 541–554, 1991.

[106] Y. Miyazaki, M. Aoki, Y. Yano, and K. Matsuzaki, “Interaction of antimicrobial peptide magainin 2 with gangliosides as a target for human cell binding.,” *Biochemistry*, vol. 51, no. 51, pp. 10229–35, 2012.

[107] C. M. Huang, H. C. Chen, and C. H. Zierdt, “Magainin analogs effective against pathogenic protozoa.,” *Antimicrob. Agents Chemother.*, vol. 34,

no. 9, pp. 1824–1826, 1990.

[108] J. H Cuervo, B. Rodriguez, and R. Houghten, "The magainins: Sequence factors relevant to increased antimicrobial activity and decreased hemolytic activity," *Peptide Research.,* vol. 1., pp. 81-86, 1988.

[109] A. Rodríguez, E. Villegas, A. Montoya-Rosales, B. Rivas-Santiago, and G. Corzo, "Characterization of Antibacterial and Hemolytic Activity of Synthetic Pandinin 2 Variants and Their Inhibition against *Mycobacterium tuberculosis*.," *PLoS One*, vol. 9, no. 7, p. e101742, 2014.

[110] C. Dempsey, R. Bazzo, and T. Harvey, "Contribution of proline-14 to the structure and actions of melittin," *FEBS Lett.*, vol. 281, no. 1, pp. 240–244, 1991.

[111] F. Azmi and M. Skwarczynski, "Towards the development of synthetic antibiotics: Designs inspired by natural antimicrobial peptides," *Curr. Med. Chem.*, vol. 23, no. 41, pp. 4610–4624, 2016.

[112] S. J. Lam, E. H. H. Wong, C. Boyer, and G. G. Qiao, "Antimicrobial polymeric nanoparticles," *Prog. Polym. Sci.*, vol. 76, pp. 40–64, 2018.

[113] E. F. Palermo, S. Vemparala, and K. Kuroda, "Cationic spacer arm design strategy for control of antimicrobial activity and conformation of amphiphilic methacrylate random copolymers," *Biomacromolecules*, vol. 13, no. 5, pp. 1632–1641, 2012.

[114] Z. Liu *et al.*, "Length effects in antimicrobial peptides of the $(RW)_n$ series," *Antimicrob. Agents Chemother.*, vol. 51, no. 2, pp. 597–603, 2007.

[115] A. C. Nilsson *et al.*, "Ltx-109 is a novel agent for nasal decolonization of methicillin-resistant and -sensitive *Staphylococcus aureus*," *Antimicrob.*

Agents Chemother., vol. 59, no. 1, pp. 145–151, 2015.

[116] J. Wang *et al.*, "High specific selectivity and Membrane-Active Mechanism of the synthetic centrosymmetric α-helical peptides with Gly-Gly pairs," *Sci. Rep.*, vol. 5, no. April, pp. 1–19, 2015.

[117] M. Bruschi *et al.*, "Synthesis, characterization, antimicrobial activity and LPS-interaction properties of SB041, a novel dendrimeric peptide with antimicrobial properties," *Peptides*, vol. 31, no. 8, pp. 1459–1467, 2010.

[118] A. Makovitzki, D. Avrahami, and Y. Shai, "Ultrashort antibacterial and antifungal lipopeptides," *Proc. Natl. Acad. Sci.*, vol. 103, no. 43, pp. 15997–16002, 2006.

[119] T. T. Tran, J. M. Munita, and C. A. Arias, "Mechanisms of Drug Resistance: Daptomycin Resistance," *Ann. N. Y. Acad. Sci.*, vol. 1354, no. 1, pp. 32–53, 2015.

[120] E. R. Turpin, B. B. Bonev, and J. D. Hirst, "Stereoselective disulfide formation stabilizes the local peptide conformation in nisin mimics.," *Biochemistry*, vol. 49, no. 44, pp. 9594–603, 2010.

[121] B. Bonev, J. Hooper, and J. Parisot, "Principles of assessing bacterial susceptibility to antibiotics using the agar diffusion method," *J. Antimicrob. Chemother.*, vol. 61, no. March, pp. 1295–1301, 2008.

[122] Sigma, "Regeneration of DEAE-Cellulose." [Online]. Available: http://www.sigmaaldrich.com/content/dam/sigma-aldrich/docs/Sigma/Product_Information_Sheet/d6418pis.pdf.

[123] E. Breukink *et al.*, "Lipid II is an intrinsic component of the pore induced by nisin in bacterial membranes," *J. Biol. Chem.*, vol. 278, no. 22, pp.

19898–19903, 2003.

[124] A. B. M. Lanne *et al.*, “Molecular recognition of lipopolysaccharide by the lantibiotic nisin,” *Biochim. Biophys. Acta - Biomembr.*, vol. 1861, no. 1, pp. 83–92, 2019.

[125] K. Tiyanont, T. Doan, M. B. Lazarus, X. Fang, D. Z. Rudner, and S. Walker, “Imaging peptidoglycan biosynthesis in *Bacillus subtilis* with fluorescent antibiotics,” *Proc. Natl. Acad. Sci.*, vol. 103, no. 29, pp. 11033–11038, 2006.

[126] J. Schindelin *et al.*, “Fiji - an Open Source Platform for Biological Image Analysis,” *Nat. Methods*, vol. 9, no. 7, pp. 1–15, 2012.

[127] R. Hussain *et al.*, “CDApps: Integrated software for experimental planning and data processing at beamline B23, Diamond Light Source,” *J. Synchrotron Radiat.*, vol. 22, no. 2, pp. 465–468, 2015.

[128] S. M. Kelly, T. J. Jess, and N. C. Price, “How to study proteins by circular dichroism,” *Biochim. Biophys. Acta - Proteins Proteomics*, vol. 1751, no. 2, pp. 119–139, 2005.

[129] Dassault Systèmes BIOVIA, “Discovery Studio Visualiser, v17.2.0.16349.” 2017.

[130] S. Jo, T. Kim, V. G. Iyer, and W. Im, “CHARMM-GUI: A Web-Based Graphical User Interface for CHARMM,” *J. Comput. Chem.*, vol. 29, no. 11, pp. 1859–1865, 2008.

[131] J. Lee *et al.*, “CHARMM-GUI Input Generator for NAMD, GROMACS, AMBER, OpenMM, and CHARMM/OpenMM Simulations Using the CHARMM36 Additive Force Field,” *J. Chem. Theory Comput.*, vol. 12, no.

1, pp. 405–413, 2016.

[132] J. C. Phillips *et al.*, “Scalable Molecular Dynamics with NAMD,” *J. Comput. Chem.*, vol. 26, no. 16, pp. 1781–1802, 2005.

[133] W. Humphrey, A. Dalke, and K. Schulten, “VMD: Visual Molecular Dynamics,” *J. Mol. Graph.*, vol. 14, no. October 1995, pp. 33–38, 1996.

[134] J. R. Winther and C. Thorpe, “Quantification of Thiols and Disulfides,” *Biochim. Biophys. Acta*, vol. 1840, no. 2, 2014.

[135] J. C. Phillips *et al.*, “Scalable Molecular Dynamics with NAMD,” *J. Comput. Chem.*, vol. 26, no. 16, pp. 1781–1802, 2005.

[136] L. Otvos, C. Snyder, B. Condie, P. Bulet, and J. D. Wade, “Chimeric Antimicrobial Peptides Exhibit Multiple Modes of Action,” *Int. J. Pept. Res. Ther.*, vol. 11, no. 1, pp. 29–42, 2005.

[137] S. R. Dennison and D. a. Phoenix, “Susceptibility of sheep, human, and pig erythrocytes to haemolysis by the antimicrobial peptide Modelin 5,” *Eur. Biophys. J.*, vol. 43, no. 8–9, pp. 423–432, 2014.

[138] I. D. Campbell, *Biophysical Techniques*. Oxford University Press, 2012.

[139] U. of C. Department of Chemistry, “An introduction to circular dichroism spectroscopy,” 2010. [Online]. Available: www.chem.uci.edu/~dmitryf/manuals/CD spectroscopy.pdf.

[140] C. J. Arnusch, R. J. Pieters, and E. Breukink, “Enhanced Membrane Pore Formation through High- Affinity Targeted Antimicrobial Peptides,” *PLoS One*, vol. 7, no. 6, pp. 1–5, 2012.

[141] H. E. Hasper *et al.*, “An alternative bactericidal mechanism of action for lantibiotic peptides that target lipid II.,” *Science*, vol. 313, no. 5793, pp.

1636–7, 2006.

[142] R. A. Daniel and J. Errington, “Control of Cell Morphogenesis in Bacteria,” *Cell*, vol. 113, no. 6, pp. 767–776, 2003.

[143] M. C. A. Lages, K. Beilharz, D. Morales Angeles, J. W. Veening, and D. J. Scheffers, “The localization of key *Bacillus subtilis* penicillin binding proteins during cell growth is determined by substrate availability,” *Environ. Microbiol.*, vol. 15, no. 12, pp. 3272–3281, 2013.

[144] L. Turchi, T. Santini, E. Beccari, and C. Di Franco, “Localization of new peptidoglycan at poles in *Bacillus mycoides*, a member of the *Bacillus cereus* group,” *Arch. Microbiol.*, vol. 194, no. 10, pp. 887–892, 2012.

[145] A. Atrih, M. P. Williamson, G. Bacher, and S. J. Foster, “Analysis of Peptidoglycan Structure from Vegetative Cells of,” *Society*, vol. 181, no. 13, pp. 3956–3966, 1999.

[146] M. Borisova, R. Gaupp, A. Duckworth, A. Schneider, D. Dalügge, and M. Mühleck, “Peptidoglycan Recycling in Gram-Positive Bacteria Is Crucial for Survival in Stationary Phase,” *MBio*, vol. 7, no. 5, pp. 1–10, 2016.

[147] J. Reith and C. Mayer, “Peptidoglycan turnover and recycling in Gram-Positive bacteria,” *Appl. Microbiol. Biotechnol.*, vol. 92, no. 1, pp. 1–11, 2011.

[148] K. Wakamatsu, A. Takeda, T. Tachi, and K. Matsuzaki, “Dimer structure of magainin 2 bound to phospholipid vesicles,” *Biopolymers*, vol. 64, no. 6, pp. 314–327, 2002.

[149] K. P. Santo and M. L. Berkowitz, “Difference between magainin-2 and melittin assemblies in phosphatidylcholine bilayers: Results from coarse-

grained simulations," *J. Phys. Chem. B*, vol. 116, no. 9, pp. 3021–3030, 2012.

[150] C. E. Dempsey, S. Ueno, and M. B. Avison, "Enhanced membrane permeabilization and antibacterial activity of a disulfide-dimerized magainin analogue," *Biochemistry*, vol. 42, no. 2, pp. 402–409, 2003.